

STRENGTH OF ANISOTROPIC WOOD AND  
SYNTHETIC MATERIALS

Ye.K. Ashkenazi

Translation of "Prochnost' anizotropnykh  
drevesnykh i sinteticheskikh materialov".  
"Lesnaya Promyshlennost'" Press, Moscow,  
1966, pp 1-168

(NASA-TM-76535) STRENGTH OF ANISOTROPIC  
WOOD AND SYNTHETIC MATERIALS (National  
Aeronautics and Space Administration) 185 p  
HC A09/MF A01 CSCL 20K

No 1-22417

Unclas  
G3/39 21913

NATIONAL AERONAUTICS AND SPACE ADMINISTRATION  
WASHINGTON, DC 20546  
APRIL 1981



## STANDARD TITLE PAGE

1. Report No. NASA TM-76535	2. Government Accession No.	3. Recipient's Catalog No.	
4. Title and Subtitle STRENGTH OF ANISOTROPIC WOOD AND SYNTHETIC MATERIALS		5. Report Date APRIL 1981	
		6. Performing Organization Code	
7. Author(s) Ye. K. Ashkenazi		8. Performing Organization Report No.	
		10. Work Unit No.	
9. Performing Organization Name and Address SCITRAN Box 5456 Santa Barbara, CA 93108		11. Contract or Grant No. NASW-3198	
		13. Type of Report and Period Covered Translation	
12. Sponsoring Agency Name and Address National Aeronautics and Space Administration Washington, D.C. 20546		14. Sponsoring Agency Code	
15. Supplementary Notes  Translation of "Prochnost' anizotropnykh drevesnykh i sinteticheskikh materialov," "Lesnaya Promyshlennost'" Press, Moscow, 1966, pp. 1-168			
16. Abstract  This book covers strength studies of anisotropic nonmetallic materials. It shows the possibility of using general formulas for different anisotropic materials. The practical application of the theoretical formulas is confirmed by the test results of different materials. Data are cited on the strength of wood, plywood, laminated wood plastics, fiber glass-reinforced plastics and directed polymer films.			
17. Key Words (Selected by Author(s))		18. Distribution Statement  UNLIMITED-Unclassified	
19. Security Classif. (of this report) Unclassified	20. Security Classif. (of this page) Unclassified	21. No. of Pages 185	22. Price

## Table of Contents

Preface	1
Chapter I. Tensorial Formulas to Compute the Strength Characteristics Depending on the Orientation of Stresses in Material	1
1. History of the Problem	1
2. Introduction	6
3. Strength Characteristics of Anisotropic Bodies as Tensorial Quantities	12
4. Study of the Components of Strength Tensor of Orthotropic Material	20
5. Strength Tensor of Fourth Order for Transversely Isotropic Material	29
Chapter II. Technique for Mechanical Tests of Anisotropic Materials	38
6. Features of Elastic Deformation of Anisotropic Bodies	38
7. Errors in Experimental Analysis of Strength Characteristics during Stretching and During Compression	46
8. Testing Methods for Simple Shearing and For Shearing	56
9. Evaluating the Structural Strength of Anisotropic Materials from Results of Mechanical Tests	63
Chapter III. Results of Experimental Study on Anisotropy of Mechanical Properties of Structural Materials	69
10. Wood and Wood Materials	69
11. Stretching of Uniaxially Oriented Crystal Polymer Films	103
12. Fiber Glass-Reinforced Plastics	104
13. Metals	129
14. Determination of Ultimate Strength for Simple Shearing from Results of Testing for Stretching or Compression of Wood Samples and Directed Fiber Glass-Reinforced Plastics	136
15. Experiments on Biaxial Compression	142
Chapter IV. Strength Anisotropy in Complex Stresses	145
16. Study of Applicability of Mises' Plasticity Conditions as Strength Conditions of Anisotropic Materials	145
17. Approximate Structure of Surface of Equally Dangerous Planar Stresses from Experimental Data	159
18. Possible Forms of Strength Conditions for Strongly Anisotropic Bodies	165
Conclusion	169
References	173

### ANNOTATION

This book covers strength studies of anisotropic nonmetallic materials. It shows the possibility of using general formulas for different anisotropic materials.

The practical application of the theoretical formulas is confirmed by the test results of different materials for the effect of static, impact loads, and for fatigue. Data are given on the strength of wood, plywood, laminated wood plastics, fiber glass-reinforced plastics, and directed polymer films.

The book is designed for engineering and technical workers, workers of scientific research institutes, and design offices of the wood working industry.



This work studies questions of strength that are common to all anisotropic materials used in machine parts and designs: wood, plywood, wood and fiber glass-reinforced plastics, rolled metals and directed polymer films. The results of an experimental strength study of different anisotropic structural materials are generalized in this work using the mathematical apparatus of tensor algebra.

The author solved questions of strength that are common to all anisotropic structural materials, based on two main assumptions: 1) the possibility of viewing anisotropic structural materials as homogeneous continuums, and 2) the possibility of classifying the strength characteristics of anisotropic bodies among the directed quantities that are expressed by fourth order (rank) tensors.<sup>1</sup>

The experimental study that was conducted confirms the correctness of these assumptions. They comply with reality with a degree of approximation that is sufficient for use in engineering practice.

Only one of all the urgent and complicated problems of materials mechanics is examined in the work, namely, strength anisotropy.

The methods for computing the strength of metal parts have been created by many generations of engineers and scientists. They have been verified by practice over decades. Applicable methods of computing the strength of machine parts made of anisotropic materials have not yet been produced. The incomplete and scattered data about the characteristics of the mechanical properties of these materials have not been generalized into a single harmonious system.

The purpose of this work is to make a feasible contribution to resolving this urgent problem of modern technology.

Chapter 1. Tensorial Formulas to Compute the Strength Characteristics Depending on the Orientation of Stresses in Material /5

1. History of the Problem

Wood is one of the most ancient construction materials for erecting buildings, bridges and other engineering structures. It was displaced at the end of the 19th century by the more economical metal and reinforced concrete. It was again employed in the World War I period.

\*Numbers in margin indicate pagination in original text.

<sup>1</sup>This work only uses the Cartesian coordinate system.

Perfected methods of designing, and especially, new methods of joining elements of wood structures guaranteed their broad application in engineering structures, special shipbuilding and aircraft construction. It is natural that the methods of calculation and studies on the mechanical properties of wood acquired great value.

Collapse and shearing of the wood at a certain angle to the fibers occur in almost all types of connections of wood design assemblies. The problem of the dependence of strength under the influence of perpendicular (collapsing) and tangential (shearing) stresses on the incline angle of the wood fiber therefore developed a long time ago. It was the subject of experimental and theoretical study in many works, starting with the time of D. I. Zhuravskiy [3].

It was essentially Zhuravskiy who first centered attention on the difference between the radial and tangential directions in wood when it is loaded transverse to the fibers. The known studies of Chevandier and Wortheim (1848-1861) did not differentiate between these directions. After noting the different resistance of wood during bending in radial and tangential planes, Zhuravskiy made a very interesting explanation for the difference in the resistance of a pine beam with different arrangement of the fibers [3]. Zhuravskiy made the first tests in Russia on wood for strength during stretching, compression and shearing.

/6

The monograph of F. Kollman [102] gives a detailed survey of works on wood strength.

Kollman [101], using the experiments of Bauman (1922), suggested the known empirical formula to compute the ultimate compression strength of wood  $\sigma_\alpha$  depending on the angle of incline of fibers  $\alpha$ :

$$\sigma_\alpha = \frac{\sigma_0 \cos^2 \alpha}{\sigma_{90} \cos^n \alpha} + \frac{\sigma_0 \sin^2 \alpha}{\sigma_0 \sin^n \alpha} \quad (1.1)$$

In the American literature, this same formula was suggested by Hankinson [108] with  $n=2$ .

Stussi [110] suggested another, also empirical formula that has become less popular:

$$\sigma_\alpha = \frac{\sigma_0 \cos^2 \alpha}{1 - C_1 \sin^2 \alpha} + \frac{\sigma_{90} \sin^2 \alpha}{1 - C_2 \cos^2 \alpha} \quad (1.2)$$

Here  $\sigma_0$ --ultimate strength during compression along, while  $\sigma_{90}$ --transverse to, the fibers.

The exponent  $n$  in the empirical formula (1.1) accepted by Kollman and Hankinson, for a long time was the subject of discussion abroad and in the USSR. G. Takhtamyshev assumed  $n$  to be equal to  $3/2$  [20]. The Standards and Specifications (NiTU) for planning wood structures, 1939 (OST 90001-38) assumed  $n$  to be equal to 2. A later issue of the NiTU (1948) assumes it to be equal to 3.

The currently active SNIIP [Construction Standards and Regulations] II-V.4-62\* provide an analogous formula with  $n=3$  for the amount  $R_\alpha$  (resistance of wood to collapse at angle  $\alpha$  to the fibers).

$$R_\alpha = \frac{R_0}{1 - \left( \frac{R_0}{R_{90}} - 1 \right) \sin^3 \alpha}. \quad (1.3)$$

Detailed experimental studies that were apparently made for the first time by Karlsen [41]\*\* on wood collapse at an angle to the fibers, resulted in an empirical formula (1.4) for the resistance to shearing at angle  $\alpha$  to the fibers ( $R_{ck,\alpha}$ ). This formula also previously (OST 90001-38) assumed that  $n=2$ . In NiTU 122-55 and SNIP V.4-62, this formula has the following appearance (with  $n=3$ ):

$$R_{ck,\alpha} = \frac{R_{ck,0}}{1 - \left( \frac{R_{ck,0}}{R_{ck,90}} - 1 \right) \sin^3 \alpha}. \quad (1.4)$$

Thus, even very extensive and detailed experimental studies with a purely empirical approach to the problem resulted in controversial results. The type of the formula could depend on the nature of the wood and the testing circumstances. As always in an empirical approach, new and numerous experiments would have been required if a new material was used, or even if the condition of the material was somewhat altered.

This work has shown that formula (1.3) is incorrect in principle, since in order to compute the amount  $R_\alpha$ , it is necessary to know not two, but three experimentally definable quantities:  $R_0(\sigma_0)$ ,  $R_{90}(\sigma_{90})$  and  $R_{45}(\sigma_{45})$ \*\*\*. The determination of precisely these three quantities

\*Construction Standards and Regulations, part II, section V, chapter 4 "Wood Structures. Design Standards," Moscow, 1962. Formulas (1.3) and (1.4) preserve the designations adopted in the SNIIP.

\*\*See also chapter III, fig. 3.11.

\*\*\*The works of A. L. Rabinovich have obtained formulas that include two quantities  $R_0(\sigma_0)$  and  $R_{90}(\sigma_{90})$ , and also elastic constants of the material.

is generally accepted for aviation plywood [16]. Formula (1.4), according to the data of this work, must have an exponent of  $n=2$  (see chapter 1, section 3).

It should be noted that the NiTU views wood as a material that is transversely isotropic (transtropic). It does not distinguish between tangential and radial directions transverse to the fibers. At the same time, GOST 6336-52 [state standard] "Methods of Physical-Mechanical Wood Tests," stipulates separate testing of all types of samples in radial and tangential directions. Consequently, wood is viewed here as an orthotropic material.

When elastic properties of boards, beams and other large structural elements are studied, they should be classified as transtropic bodies. The board is usually arranged lengthwise along the wood fibers, but it does not have a definite orientation of the cross section in relation to the annual rings. In this case, the elastic properties can be considered the same in different directions transverse to the fibers since the continual change in the incline of the annual rings in the cross section plane averages the elastic properties in different directions in this plane [51]. This averaging does not occur in relation to the strength properties since strength is always determined not by the average, but the least amount of resistance. Transverse isotropy of the wood strength properties in structures is a rougher approximation than the plan of transverse isotropy of its elastic properties. Strength in a direction perpendicular to the fibers cannot be assumed to be equal to the average or intermediate quantity between strength in radial and tangential directions. In establishing the ultimate and calculated resistances, it would be more accurate to start from an orthogonal plan of strength anisotropy, and distinguish, where this is possible, the orientation of forces not only in relation to the fibers, but also in relation to the annual layers of the wood.

/8

The question of how wood strength depends on the direction of the fibers was theoretically examined for the first time in 1939 in the United States in the Madison Laboratory of Forestry Products. Norris in his work [108] attempted to derive a corresponding formula based on the tenets of Hanke's theory of plasticity. During simple compression in different directions in relation to the fibers, Norris

obtained a formula to compute the ultimate resistance

$$\frac{1}{\tau_a^2} = \frac{\sin^4 \alpha}{\tau_0^2} + \frac{\sin^2 \alpha \cos^2 \alpha}{N} + \frac{\cos^4 \alpha}{\tau_{90}^2}, \quad (1.5)$$

where  $N$  is the shear modulus.

These ideas were developed in the further works of Norris, Werren and other workers in the Madison laboratory. They derived a number of more advanced formulas. We unfortunately do not have the derivations of these formulas. Summary formulas are given in Werren's work [113]. They are used for anisotropic fiber glass-reinforced plastics. Equations of limit states were the initial equations in their derivation. They contained only second order components (relative to stresses) as accepted in the Hanke-Mises-Hill theory (see chapter IV, p146).

Werren presents the following equation:

$$\frac{1}{\tau_a^2} = \frac{\sin^4 \alpha}{\tau_0^2} + \frac{\sin^2 2\alpha}{4\tau_0^2} + \frac{\cos^4 \alpha}{\tau_{90}^2}. \quad (1.6)$$

If in formula (1.5)

$$N = \tau_0^2,$$

then it is obtained from equation (1.6).

The Madison laboratory formula has the following appearance for a section at angle  $\alpha$  to the fibers

$$\frac{1}{\tau_a^2} = \frac{\cos^2 2\alpha}{\tau_0^2} + \left( \frac{1}{\tau_0^2} + \frac{1}{\tau_{90}^2} \right) \sin^2 2\alpha. \quad (1.7)$$

Werren obtained a good correspondence of formula (1.6) for fiber glass-reinforced plastics to the experimental data (see chapter III, fig. 3.25 where Werren's curve is presented), but did not obtain any correspondence during shear. [103]

The German literature [102] presents formulas to compute the amount of resistance of orthotropic wood materials during shear. It coincides with our formula (1.24) (see section 4). Kollman cites this formula without the derivation, referring to the work of R. Keylwerth that was done during World War II for the aircraft construction plants of the Junkers firm. The formula is confirmed by the experiments of Keylwerth (see fig.3.14) for shear of samples of laminated wood materials. They

were published in Kollman's book. Keylwerth's work that is cited by Kollman is not available in the USSR, therefore it is difficult to say precisely how this formula was derived.

The work of A. L. Rabinovich [58] was published almost at the same time as the article of Keylwerth and Kollman. Besides a comprehensive examination of the tensor of elastic constants for orthotropic wood materials, it suggested a formula to compute the ultimate strengths during stretching and compression based on deformation assumptions. A. L. Rabinovich did not examine questions of strength under the influence of tangential stresses. He obtained a formula for resistance to the effect of perpendicular stresses that practically coincides with the tensorial formula (1.22) (see section 4).

The concept introduced below on the strength tensor makes it possible to produce more general formulas of ultimate resistances not only during stretching and compression, but also during shear. This has definite practical importance for wood and modern synthetic materials.

## 2. Introduction

Since the time of Savart (1830) and Saint-Venant (1856), a plan of orthogonal anisotropy of elastic properties has been attributed to wood by analogy with cubic system crystals. Experimental study of the characteristics of wood and wood materials elastic properties viewed as a homogenous continuum made it possible to apply methods of the mathematical theory of elasticity of anisotropic bodies.

A vast class of new synthetic anisotropic materials has appeared in recent years. It is sometimes difficult to use them in machine construction and construction due to the lack of reliable strength calculation methods and data on the mechanical properties of these materials.

The reinforced plastics are the strongest of the synthetic materials and the most promising in their mechanical properties. The reinforcing fibers in them, no matter what their arrangement, are linked into a unit by a polymer binding agent. These plastics have two characteristic features that distinguish them from metals, and bring them closer to wood materials: first, the effect of the time factor and the size of the samples on the mechanical characteristics, and second, the

/10

anisotropy of all mechanical properties.

This work does not examine the first feature. It is therefore assumed that in studying the mechanical properties of the material, the dimensions of the samples, testing temperature and rate of deformation have the same order in all stress states and for all structural directions.

Of all the urgent and complicated questions in mechanics of materials, this work examines only one, anisotropy of their mechanical strength under different homogeneous stresses.

Anisotropy is viewed in the first approximation in isolation from many factors that significantly influence the strength properties.

Investigation of the mechanical strength of anisotropic bodies is an urgent problem of modern technology. It develops when the sphere of application of synthetics, reinforced plastics and wood, reinforced plastics in machine construction, and directed polymers in light industry expands.

Certain questions of strength, plasticity and especially fatigue of polycrystalline quasiisotropic steel also make it necessary to investigate the mechanical properties of anisotropic crystallites. The "whiskers" of pure metals are anisotropic. The anisotropy of certain high-strength pressure-treated metal alloys is significant [119]. In solving the problems of the mechanics of anisotropic materials, it is useful to employ methods of a related science, crystal physics. Until recently it was almost exclusively involved with studying the physical and mechanical properties of anisotropic bodies.

In physics, the properties of crystals have been studied since W. Voigt using mathematical quantities called tensors.

Tensors are used to describe those properties of crystals whose characteristics can be obtained for all structural directions.

Tensors of a different order (rank) correspond to various physical properties of a crystal. The tensor order depends on precisely which crystal property is being examined, while the number of tensor components that differ from zero is determined by the group of structural symmetry of the studied crystal.

This mathematical description of the physical properties of a crystal require that it be viewed as a homogeneous, continuous anisotropic

medium that has a certain symmetry.

In the works of A. V. Shubnikov and V. A. Bazhenov, the main method of crystallography, the science of the symmetry of a medium and the tensor presentation of the characteristics of its physical properties, covers the noncrystalline anisotropic structures (wood and wood materials) in relation to the piezoelectric properties of these structures. /11

This work attempted to use these methods to investigate the strength property characteristics of a broad class of anisotropic materials used in technology.

The use of the tensor apparatus requires a preliminary generalization of the concept on the strength property characteristics of anisotropic bodies. This generalization that follows from the problem of technical strength calculations of anisotropic parts, can reject a detailed description of the nature of the physical process that transfers the material to a dangerous state.

Introduction of the dangerous state concept complies with the calculation methods used in evaluating the efficiency and practical suitability of machine parts and design elements. This concept is the basis for the modern science regarding resistance of materials. It naturally can be the basis for examining resistance of those materials whose properties differ in various directions.

Anisotropy of the majority of structural materials is a consequence of the primary orientation of their structural elements. These materials are usually orthotropic (orthogonally anisotropic), i.e., they have three mutually perpendicular planes of structural symmetry. These are uneven plywood, DSP [laminated wood plastic], SVAM [fiber glass anisotropic material] and other fiber glass plastics that are reinforced with continuous fiber glass (AG-4S), different textolites and glass textolites (KAST), rolled metals, and directed polymer films.

If these materials are laminated sheets (plywood, DSP, SVAM), then the anisotropy in the sheet plane is determined by the fibrous structure of the individual layers and their mutual arrangement.

If the sheet material is transverse-isotropic (transtropic), then all the directions lying on the sheet plane are equivalent, and the sheet plane is a plane of isotropy.



The sheet plane of laminated material can be a plane of isotropy in two cases:

1. If the layers are isotropic. The anisotropy of the material is then determined only by the difference between its properties in the sheet plane and its properties in the direction perpendicular to the sheet plane. The latter direction is usually weaker due to the effect of the binding agent (glued interlayers between the layers).

2. If the layers are anisotropic, but turned towards each other so that the sheet as a whole has an axis of symmetry on the order of  $\frac{2\pi}{5}$  or higher ("stellar" arrangement of layers with size of the angle between the fibers in adjacent layers no more than  $72^\circ$ ) (see section 4). /12

In the elements of wood structures, the calculated plan of anisotropy is determined by the shape, dimensions and arrangement of the sections in relation to the annual rings. With fairly large dimensions of the sections, and in the absence of regular orientation (boards, beams, laths) one can, as A. N. Mitinskiy [51] demonstrated, approximately consider the direction of the wood fibers to be the axis of symmetry of its structure, and the plane perpendicular to this axis, to be the plane of isotropy of all of its properties.

As applied to the elementary volumes of wood, the hypothesis on orthogonal anisotropy fits its structure best. This hypothesis corresponds to the test results of small pure samples. It is based on an assumption regarding the existence of three planes of symmetry in the elementary volume of wood [49].

The plane that is perpendicular to the fibers is considered the plane of symmetry of the wood strength properties if one ignores the change in these properties over the length of the trunk. In the first approximation, this assumption is justified by the circumstance that a change in strength over the trunk is usually small as compared to the changes governed by the difference in axial orientation of the sample in relation to the direction of the fibers.

One can take the radial plane as the plane of symmetry of the wood strength characteristics on the condition that the curvature of the annual rings is small within the examined volume.

The tangential plane can be conditionally taken as the plane of symmetry if one ignores the change in strength over the diameter of

the trunk and does not take into account the differences in the properties of the early and late zones of the annual layers.

Wood of all types is characterized by a very pronounced anisotropy. Its moduli of elasticity for directions along and transverse to the fibers differ in quantity almost 20-fold, and the ultimate strengths differ 40-fold. The derived wood materials, plywood, different laminated wood plastics (DSP-B, DSP-V) are also anisotropic. The anisotropy is significant for all mechanical properties and in the crystal polymers directed by preliminary stretching.

The high-strength plastics reinforced with fiber glass that are employed in technology are also anisotropic. Anisotropy is very significant in the case of reinforcement with unidirectional fiber glass or spun glass thread (SVAM, STER, AG-4S and others).

The work experimentally studied the strength of fiber glasses of two main types of reinforcement: fabric and fibrous (directed). The obtained relationships (but not the absolute quantities of the strength characteristics) will apparently be suitable for other fiber glasses of random symmetrical reinforcement.

/13

Anisotropy of steel mechanical properties is often a consequence of the primary orientation of the crystals after plastic deformation (drawing or rolling). The assumption regarding the anisotropy of steel mechanical properties in this case is closer to reality than the standard assumption that views steel as a quasiisotropic material. Certain high-strength alloys also have anisotropic mechanical properties [119]. Metals are generally less anisotropic than the fiber glass plastics or wood. At the same time, there are known cases of failures in metal parts when the designers do not consider the anisotropy of the metal [22].

Crystals where the shapes of symmetry are varied are distinguished by considerable anisotropy of all the properties. Great advances have therefore been made in crystal physics in investigating the symmetry of structure and the symmetry of physical properties of anisotropic bodies.

The main method of modern crystal physics, the science of symmetry, can be widely employed in the mechanics of anisotropic materials. New potentialities are thus afforded for a study of the mechanical properties of anisotropic bodies and for generalization of their testing results.

The symmetry of crystal bodies is a consequence of their regular internal structure. Therefore, not only the shape but also the properties of crystals are symmetrical.

In crystal physics, the link between the symmetry of the crystal and the symmetry of the physical properties is viewed on the basis of Neumann's principle. According to this principle, the elements of symmetry in a physical property must include the elements of symmetry of the point crystal group. The symmetry of the physical property is generally higher than the symmetry of the crystal structure. An example is the fact that all the characteristics of elastic properties and strength of crystals of any structure have a center of symmetry since neither stresses nor deformations can be altered during inversion. The physical property can generally have natural symmetry. It is manifest regardless of the group of crystal symmetry [52].

The elastic properties of anisotropic construction materials are usually examined based on an analysis of their symmetry [43, 45, 49, 58]. The study of elastic properties views all anisotropic materials, including those with heterogeneous structure (for example, laminated and fibrous), based on the hypothesis of a continuous, homogeneous continuum. /12

Within the limits of the tasks set in this work, this hypothesis refers to all the mechanical properties of anisotropic materials. The specific structural features are not taken into consideration. This permits a study of the laws governing the anisotropy of mechanical properties that are common for a large number of diverse materials.

The necessary premises for such an approach to the problem coincide with the requirements that are usually made for construction materials. They are: first, monolithic nature of the material that is guaranteed, for example, for fiber glass-reinforced plastics, by definite correlations between the properties of the fiber and the binding agent; second, invariability of the mechanical properties of the material with an assigned temperature-velocity regime during a certain time interval that depends on the purpose of the structure; third, the size of the item or sample that is fairly great as compared to the dimensions of the structural elements (the diameter of the glass fiber or the size of the wood cells), and at the same time, is

fairly small so that it could be ignored (for example, curvature of annual wood rings), attributing to it an orthogonal calculated plan of anisotropy.

The application of the hypothesis on the homogeneous continuum to an examination of the strength properties of anisotropic materials of varying structure is only possible as a first approximation with the same degree of accuracy as, for example, the application of the hypothesis on the homogeneous and isotropic elastic medium to polycrystalline steel.

In both cases, these hypotheses are not suitable in studying the true physical essence of the failure of body continuity [66]. This does not prevent us from constructing all the main sectors of a science on the resistance of materials on the second of the mentioned hypotheses.

Further evolution of the mechanics of anisotropic materials will possibly result in a rejection of the continuum hypothesis and its replacement, for example, with ideas on the heterogeneous-periodic medium-structure [66].

For a resolution of the limited task set in this work of studying the anisotropic characteristics of technical strength, the continuum hypothesis is justified since the results of its application are confirmed by practical data.

### 3. Strength Characteristics of Anisotropic Bodies as Tensorial Quantities /15

A general definition of a tensor can be formulated as follows: if for the Cartesian coordinate system we have a set of quantities that are formed during the rotation of coordinate axes according to definite linear laws, then this set defines the tensor whose order (rank) depends on the form of the transformation law.

W. Voigt essentially initiated the view of the strength characteristics of crystals as directed (tensorial) quantities [69]. This view was not developed, however, since a study of the physical features and reasons for a certain type of strength failure dominated further in crystal physics: shear formation, twinning, separation. The law of critical tangential stress was thus established. It defines the beginning of plastic deformation of crystals. The law of critical

normal stress (Zonke's law) was established. It defines their brittle failure [80]. Neither law can answer how the strength characteristics of an anisotropic material change depending on the orientation of the active force. At the same time, this question becomes very urgent when the strength of anisotropic construction materials that are used more extensively in technology is examined.

W. Voigt in his classic work on crystal physics [114] for the first time made a detailed study of almost all the physical properties of crystal bodies. He viewed the characteristics of these properties as directed quantities (vector and tensor). W. Voigt for the first time applied the concept of different order tensors to continuum mechanics. He made especially detailed studies of elastic deformations and elastic constants of crystals [114]. In his vast monograph, W. Voigt only devoted several pages to the strength symmetry of crystals.

W. Voigt notes correctly that the phenomenon of strength deterioration by its nature has a center of symmetry. It can therefore be presented using directed quantities of only an even order. For the first time W. Voigt advanced the hypothesis that the phenomenon of strength deterioration in anisotropic bodies can be described by a fourth order tensor. On this basis, he wrote an equation for the ultimate strength during stretching. Comparison of this equation with the results of the incomplete experiments of Zonke led W. Voigt to the conclusion that the fourth order of the tensor is not sufficient to describe the phenomenon of strength deterioration. The higher sixth order is too complicated. Zonke's experiments, whose results are cited by W. Voigt, consisted of stretching variously oriented prismatic square-section samples made of rock salt crystals. The experiments were very incomplete since the crystals apparently had structural defects or inclusions that had little effect on the amount of elastic deformation, but resulted in considerable scattering of the results from determining the strength characteristics of the samples. W. Voigt limited himself to this in examining the quantitative aspect of crystal strength. /16

The current state of technology requires an examination of a broader class of anisotropic media. It is essentially necessary for many anisotropic construction materials to obtain general laws that express

their strength characteristics depending on the orientation of stresses and on the symmetry of the medium. This circumstance determines the need to return to W. Voigt's hypothesis regarding the existence of a strength tensor.

We introduce the term tensoriality here in the sense that a change in the technical strength characteristics of anisotropic bodies, depending on the orientation of stresses in the material, is approximated by transformation formulas of the tensor components during rotation of the coordinate axes. The suitability of this hypothesis can be verified by its correspondence to the results of an experimental study of strength of different anisotropic materials.

In passing to a substantiation of the order of the strength tensor, it is necessary to take into consideration that the phenomenon has a symmetry center. It can therefore be described not only by a fourth order tensor. The second order tensor used, for example, in the work of Ya. B. Fridman and Ye. M. Morozov [73] could be the most convenient and simplest tensor for this purpose.

We will investigate whether the second order tensor can be considered suitable to describe the phenomenon of strength deterioration of anisotropic bodies.

In a three-dimensional space, the symmetry of any property of an anisotropic continuum (and consequently, the order of the corresponding tensor) can be studied by analyzing the symmetry of the geometric figure (surface) that depicts the change in the quantities that determine this property when the direction in this medium changes.

The surface that is called characteristic [52] or directive [58] can be used for a graphic presentation of the amount of resistance to stretching. Depending on the order of this surface, it will have a certain appearance for the material with definite symmetry. For an isotropic material, the characteristic surface of strength, regardless of its order, must, of course, become spherical.

/17

If axes of symmetry of an orthotropic body  $x_1$ ,  $x_2$  and  $x_3$  are selected as the coordinate axes, then each point of the characteristic surface will be separated from the beginning of the coordinates by the quantity of the radius-vector  $r$ , while its projection on the coordinate

axis is determined from the expressions

$$\left. \begin{aligned} x_1 &= rC_{11} \\ x_2 &= rC_{12} \\ x_3 &= rC_{13} \end{aligned} \right\} \quad (1.8)$$

where  $C_{ik}$ --direction cosines of vector  $r$  that is superposed with the axis  $x_i'$  during rotation of the coordinates.

Rotation of the coordinate axes is determined by the cosine scheme

$$\begin{array}{cccc} & x_1 & x_2 & x_3 \\ x_1' & C_{11} & C_{12} & C_{13} \\ x_2' & C_{21} & C_{22} & C_{23} \\ x_3' & C_{31} & C_{32} & C_{33} \end{array}$$

The assumption on the second order tensor means that when the coordinate axes turn, the change in the amount of resistance of the orthotropic material, for example to stretching, must occur according to the law

$$a_{1'1'} = \sum_{i=1}^3 \sum_{k=1}^3 a_{ik} C_{1i} C_{1k}, \quad (1.9)$$

where  $a_{i'i'}$ --a quantity linked to the material resistance in direction of the axis  $x_i'$ , i.e., in the direction of the vector radius;  
 $a_{ik}$ --the same quantities in the direction of the material symmetry axes.

After substituting an expression for the direction cosines from (1.8) and after developing formula (1.9), we obtain:

$$a_{1'1'} r^2 = a_{11} x_1^2 + a_{22} x_2^2 + a_{33} x_3^2,$$

or, after assuming  $r = \frac{1}{\sqrt{a_{1'1'}}}$ , we arrive at the equation for the

characteristic surface of second order in the following form:

$$a_{11} x_1^2 + a_{22} x_2^2 + a_{33} x_3^2 = 1. \quad (1.10)$$

The second order surface (1.10) can meet complete isotropy (be turned into a sphere) with the unique condition

$$a_{11} = a_{22} = a_{33}.$$

Thus, the assumption on the second order of the characteristic surface that follows from the second rank of the resistance tensor, leads to the following conclusion. If there is a known orthotropic material whose quantity of the strength characteristic during stretching is the same in the direction of the symmetry axes  $x_1$ ,  $x_2$  and  $x_3$ , then this material must have complete isotropy of resistance.

However, in the case of a planar problem, the experimental data on rupture strength for such an orthotropic sheet material as, for example, SVAM with fiber ratio 1:1 [12], metal alloys [119] or DSP-V [19] show that even when the ultimate strengths are equal in two main directions ( $\sigma_0 = \sigma_{90}$  or  $a_{11} = a_{22}$ ), the curve of ultimate strengths in the sheet plane does not become a circle since the ultimate strength in the intermediate (most often diagonal) direction is considerably lower than in the main direction:  $\sigma_{45} < \sigma_0$ , i.e., the intersection track of the characteristic surface with the sheet plane does not produce a circle (see the detailed experimental data in chapter III).

The order of the surface must thus be higher than the second.

We will study the nearest even order, the fourth.

It is known that the spatial figures that depict, for example, the dependence of the elasticity modulus  $E$  of an orthotropic material on the stress orientation, are restricted to a fourth order.

The work of A. L. Rabinovich [58] presents the equations for the directive surface and the directive curve of the  $E$  modulus.

The external appearance of the spatial figures that depict the change in the strength characteristics of the orthotropic bodies depending on the orientation of stresses in the material is analogous to the external appearance of the figures that depict the change in the characteristics of the elastic properties of these same materials ([5], section 12).

It is impossible to understand the analogy between the aforementioned spatial figures as a simple proportionality between the corresponding characteristics of strength and elasticity.

The following ratio that is suggested, for example, in the work of N. T. Smotrin and V. M. Chebanov [67]

$$\frac{\sigma_0}{E_0} = \frac{\sigma_{90}}{E_{90}}$$



is not fulfilled even for wood. For pine, the ultimate strength during compression in a tangential direction tranverse to the fibers is higher than in a radial direction. The modulus of elasticity E in the tangential direction is lower than in the radial.

The analogy of the external appearance of the figures for the change in strength characteristics and the characteristics of elastic properties makes it possible to only hypothesize the same tensor rank to describe these quantities. /19

We will show that the assumption regarding the fourth tensor rank of resistances results in the fourth order of the characteristic surface, for example, for resistances to stretching.

The assumption on the fourth order of the resistance tensor means that when the coordinate axes turn, the change in the amount of resistance to stretching should occur according to the law

$$a_{1'1'1'1'} = \sum_{i=1}^3 \sum_{k=1}^3 \sum_{l=1}^3 \sum_{p=1}^3 a_{iklp} C_{1i} C_{1k} C_{1l} C_{1p} =$$

$$= a_{1111} C_{11}^4 + a_{2222} C_{12}^4 + a_{3333} C_{13}^4 + K_{12} C_{11}^2 C_{12}^2 + K_{23} C_{12}^2 C_{13}^2 + K_{31} C_{13}^2 C_{11}^2,$$

or [see formula (1.8)]

$$a_{1'1'1'1'} r^4 = a_{1111} x_1^4 + a_{2222} x_2^4 + a_{3333} x_3^4 + K_{12} x_1^2 x_2^2 + K_{23} x_2^2 x_3^2 + K_{31} x_3^2 x_1^2 ;$$

after taking  $r = \frac{1}{\sqrt{a_{1'1'1'1'}}}$ , we obtain an equation for the charac-

teristic surface of the fourth order in axes of symmetry of the material

$$a_{1111} x_1^4 + a_{2222} x_2^4 + a_{3333} x_3^4 + K_{12} x_1^2 x_2^2 + K_{23} x_2^2 x_3^2 + K_{31} x_3^2 x_1^2 = 1. \quad (1.11)$$

The coefficients  $a_{ikop}$  in these equations depend on the quantities of the strength characteristics of the material during stretching in the direction of the axis of symmetry. The uneven coordinate orders drop out on the condition of the orthogonal symmetry of the material.

The fourth order surface (1.11) on the condition that  $a_{1111} = a_{2222} = a_{3333}$  still does not depict a spherical surface, i.e., does not result in the conclusion that the material is isotropic.

It is also necessary that

$$2a_{1111} = K_{12} = K_{23} = K_{31}$$

only then will equation (1.11) adopt the appearance

$$x_1^2 + x_2^2 + x_3^2 = \frac{1}{V a_{1111}},$$

i.e., will correspond to the case of complete isotropy and be depicted by a spherical surface.

Thus, the assumption on the fourth order of the characteristic surface corresponds to that feature of change in the strength characteristic that even when the quantities of resistance are equal in the direction of the three symmetry axes, these figures are not transformed into a sphere and do not comply with the isotropy of the material. The characteristic surfaces of elastic constants (for example, elasticity modulus of an orthotropic body) naturally possess the same property.

The spatial figures for the change in strength and elastic properties are analogous in the sense that both of them are fourth order surfaces. Equation (1.11) for orthotropic materials can be equally adopted as the characteristic surface to describe the change in the characteristics of the elastic and strength properties during stretching. /20

We will show that the fourth order of the algebraic surface that can be used to present a geometrical spatial figure, really conforms to the fourth rank of the tensor compiled from the equation coefficients of this surface. Then the same rank of the tensor will follow from the same order of the equation of directive surfaces.

The works of Academician A. V. Shubnikov demonstrated that the symmetry operations of a three-dimensional figure can be viewed as affine orthogonal transformations of the point coordinate of the figure.

Here certain operations of symmetry for flat figures (rotation by 180° around an axis that lies in the figure plane) make it necessary to solve the problem in a three-dimensional space, although as a result of the operation, the figure remains in its plane.

Generalization of the symmetry operations for a three-dimensional space (negative operation of antisymmetry) also requires a formal examination in a higher, four-dimensional space.

The equation for the fourth order surface that was previously

written in the symmetry axes (1.11), can be written in a more general form in the four-dimensional space

$$\sum_{i=1}^3 \sum_{k=1}^3 \sum_{o=1}^3 \sum_{p=1}^3 a_{ikop} x_i x_k x_o x_p = 1. \quad (1.12)$$

Here the fourth coordinate is formally introduced. It is assumed that all four coordinates are transformed when the coordinate axes rotate according to the standard formulas of affine orthogonal transformation

$$\begin{aligned} x_i &= \sum_{l=1}^3 x_l C_{l'i} \\ C_{l'i} &= \frac{\partial x_{l'}}{\partial x_i}. \end{aligned} \quad (1.13)$$

Each of the four coordinates can be viewed (with a change in the index from 1 to 3) as a square Cartesian coordinate. The rotation of the Cartesian coordinate system is determined by the cosine table given above. By substituting (1.13) into (1.12) we obtain

$$\begin{aligned} \sum_{i=1}^3 \sum_{k=1}^3 \sum_{o=1}^3 \sum_{p=1}^3 \sum_{i'=1}^3 \sum_{k'=1}^3 \sum_{o'=1}^3 \sum_{p'=1}^3 a_{ikop} C_{i'i} C_{k'k} C_{o'o} C_{p'p} x_{i'} x_{k'} x_{o'} x_{p'} &= \\ &= \sum_{i'=1}^3 \sum_{k'=1}^3 \sum_{o'=1}^3 \sum_{p'=1}^3 a_{i'k'o'p'} x_{i'} x_{k'} x_{o'} x_{p'} \\ a_{i'k'o'p'} &= \sum_{i=1}^3 \sum_{k=1}^3 \sum_{o=1}^3 \sum_{p=1}^3 a_{ikop} C_{i'i} C_{k'k} C_{o'o} C_{p'p}. \end{aligned} \quad (1.14)$$

Formula (1.14) makes it possible to assert that the algebraic coefficients of a uniform polynomial of the fourth degree (1.11) are actually transformed when the coordinate axes turn as components of the fourth order tensor.

Equation (1.14) can be written in a more general appearance as

$$a_{i'k'o'p'} = \sum_{i=1}^3 \sum_{k=1}^3 \sum_{o=1}^3 \sum_{p=1}^3 a_{ikop} \frac{\partial x_{i'}}{\partial x_i} \frac{\partial x_{k'}}{\partial x_k} \frac{\partial x_{o'}}{\partial x_o} \frac{\partial x_{p'}}{\partial x_p}. \quad (1.15)$$

This is also a general definition of the tensor of fourth rank (order, valency) in a three-dimensional Euclidean space [26].

Thus, the same order of surfaces that in a three-dimensional space depicts a change in the characteristics of elastic and strength properties of orthotropic bodies, makes it possible to assert that the

rank of the corresponding tensors must also be the same, i.e., fourth.

The same rank of the tensor of elasticity and the tensor of ultimate resistances with the same nature of symmetry of the corresponding surfaces results in an assumption regarding the same physical dimensionality of the components of both tensors, i.e., to a hypothesis that in formula (1.14) the value  $a$  is inversely proportional to the value of the ultimate resistance  $\sigma_{ikop} = \sigma_b$ , taken in the first degree

$$a_{ikop} = \frac{1}{\sigma_{ikp}}. \quad (1.16)$$

The assumption advanced in this paragraph about the possibility of examining the ultimate resistances of the anisotropic bodies as components of the fourth order tensor is experimentally verified later in chapter III. The results of mechanical tests on different anisotropic materials are compared in chapter III with formula (1.14). It can be viewed as a definition of the fourth order tensor.

We will pass to a detailed study of this formula.

#### 4. Study of the Components of the Strength Tensor of Orthotropic Material

/22

A change in mechanical properties depending on the direction in orthotropic material can be graphically illustrated by a certain symmetrical figure. Assume that the figure (characteristic surface) that illustrates the strength properties (ultimate resistances) of the orthogonally-anisotropic material is classified as a square coordinate system  $x_1, x_2$  and  $x_3$ . Its origin coincides with the center of the figure. We will replace this system with a new coordinate system,  $x_1', x_2'$  and  $x_3'$ , leaving the origin of the coordinates in place, and only turning the axis. We are only interested in the mutual arrangement of the figure and the coordinate system. The rotation of the axes therefore yields the same results as rotation of the figure itself when the coordinate system is fixed. The formulas for transformation of the coordinates during axis rotation can be used to compute the resistance of the examined material depending on the direction.

The formulas for transformation of the point coordinates of the figure contain angle cosines between the new and old directions of the

axes that can be designated, for example, by the letter C with two indices. Assume that the first corresponds to the number of the new, turned axis, and the second to the number of the old axis. For example,

$$C_{13} = \cos(x'_1, x_3).$$

The cosines of the angles during the rotation of the coordinate axes are completely presented in the scheme (p. 15, section 3).

The transformation formulas for the equation coefficients of the characteristic surface during rotation of the coordinate axes can be constructed in different ways. They can contain derivatives of two, three or a greater number of cosines depending on the nature of the surface that complies with certain properties of the material, on the nature of these properties, or in other words, on the order of the tensor that corresponds to the examined property of the anisotropic material.

We substantiated above the assumption on the fourth order of the tensor of ultimate resistances. According to this hypothesis, the transformation formulas of the equation coefficients for the characteristic surface of the strength properties, and consequently, the formulas to compute the resistances in different directions must contain derivatives of four direction cosines.

The components of the fourth order tensor in a three-dimensional space change when the coordinate axes rotate according to the law expressed by formula (1.14). Here  $a_{ikop}$  is the quantity of the component that is assigned in the initial (main) coordinate system,  $a_{i'k'o'p}$  is its quantity after axial rotation;  $i, k, o$  and  $p$  are the numbers of the old axes, while  $i', k', o'$  and  $p'$  are the numbers of the same axes after their rotation. Each of the four letters can adopt a value from one to three.

/23

When reflected in the symmetry plane, the components of the strength tensor of the orthogonally anisotropic material must not change their quantities. This reflection is equivalent [79] to transformation of coordinates according to one of the following three schemes of direction cosines

1)	$x_1$	$x_2$	$x_3$	2)	$x_1$	$x_2$	$x_3$	3)	$x_1$	$x_2$	$x_3$
$x_1'$	1	0	0	$x_1'$	1	0	0	$x_1'$	-1	0	0
$x_2'$	0	-1	0	$x_2'$	0	1	0	$x_2'$	0	1	0
$x_3'$	0	0	1	$x_3'$	0	0	-1	$x_3'$	0	0	1

It is assumed in the first scheme that the symmetry plane is the plane  $x_1x_3$ , in the second,  $x_1x_2$ , and in the third,  $x_2x_3$ . The existence of three symmetry planes (i.e., orthogonal anisotropy of the material) requires that the substitution of the cosines from these three schemes into formula (1.14) does not change the quantities of the components.

This condition is only fulfilled with the transformation of such components  $a_{ikop}$  where either all four signs are the same, or the signs are equal in pairs since in this case, the negative unit will enter the product of cosines in the square, and the sign of the corresponding component does not change. Consequently, the condition for symmetry will be fulfilled. Thus, in the main axes of symmetry, the strength tensor (asymmetrical) can have not  $3^4=81$ , but only 21 components that differ from zero, including three main components where all four indices are the same. Table 1.1 records the strength tensor in a general appearance in the symmetry axes of an orthotropic material.

In this table, the tensor is assumed to be asymmetrical, i.e., no additional assumptions are introduced on the equality of any of its components.

The main components of the tensor are defined in a three-dimensional space by the three quantities of direction cosines, i.e., one direction. They are therefore suitable to present the quantities of the strength characteristics in uniaxial stresses (stretching or compression).

Orientation of a tangential stress in space, and consequently, the ultimate strength corresponding to this stress, cannot be assigned by three direction cosines (one direction in space), therefore the tensor components that have four equal indices are not suitable for presentation of these quantities. /24

Strength in relation to the tangential stresses must be linked to two directions: one direction must determine the position of the tangential stress action area (this can be, for example, the direction

of the perpendicular to the area). The other must determine the direction of the action of the tangential stress itself on this area.

By analogy with the tensor of characteristics for elastic properties, we will assume that the components of the fourth rank tensor conform to pure shear. These components are arranged on the main diagonal of the matrix and have equal indices in pairs

$$a_{ikik} = \frac{1}{4\tau_{ikik}}, \quad (1.17)$$

where  $\tau_{ikik} = \tau_b$  -- ultimate strength of material during pure shear.

TABLE 1.1. STRENGTH TENSOR (ASYMMETRICAL) IN SYMMETRY AXES OF ORTHOTROPIC MATERIAL

	11	22	33	12	21	13	31	23	32
11	$a_{1111}$	$a_{2211}$	$a_{3311}$	0	0	0	0	0	0
22	$a_{1122}$	$a_{2222}$	$a_{3322}$	0	0	0	0	0	0
33	$a_{1133}$	$a_{2233}$	$a_{3333}$	0	0	0	0	0	0
12	0	0	0	$a_{1212}$	$a_{2112}$	0	0	0	0
21	0	0	0	$a_{1221}$	$a_{2121}$	0	0	0	0
13	0	0	0	0	0	$a_{1313}$	$a_{3113}$	0	0
31	0	0	0	0	0	$a_{1331}$	$a_{3131}$	0	0
23	0	0	0	0	0	0	0	$a_{2323}$	$a_{3223}$
32	0	0	0	0	0	0	0	$a_{2332}$	$a_{3232}$

Two different approaches are possible to examining the resistance to the tangential stresses (shear, shearing, pure shear). In one case one can start from the direct testing results. They generally do not successfully create a homogeneous stress of pure shear, and the quantity of resistance to the tangential stresses on two mutually perpendicular areas varies.

Thus, for example, the resistance to shearing along the fibers for wood is always considerably lower than the resistance to cross-cutting of the fibers, although the same tangential stresses are active in mutually perpendicular areas in the corresponding samples used to determine the quantity of these two resistances.

This approach results in an asymmetrical strength tensor and in formulas that are derived in publication [5].

Another approach complies with the classic method of viewing the theory of elasticity and plasticity. It requires symmetry of the strength tensor. Here, if there are no direct experiments,

we have to consider that under conditions of pure shear, the resistance of the material to tangential stresses on two mutually perpendicular areas is determined by the least of the two quantities that were obtained experimentally in a test for shear on these two areas. The appropriate formulas are somewhat simpler than in the first approach. They are presented below.

By convoluting the tensor (1.14), we obtain the following invariant:

$$I = \sum_{i=1}^3 \sum_{k=1}^3 a_{ikkk} = a_{1111} + a_{2222} + a_{3333} + 2a_{1122} + 2a_{2233} + 2a_{3311}.$$

After a  $45^\circ$  turn of the coordinate system around the axis "3", i.e., z, and taking formula (1.14) into consideration, we obtain

$$a_{1122} = \frac{1}{2} [4a_{1'1'1'1'}^{45} - a_{1111} - a_{2222} - 4a_{1212}].$$

or, by bearing (1.16) and (1.17) in mind,

$$a_{1122} = \frac{1}{2} \left[ \frac{4}{\sigma_{45}} - \frac{1}{\sigma_0} - \frac{1}{\sigma_{90}} - \frac{1}{\tau_0} \right]_{xy}, \quad (1.18)$$

where  $\sigma_{45} = \sigma_{1'1'1'1'}^{45}$  -- ultimate strength during stretching in a direction that lies in the symmetry plane xy and comprises a  $45^\circ$  angle with the x axis;  $\sigma_0 = \sigma_{1111}$  and  $\sigma_{90} = \sigma_{2222}$  -- ultimate strengths during stretching in a direction of the symmetry axes of the material x and y;  $\tau_0 = \tau_{1212}$  -- ultimate strength in pure shear in the same plane by tangential stresses that act in parallel to the x and y axes.

We obtain from formula (1.14)

$$4a_{1'2'1'2'}^{45} = a_{1111} + a_{2222} - 2a_{1122},$$

from which

$$2a_{1122} = a_{1111} + a_{2222} - 4a_{1'2'1'2'}^{45}, \quad (1.19)$$

or

$$a_{1122} = \frac{1}{2} \left[ \frac{1}{\sigma_0} + \frac{1}{\sigma_{90}} - \frac{1}{\sigma_{45}} \right]_{xy}.$$

Thus, the strength tensor can be presented in the developed form given in tables 1.2 and 1.3.



TABLE 1.2. SYMMETRICAL TENSOR OF STRENGTH FOR ORTHOTROPIC MATERIAL

/26

	11	22	33	12	23	31
11	$\frac{1}{\sigma_A^0}$	$\frac{1}{2} \left[ \frac{1}{\sigma_{11}} + \frac{1}{\sigma_{22}} - \frac{1}{\tau_{45}} \right]_{xy}$	$\frac{1}{2} \left[ \frac{1}{\sigma_{11}} + \frac{1}{\sigma_{33}} - \frac{1}{\tau_{45}} \right]_{xz}$	0	0	0
22	$\frac{1}{2} \left[ \frac{1}{\sigma_{11}} + \frac{1}{\sigma_{22}} - \frac{1}{\tau_{45}} \right]_{xy}$	$\frac{1}{\sigma_y^0}$	$\frac{1}{2} \left[ \frac{1}{\sigma_{11}} + \frac{1}{\sigma_{22}} - \frac{1}{\tau_{45}} \right]_{yz}$	0	0	0
33	$\frac{1}{2} \left[ \frac{1}{\sigma_{11}} + \frac{1}{\sigma_{22}} - \frac{1}{\tau_{45}} \right]_{xz}$	$\frac{1}{2} \left[ \frac{1}{\sigma_{11}} + \frac{1}{\sigma_{33}} - \frac{1}{\tau_{45}} \right]_{yz}$	$\frac{1}{\sigma_z^0}$	0	0	0
12	0	0	0	$\frac{1}{\tau_{xy}^0}$	0	0
23	0	0	0	0	$\frac{1}{\tau_{yz}^0}$	0
31	0	0	0	0	0	$\frac{1}{\tau_{zx}^0}$

TABLE 1.3. SYMMETRICAL TENSOR OF STRENGTH FOR ORTHOTROPIC MATERIAL

/27

	11	22	33	12	23	31
11	$\frac{1}{\sigma_A^0}$	$\frac{1}{2} \left[ \frac{4}{\sigma_{45}} + \frac{1}{\sigma_{11}} + \frac{1}{\sigma_{22}} - \frac{1}{\tau_{11}} \right]_{xy}$	$\frac{1}{2} \left[ \frac{4}{\sigma_{45}} + \frac{1}{\sigma_{11}} + \frac{1}{\sigma_{33}} - \frac{1}{\tau_{11}} \right]_{xz}$	0	0	0
22	$\frac{1}{2} \left[ \frac{4}{\sigma_{45}} + \frac{1}{\sigma_{11}} + \frac{1}{\sigma_{22}} - \frac{1}{\tau_{11}} \right]_{xy}$	$\frac{1}{\sigma_y^0}$	$\frac{1}{2} \left[ \frac{4}{\sigma_{45}} + \frac{1}{\sigma_{11}} + \frac{1}{\sigma_{33}} - \frac{1}{\tau_{11}} \right]_{yz}$	0	0	0
33	$\frac{1}{2} \left[ \frac{4}{\sigma_{45}} + \frac{1}{\sigma_{11}} + \frac{1}{\sigma_{22}} - \frac{1}{\tau_{11}} \right]_{xz}$	$\frac{1}{2} \left[ \frac{4}{\sigma_{45}} + \frac{1}{\sigma_{11}} + \frac{1}{\sigma_{33}} - \frac{1}{\tau_{11}} \right]_{yz}$	$\frac{1}{\sigma_z^0}$	0	0	0
12	0	0	0	$\frac{1}{\tau_{xy}^0}$	0	0
23	0	0	0	0	$\frac{1}{\tau_{yz}^0}$	0
31	0	0	0	0	0	$\frac{1}{\tau_{zx}^0}$

In tables 1.2 and 1.3,  $\sigma_0$ ,  $\sigma_{90}$  and  $\sigma_{45}$  are the ultimate strengths in the symmetry plane that is designated by the indices in brackets

$[\sigma_0]_{xy} = \sigma_x^0$ , the main axes  $x, y, z$ .

If the anisotropic material resists stretching and compression in different ways, then the strength tensor should be written twice, separately for stretching (then  $\sigma_x^0$ ,  $\sigma_y^0$  and  $\sigma_z^0$  -- resistances during stretching) and separately for compression.

After developing equation (1.14), we obtain tensorial formulas (1.20) and (1.21) to compute the strength characteristics during stretching (compression) and during pure shear. They are randomly oriented in an orthotropic body. Here the following simpler designation is adopted for the axes and the direction cosines:

$$\begin{array}{ccc} x & y & z \\ x' & n_1 & l_1 & m_1 \\ y' & n_2 & l_2 & m_2 \\ z' & n_3 & l_3 & m_3 \end{array}$$

$$\begin{aligned} \frac{1}{\sigma_b} = & \frac{n_1^4}{\sigma_x^0} + \frac{l_1^4}{\sigma_y^0} + \frac{m_1^4}{\sigma_z^0} + \left( \frac{4}{\sigma_{xy}^{45}} - \frac{1}{\sigma_x^0} - \frac{1}{\sigma_y^0} \right) n_1^2 l_1^2 + \\ & + \left( \frac{4}{\sigma_{yz}^{45}} - \frac{1}{\sigma_y^0} - \frac{1}{\sigma_z^0} \right) l_1^2 m_1^2 + \left( \frac{4}{\sigma_{zx}^{45}} - \frac{1}{\sigma_z^0} - \frac{1}{\sigma_x^0} \right) m_1^2 n_1^2; \end{aligned} \quad (1.20)$$

$$\begin{aligned} \frac{1}{\tau_b} = & \frac{1}{\tau_{xy}^0} (n_1 l_2 + l_1 n_2)^2 + \frac{1}{\tau_{yz}^0} (l_1 m_2 + m_1 l_2)^2 + \frac{1}{\tau_{zx}^0} (m_1 n_2 + n_1 m_2)^2 + \\ & + \frac{4 n_1 l_1 n_2 l_2}{\tau_{xy}^{45}} + \frac{4 l_1 m_1 l_2 m_2}{\tau_{yz}^{45}} + \frac{4 m_1 n_1 n_2 m_2}{\tau_{zx}^{45}}. \end{aligned} \quad (1.21)$$

For sheet, orthogonally anisotropic material in the case of a planar problem we obtain

$$\sigma_b = \frac{\sigma_0}{\cos^4 \alpha + b \sin^2 2\alpha + c \sin^4 \alpha}, \quad (1.22)$$

where

$$b = \frac{\sigma_0}{\sigma_{45}} - \frac{1+c}{4}; \quad c = \frac{\sigma_0}{\sigma_{90}}.$$

During pure shear in the plane of a sheet perpendicular to the  $z$  axis, i.e., for the planar problem

$$\tau_b = \frac{1}{\frac{\cos^2 2\alpha}{\tau_0} + \frac{\sin^2 2\alpha}{\tau_{45}}} \quad (1.23)$$

Publication [5] has obtained a formula to compute the ultimate strength  $\tau_b$  during shear on an area with perpendicular  $x'$ , and tangential stress active in the direction of the  $y'$  axis. It can be written in the following form:

$$\tau_b = \frac{\tau_0}{\cos^4 \alpha + c_1 \sin^2 2\alpha + c_2 \sin^4 \alpha} \quad (1.24)$$

where

$$c_1 = \frac{\tau_0}{\tau_{90}}; \quad c_2 = \frac{\tau_0}{\tau_{45}} - \frac{1 + c_1}{4}.$$

Formula (1.24) conforms to those three cases of rotation of the shear area around the symmetry axis in which the direction of the  $x'$  perpendicular to the shear area, and the direction of the tangential stresses  $y'$  remain perpendicular to this axis.

In this case, it is necessary to experimentally define the three quantities of resistance to shear:  $\tau_0, \tau_{90}$  and  $\tau_{45}$  (1.24) or the two quantities of resistance to pure shear  $\tau_0$  and  $\tau_{45}$  (1.23).

All the remaining possible cases of orientation of shear resistance  $\tau_b$  in which even one axis ( $x', y'$  or  $z'$ ) coincides with the symmetry axis of the material, do not depend on the amount of resistance  $\tau_{45}$  on the diagonal areas. They are computed according to the formula

$$\tau_b = \frac{1}{\frac{\cos^2 \alpha}{\tau_0} + \frac{\sin^2 \alpha}{\tau_{90}}} \quad (1.25)$$

Resistance to pure shear in these cases of rotation of the tangential stress area must not be changed.\*

For wood, the latter formula complies with the essentially important case of shearing in different directions on areas that are parallel to the fibers.

\*Figure 3.35 for fiber glass-reinforced plastic gives experimental confirmation of the correctness of this hypothesis: the ultimate shear strength perpendicular to the sheet plane practically does not depend on the orientation of the shear area in relation to the glass fiber.

If one hypothesizes that  $\tau_0$  is the resistance to shear along the fibers, while  $\tau_{90}$  is the resistance to shear transverse to the fibers, then formula (1.25) coincides with the empirical formula accepted to compute the shear resistance of wood at angle  $\alpha$  to the fibers. It is given in NiTU 122-55 ("Standards and Specifications for Planning Wood Designs," 1955).\*

Particular cases of applying the general formula (1.21) for fiber glass-reinforced plastics and other sheet orthotropic materials are shown in figure 1.1. /30

The hypothesis advanced by W. Voigt regarding the possible sixth order of the strength tensor can be studied by the same simple method.

The total number of components of the sixth order strength tensor in random axes will be  $3^6=729$ . For the orthotropic material in the symmetry axes, 147 components of the sixth order tensor will differ from zero.

From the general formula for transformation of the sixth order tensor components in a three-dimensional space, during rotation of the coordinate axes the following particular formula is obtained to compute the component with six identical indices under conditions of a planar problem

$$\tau_\theta = \frac{\tau_0}{\cos^6 \alpha - b_0 \sin^2 2\alpha - c \sin^6 \alpha}, \quad (1.26)$$

where, as before  $c = \frac{\tau_0}{\tau_{90}}$ ;

$$b_0 = \frac{\tau_0}{\tau_{45}} - \frac{1+c}{8}.$$

Thus, in this hypothesis, the formula is analogous to that in the hypothesis on the fourth order of the strength tensor. It is distinguished only by a higher (sixth) degree of the cosines and sines. /31

Figure 1.2 a and b present the curves for a change in the ultimate resistance during stretching and compression. They were plotted for plywood and fiber glass-reinforced plastics according to formula (1.22) and formula (1.26). The average values for the ultimate resistances according to experimental data are also designated on this figure.

Comparison of the curves with the experimental data show that the assumption about the sixth order of the strength tensor results in

\*The 1962 standards cite this same formula with exponent of 3 not 2 of the trigonometric functions (see section 1 and SNiP II-V.4-62).

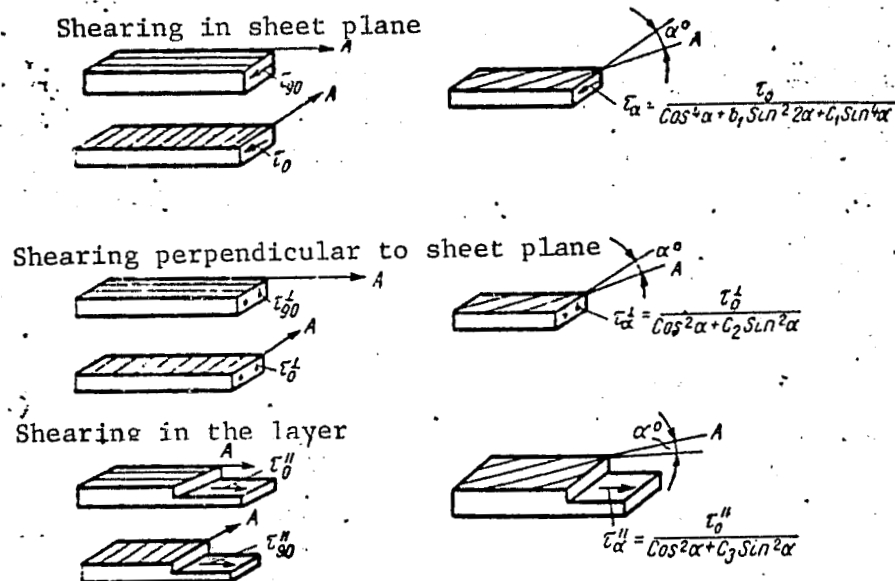


Figure 1.1. Schematic Illustration of Effect of Tangential Stresses with Different Types of Testing for Sheet Orthotropic Materials for Shear and Shearing:

$$b_1 = \frac{\tau_0}{\tau_{45}} - \frac{C_1 + 1}{4}; \quad C_1 = \frac{\tau_0}{\tau_{90}}; \quad C_2 = \frac{\tau_0^\perp}{\tau_{90}^\perp}; \quad C_3 = \frac{\tau_0''}{\tau_{90}''};$$

A--direction of fibers (axis of symmetry of material).

more complicated computations. It does not have any advantages as compared to the assumption on the fourth order of this tensor.

##### 5. Strength Tensor of Fourth Order for Transversely Isotropic Material

Plates are sometimes made of a wood veneer sheet [40, 100, 102] and of laminated fiber glass sheet [87] in which the fibers in the adjacent layers are turned towards each other at a certain angle that is smaller than a right angle. In this case the laminated material on the whole has a "stellar" structure [12]. In the majority of cases, the fibers in the fiber glass-reinforced plastic sheets are oriented in three directions at an angle of  $\alpha_0 = 60^\circ$  to each other [87]. The aviation plywood F-60 studied in publication [40] is the same. Wood plastic DSP-G is popularly used to make pistons, bushings, friction pulleys and other similar parts. The direction of fibers in the adjacent layers of the veneer sheet comprise the angle  $\alpha_0 = 30^\circ$  [19].

Laminated splint-slab sheets with oriented direction of the fibers in the layers are also made as "stellar" with  $\alpha_0 = 60^\circ$ . Keywerth [100] found that the moduli of elasticity and strength of these sheets during pure shear are higher than for sheets with the same orientation of fibers over the entire thickness.

We will examine the shape of the symmetrical strength tensor for a "stellar" sheet material, assuming that the directions of the fibers  $x_1$ ,  $x_1'$  and  $x_2'$  (fig. 1.3) are equivalent directions. They can be superposed with each other by rotation at angle  $\alpha_0 = 60^\circ = \frac{2\pi}{6}$  around the axis  $x_3$ , perpendicular to the sheet plane.

The  $x_3$  axis is thus considered to be the axis of symmetry of the sixth order. After rotation of the system of coordinate axes at angle  $\frac{2\pi}{6}$  around the axis  $x_3$ , all the components of the strength tensor must preserve their values. /33

We will use the letters  $x_1$ ,  $x_1'$  and  $x_2'$  to designate the directions of fiber arrangement (fig. 1.3,a). We will rotate the coordinate system around the axis  $x_3$  perpendicular to the drawing, by angle  $\alpha_0 = 60^\circ$ . From the general formula for transformation of the strength tensor components (1.14) in this case we obtain the following expression for the component  $a_{1'1'1'1'}$  in relation to the axis  $x_1'$

$$a_{1'1'1'1'} = C_{1'1}^4 a_{1111} + C_{1'2}^4 a_{2222} - 2C_{1'1}^2 C_{1'2}^2 R_{12},$$

or with  $\alpha_0 = 60^\circ$

$$a_{1'1'1'1'} = \frac{1}{16} a_{1111} + \frac{9}{16} a_{2222} + \frac{3}{16} (a_{1122} + a_{2211} + a_{1212} + a_{2121} + a_{1221} + a_{2112}).$$

If we hypothesize that  $a_{1'1'1'1'} = a_{1111}$  by equivalency of directions  $x_1'$  and  $x_1$ , then

$$15a_{1111} = 9a_{2222} + 2R_{12}, \quad (1.27)$$

where

$$2R_{12} = a_{1122} + a_{2211} + a_{1212} + a_{2121} + a_{1221} + a_{2112} = 2a_{1122} + 4a_{1212}.$$

The formula for transformation of the component  $a_{2'2'2'2'}$  on the condition of equivalency of the directions  $x_2'$  and  $x_1$ , i.e., with  $a_{2'2'2'2'} = a_{1111}$ , will yield

/34

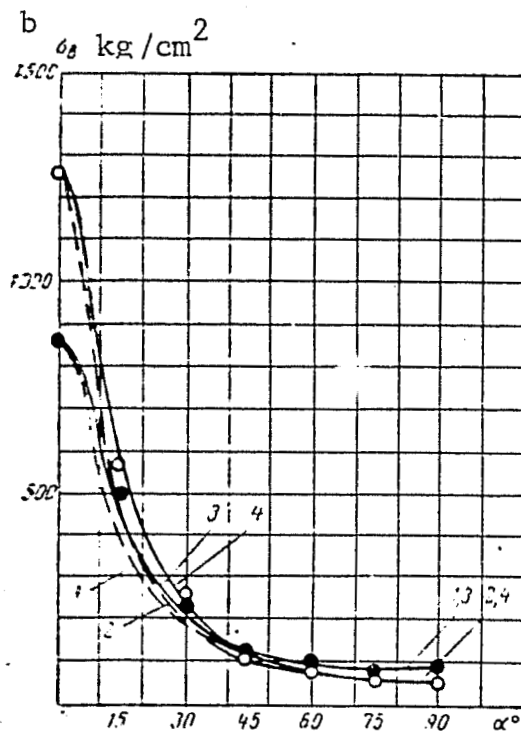
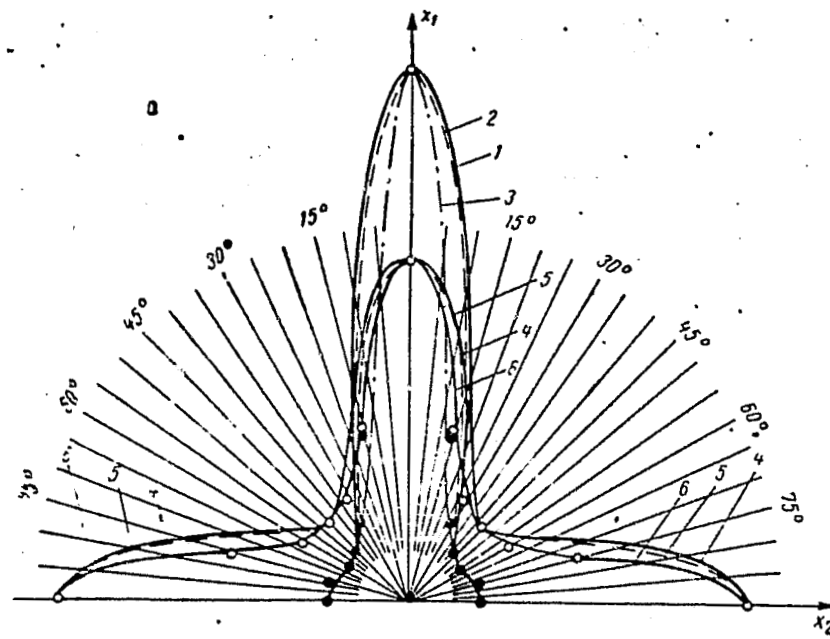


Figure 1.2. Comparison of Results of Testing Two Anisotropic Materials with Curves Constructed by Different Formulas: a--fiber glass-reinforced plastic SVAM on epoxy-phenol binding agent: curves 1,2 and 3 constructed for SVAM with fiber ratio 1:13; curves 4,5 and 6--with fiber ratio 1:1; curves 1 and 4 constructed according to formula (1.22), 2 and 5--according to formula (4.10) (see chapter IV, section 16); b--parallel plywood: curves 1 and 3 constructed for compression; 2 and 4--for stretching; 1 and 2--according to formula (1.26); 3 and 4--according to formula (1.22).

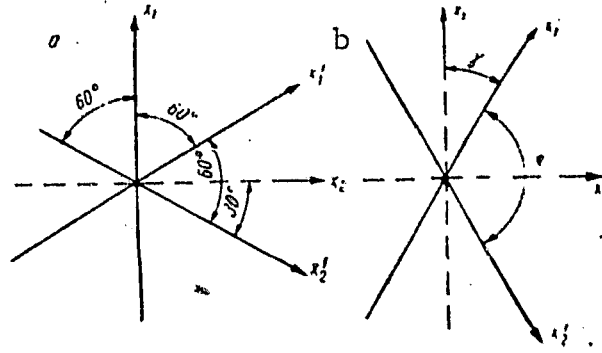


Figure 1.3. Schematic Illustration of Fiber Direction in Adjacent Layers with "Stellar" (a) and Nonorthogonal (b) Laying of Layers

$$\begin{aligned} a_{1111}c_{2,2}^4 + a_{2222}c_{2,2}^4 + 2R_{12}c_{2,1}^2c_{2,2}^2 &= a_{1111}, \\ 7a_{1111} &= a_{2222} + 6R_{12}. \end{aligned} \quad (1.28)$$

By examining formulas (1.27) and (1.28) jointly, we arrive at the equality  $a_{1111}=a_{2222}$  (1.29).

Thus, not only the directions  $x_1$ ,  $x_1'$  and  $x_2'$  are equivalent to each other, but the direction of the axis of symmetry  $x_2$  is equivalent to these directions (see fig. 1.3a).

Assuming that for the symmetrical tensor  $a_{1212}=a_{1221}=a_{2112}=a_{2121}$ , we obtain:

$$a_{1111} = a_{1122} + 2a_{1212}, \quad (1.30)$$

or

$$a_{1122} = \frac{1}{2} \frac{a_{1111}}{a_{1111}^0} - \frac{2}{4} \frac{a_{1212}}{a_{1212}^0}. \quad (1.31)$$

To compute the component of the strength tensor  $a_{1'1'1'1'}^0$  in the direction of random axis  $x_1^0$  that comprises a certain angle  $\alpha$  with the axis  $x_1$  and angle  $90^\circ$  with the axis  $x_3$ , formula (1.14) adopts the following appearance:

$$a_{1'1'1'1'}^0 = a_{1111} \cos^4 \alpha + a_{2222} \sin^4 \alpha + 2R_{12} \sin^2 \alpha \cos^2 \alpha. \quad (1.32)$$

If we substitute the ratios (1.29) and (1.30) into formula (1.32), i.e.  $a_{1111}=a_{2222}=R_{12}$ , then it happens that  $a_{1'1'1'1'}^0 = a_{1111}$ , i.e., the random



direction  $x_1^0$  is equivalent to the direction of the  $x_1$  axis of symmetry.

It thus turns out that the plan that is perpendicular to the axis of symmetry of the sixth order is a plane of isotropy, i.e., all the directions lying in this plane are equivalent to each other.

Table 1.1 presents a general view of an asymmetrical strength tensor for orthotropic material. The strength properties of this material are characterized by the following nine independent components of a symmetrical tensor (see table 1.3):  $a_{1111}, a_{2222}, a_{3333}, a_{1122}, a_{1133}, a_{2233}, a_{1212}, a_{1313}, a_{2323}$ .

Taking into account the equivalency of the directions  $x_1$  and  $x_2$ , we find that  $a_{1111}=a_{2222}$ ;  $a_{1313}=a_{2323}$  and  $a_{1133}=a_{2233}$ . In addition, it was proved above that  $a_{1111}=a_{1122}+2a_{1212}$ .

Thus, the material examined above that has a sixth order axis of symmetry, is characterized by five independent components of the strength tensor.

If a sixth order axis of symmetry is present, the material in its strength properties<sup>1</sup> has a plane of isotropy that is perpendicular to this axis, and can be called transverse or transversely-isotropic (transtropic).

In the limits of an assumption on the continuous and homogeneous continuum, the plates that are made of anisotropic layers where the angle between the direction of fibers in the adjacent layers does not exceed  $60^\circ$ , can be considered isotropic in the plate plane. Here the layers must be arranged so that the middle plane is the plane of plate symmetry. The view of the fourth order tensor for this case is presented in table 1.4. In this case, the tensor has six different components that are not equal to zero. If one considers correlation (1.30), then the five components of the tensor<sup>2</sup> in the main symmetry axes are independent.

Table 1.5 records the same tensor as in table 1.4, but here the hypothesis is introduced that its components equal the quantities that are inverse to the ultimate strengths. Instead of  $\tau_{xz}^{45}$  in table 1.5, one can introduce  $\sigma_{xz}^{45}$ , by using the invariant correlation (see formula 1.30).<sup>1</sup> Lyav [45] proves this in relation to elastic properties.

<sup>2</sup>In the case of transverse-isotropic (transtropic) material, the tensor of elastic constants, as is known, also contains five independent components in the main symmetry axes.

TABLE 1.4. SYMMETRICAL TENSOR OF FOURTH ORDER  
FOR TRANSVERSE-ISOTROPIC MATERIAL

	11	22	33	12	13	23
11	$a_{1111}$	$a_{1122}$	$a_{1133}$			
22	$a_{1122}$	$a_{1111}$	$a_{1133}$			
33	$a_{1133}$	$a_{1133}$	$a_{3333}$			
12	—	—	—	$4c_{1212}$		
13	—	—	—	—	$4c_{1313}$	
23	—	—	—	—	—	$4a_{1313}$

1.19 and 1.18):

$$\frac{1}{\sigma_0} + \frac{1}{\tau_{90}} - \frac{4}{\tau_{45}} = \frac{4}{\sigma_{45}} - \frac{1}{\tau_0} - \frac{1}{\tau_{90}} - \frac{1}{\tau_0} \quad (1.33)$$

The strength tensor presented in table 1.5 refers to any material that possesses symmetry of the transverse-isotropic (transotropic) continuum. These materials, besides those examined above, include laminated slabs consisting of isotropic layers with weaker interlayers. By ignoring the differences in strength transverse to the fibers, one can also classify wood among the transverse-isotropic materials. Back in the works of V. P. Yermakov<sup>1</sup> it was shown that a steel wire, stretched through a draw plate, can also be classified with the transversely-isotropic bodies. /37

If the material is isotropic, then the symmetrical strength tensor adopts the appearance presented in table 1.6.

This tensor contains three components that differ from zero. Taking correlation (1.30) into consideration, one can believe that the two components are independent and the strength tensor will adopt the appearance presented in table 1.7. It thus turns out that the complete set of strength characteristics of an isotropic material consists of the amount of its resistance to the perpendicular stresses  $\sigma_0$  and the amount of its resistance to tangential stresses under conditions of pure shear  $\tau_0$ . In the same way as above, it is assumed that if the amounts of stretching resistance differ from the amounts of compression resis-

<sup>1</sup>The concept of transverse-isotropic bodies and the very name in Russian were apparently first introduced by Yermakov in publication [32]. Using the approach of M. F. Okatov [54], Yermakov examined the number of elastic constants in anisotropic bodies, based on the mutual arrangement of the ellipsoids of deformation and stresses. He called the latter the surface of elastic forces. In the same work, Yermakov examines the equilibrium of an elastic cylinder in the general case of anisotropy when random forces and moments act on its ends.

TABLE 1.5. SYMMETRICAL STRENGTH TENSOR FOR TRANSVERSE-ISOTROPIC MATERIAL

	11	22	33	12	13	23
11	$\frac{1}{\sigma_x^0}$	$\left[ \frac{1}{\sigma_0} - \frac{1}{2\tau_0} \right]_{xy}$	$\frac{1}{2} \left[ \frac{1}{\sigma_0} + \frac{1}{\sigma_{90}} - \frac{1}{\tau_{45}} \right]_{z,x}$	0	0	0
22	$\left[ \frac{1}{\sigma_0} - \frac{1}{2\tau_0} \right]_{xy}$	$\frac{1}{\sigma_x^0}$	$\frac{1}{2} \left[ \frac{1}{\sigma_0} + \frac{1}{\sigma_{90}} - \frac{1}{\tau_{45}} \right]_{z,x}$	0	0	0
33	$\frac{1}{2} \left[ \frac{1}{\sigma_0} + \frac{1}{\sigma_{90}} - \frac{1}{\tau_{45}} \right]_{z,x}$	$\frac{1}{2} \left[ \frac{1}{\sigma_0} + \frac{1}{\sigma_{90}} - \frac{1}{\tau_{45}} \right]_{z,x}$	$\frac{1}{\sigma_z^0}$	0	0	0
12	0	0	0	$\frac{1}{\tau_{xy}^0}$	0	0
13	0	0	0	0	$\frac{1}{\tau_{xy}^0}$	0
23	0	0	0	0	0	$\frac{1}{\tau_{xz}^0}$

tance, then a separate strength tensor can be written for the first and a separate for the second resistances.

The strength tensor for isotropic material is given here to complete the study as a limit case since it shows that the adopted approach to the strength question for isotropic material requires determination of the ultimate pure shear resistance according to experimental data. It cannot be computed by any criterial theory (an analogous conclusion was accepted in the famous theory of strength of Mohr).

The formulas for the change in ultimate strengths for transverse-isotropic material, depending on the orientation of the stress in relation to the material's axis of symmetry, can be obtained directly from the formulas given in section 4, on the condition that the axes  $x_1$  and  $x_2$  are equivalent. These formulas are of practical importance for wood which is viewed as a transverse-isotropic material. It is easy to see that in the case of stretching or compression in a direction that

TABLE 1.6. SYMMETRICAL FOURTH-ORDER TENSOR  
FOR ISOTROPIC MATERIAL

	11	22	33	12	13	23
11	$a_{1111}$	$a_{1122}$	$a_{1122}$	0	0	0
22	$a_{1122}$	$a_{1111}$	$a_{1122}$	0	0	0
33	$a_{1122}$	$a_{1122}$	$a_{1111}$	0	0	0
12	0	0	0	$a_{1212}$	0	0
13	0	0	0	0	$4a_{1212}$	0
23	0	0	0	0	0	$4a_{1212}$

TABLE 1.7. STRENGTH TENSOR FOR ISOTROPIC MATERIAL

	11	22	33	12	13	23
11	$\frac{1}{\sigma_0}$	$\frac{1}{\sigma_0} - \frac{1}{2\tau_0}$	$\frac{1}{\sigma_0} - \frac{1}{2\tau_0}$	0	0	0
22	$\frac{1}{\sigma_0} - \frac{1}{2\tau_0}$	$\frac{1}{\sigma_0}$	$\frac{1}{\sigma_0} - \frac{1}{2\tau_0}$	0	0	0
33	$\frac{1}{\sigma_0} - \frac{1}{2\tau_0}$	$\frac{1}{\sigma_0} - \frac{1}{2\tau_0}$	$\frac{1}{\sigma_0}$	0	0	0
12	0	0	0	$\frac{1}{\tau_0}$	0	0
13	0	0	0	0	$\frac{1}{\tau_0}$	0
23	0	0	0	0	0	$\frac{1}{\tau_0}$

constitutes the angle  $\alpha$  with direction of the symmetry axis of infinite order  $x_3$  (i.e., with direction of the wood fibers), the tensorial formula for transverse-isotropic material is written in the same way as for orthotropic material

$$\sigma_b = \frac{\sigma_0}{\cos^4 \alpha - b \sin^2 2\alpha - c \sin^4 \alpha}$$

$$b = \frac{\sigma_0}{\sigma_{45}} - \frac{1+c}{4}; \quad c = \frac{\sigma_0}{\sigma_{90}};$$

where

$\sigma_0$ --ultimate strength in direction of  $x_3$  axis of infinite symmetry (along wood fiber);

$\sigma_{90}$ --ultimate strength in direction lying in plane of isotropy (transverse to wood fibers).

Resistance to tangential stresses is of practical importance for wood. It is viewed as a transverse-isotropic material when shearing resistance is computed at an angle to the fibers. Ignoring the difference in the resistance values during shearing transverse to the fibers in the radial and tangential planes, and considering that during shearing along the fibers, the resistances on the radial and tangential planes are also the same, we obtain the following formula to compute the amount of shearing resistance at angle  $\alpha$  to the fibers [5]:

$$\tau_b = \frac{\tau_0}{1 - \left( \frac{\tau_0}{\tau_{90}} - 1 \right) \sin^2 \alpha} \quad (1.34)$$

where:

$\tau_0$ --shearing resistance along fibers;

$\tau_{90}$ --shearing resistance transverse to fibers.

In both cases, the perpendicular to the shearing area lies in the plane that is perpendicular to the fibers. The shearing force acts on this area in the first case along the fibers, and in the second, transverse to them.

In designing wood structures, the quantities for calculated shearing resistance  $\tau_b = R_{ck}$  are usually taken from the plan of transverse isotropy of wood, i.e., no difference is made between the radial and tangential directions.

In the practice of using laminated fiber glass materials there are known cases of nonorthogonal placement of the layers. Here the axis that is perpendicular to the sheet plane cannot be considered the axis of infinite symmetry. This occurs when the fibers are laid in two directions  $x_1'$  and  $x_2'$  (fig. 1.3.b) arranged in the sheet plane such that the angles between these directions are not equal to each other ( $2\gamma = \beta$ ). Figure 1.3b has a schematic illustration of the axial arrangement in the sheet plane in this case. The fibers are laid parallel to the  $x_1'$  and  $x_2'$  axes. It is easy to see that the symmetry axes are the axes  $x_1$  and  $x_2$ . The  $x_2$  axis is the bisector of the  $\beta$  angle, while the  $x_1$  axis is the bisector of angle  $2\gamma$ . This material can be viewed as orthogonally-anisotropic on the condition that the layers with fibers lying in directions  $x_1'$  and  $x_2'$  alternated regularly. In this case,

the symmetry planes will be the middle plane of the sheet and the two planes that are perpendicular to the first and contain the  $x_1$  and  $x_2$  axes.

The strength isotropy of "stellar" sheet materials in the sheet plane with  $\alpha_0=60^\circ$  follows from the following theorem proved by V. L. German [28] and generalizing Neumann's principle for the case of anisotropic continuums. If the medium has an axis of structural symmetry of  $n$ th order, then it is axially isotropic in relation to this axis for all physical properties whose characteristics are determined by tensors of rank  $r < n$ . Thus, for the strength properties ( $r=4$ ), already with a symmetry axis of the fifth order ( $n=5$ ), i.e., if the angle between the fiber directions in the adjacent layers of the "stellar" material is no more than  $72^\circ$  /40

$$\alpha_0 \leq \frac{2\pi}{n} = 72^\circ,$$

then all the directions in the sheet plane must be equivalent to each other.

## Chapter II. Technique for Mechanical Tests of Anisotropic Materials /41

### 6. Features of Elastic Deformation of Anisotropic Bodies

In passing to an experimental study of anisotropy in the mechanical properties of structural materials, it is necessary to dwell on the technique for testing them. Materials with very pronounced anisotropy are deformed very uniquely. They refute certain generally accepted ideas regarding deformations that have been formed in the practice of testing isotropic metal samples. For example, with central compression of wood samples that are oriented in a definite manner, they receive, besides shortening, very pronounced skewing of the edges. Sometimes they are twisted around the axis that coincides with the direction of the compressing force.

The testing technique that is accepted for isotropic samples needs to be critically evaluated and reworked as applied to anisotropic materials. Errors in defining the strength characteristics are usually associated with heterogeneity of the stress in the sample. They depend on the method of its securing in the machine. These errors increase because of the unique nature of deformations in anisotropic bodies.

N. G. Chentsov [76] who in 1936 studied the elastic deformations of plywood as an orthotropic plate, noticed that in directions not coinciding with the main symmetry axes of the material, the elongations will depend not only on the perpendicular, but also on the shear forces. The shears will be induced not only by the shear forces, but also by the perpendicular.

To illustrate this phenomenon, Keylwerth [99] presents a photograph of a wood sample during free compression beyond the elasticity limit (fig. 2.1). Compression occurs at a  $45^\circ$  angle to the fibers in a radial plane. The upper pillow of the press is designed so that it can move freely and turn in relation to the lower. Figure 2.1 shows the skewing of the sample. This is not a consequence of its inaccurate installation, but a result of shear during compression.

/42

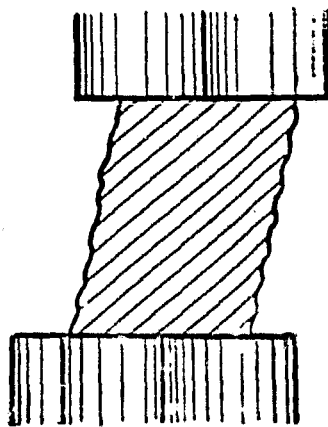


Figure 2.1. Free Compression of Wood Sample Cut at a  $45^\circ$  Angle to Fibers

A. L. Rabinovich [58] presents corrugated plate as a model of an anisotropic material. When it is stretched, the angles between the edges change. The angle (initially right angle) is reduced within which the axis of the least rigidity of the plate passes.

Hooke's law for anisotropic material with random orientation of the perpendicular  $\sigma_x$  and  $\sigma_y$  and tangential  $\tau_{xy}$  stresses under conditions of planar stress has the following appearance:

$$\begin{aligned}
\varepsilon_x &= \frac{\sigma_x}{E_x} - \frac{\mu_{xy}\sigma_y}{E_y} + \frac{\nu_{xy,xy}\tau_{xy}}{G_{xy}}; \\
\varepsilon_y &= -\frac{\mu_{yx}\sigma_x}{E_x} + \frac{\sigma_y}{E_y} + \frac{\nu_{yx,xy}\tau_{xy}}{G_{xy}}; \\
\gamma_{xy} &= \frac{\nu_{xy,xy}\sigma_x}{E_x} + \frac{\nu_{yx,xy}\sigma_y}{E_y} + \frac{\tau_{xy}}{G_{xy}},
\end{aligned}
\tag{2.1}$$

where  $\varepsilon_x$  and  $\varepsilon_y$ --relative elongations in direction of perpendicular stresses  $\sigma_x$  and  $\sigma_y$ , while  $\gamma_{xy}$ --relative shear or change in the angle between the areas on which these stresses act.  $E$ ,  $G$  and  $\mu$  in formulas (2.1) are respectively the moduli of normal elasticity, the shear moduli and the coefficient of transverse deformation of material in the corresponding directions. The first index for the coefficients  $\mu$  designates the direction of transverse deformation, while the second designates the direction of the force that induces this deformation.

$\nu_{x,xy}$  and  $\nu_{y,xy}$  in formulas (2.1) are the coefficients that determine the ratio of linear deformation to the relative shear under the influence of tangential stresses alone (fig. 2.2b).  $\nu_{xy,x}$  and  $\nu_{xy,y}$  are coefficients that determine the ratio of angular deformation (shear) to linear deformation under the influence of perpendicular stresses alone (fig. 2.2a). A. N. Mitinskiy [49] calls these quantities the coefficients of transverse and angular deformation of the second order. S. G. Lekhnitskiy [43] calls them secondary coefficients, while A. L. Rabinovich [58] calls them the coefficients of mutual influence. The deformations that comply with formulas (2.1) with  $\sigma_y = \tau_{xy} = 0$  are shown in figure 2.2a, and with  $\sigma_x = \sigma_y = 0$  in figure 2.2,b.

In figure 2.2, I, the coefficient of transverse deformation  $\mu_{xy}$  is assumed to be positive; therefore, stretching of the plate is accompanied by a decrease in its cross dimensions.

It should be noted that for wood, the coefficients of transverse deformation become negative for certain directions [1,2,8,49,60, 94].

The coefficients of mutual influence  $\nu_{x,xy}$  and  $\nu_{y,xy}$  always maintain the same signs. They can either both be positive or both negative.

Figure 2.2,a,II shows the appearance of deformation for the cases a and b with negative Poisson's coefficient  $\mu_{yx}$  and positive coefficients

/44



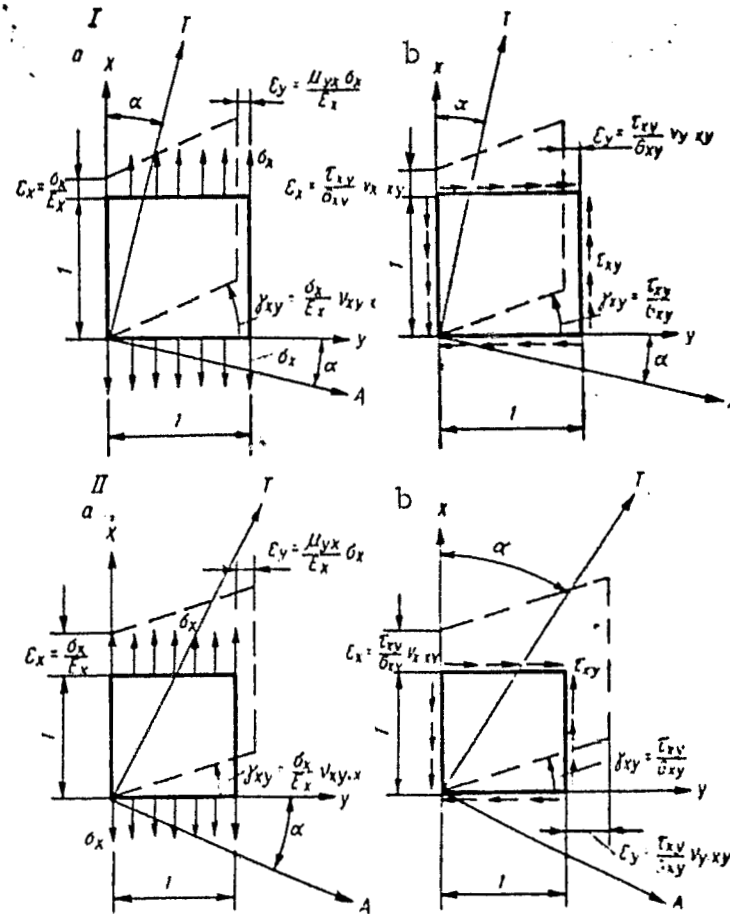


Figure 2.2. Schematic Illustration of Deformation of Anisotropic Material  
a--with free stretching; b--with pure shear;  
I--with positive and II--with negative value  
of coefficient of cross deformation

of mutual influence, i.e., with  $\mu_{yx} < 0$  and  $\nu_{x,xy} > 0$ . This deformation is characteristic for certain orientations in wood, material with very pronounced anisotropy.

When a wood sample is stretched in a direction that forms a  $45^\circ$  angle to the fibers and lies in the tangential plane, the elastic deformations have the appearance illustrated in fig. 2.2.II.

Crystal physics usually writes formula (2.1) in a form in which the coefficients of deformation and the moduli of elasticity (i.e., the technical elastic constants) are replaced by physical elastic constants [43]

$$\left. \begin{aligned} \varepsilon_x &= a_{11}\sigma_x + a_{12}\sigma_y + a_{16}\tau_{xy}; \\ \varepsilon_y &= a_{21}\sigma_x + a_{22}\sigma_y + a_{26}\tau_{xy}; \\ \gamma_{xy} &= a_{61}\sigma_x + a_{62}\sigma_y + a_{66}\tau_{xy}; \\ a_{16} &= a_{61} = \frac{\nu_{xy,xy}}{G_{xy}} = \frac{\nu_{xy,x}}{E_x}; \end{aligned} \right\} \quad (2.2)$$

$$\left. \begin{aligned} a_{26} &= a_{62} = \frac{\nu_{y,xy}}{G_{xy}} = \frac{\nu_{xy,y}}{E_y}; \\ a_{12} &= a_{21} = \frac{-\nu_{yx}}{E_x} = \frac{-\nu_{xy}}{E_y}; \\ a_{11} &= \frac{1}{E_x}; \quad a_{22} = \frac{1}{E_y}; \quad a_{66} = \frac{1}{G_{xy}}. \end{aligned} \right\} \quad (2.3)$$

In figure 2.3,a, the solid lines show the typical graphics constructed by Hearmon [94] for the change in elastic constants  $a_{11}$ ,  $a_{66}$  and  $a_{16}$  for wood, depending on the direction in relation to the fibers.

It follows from these graphs that the secondary linear deformation  $\varepsilon_x$  under the influence of tangential stresses  $\tau_{xy}$  (determined by the quantity  $a_{16}$ ) can have a quantity of the same order for wood as the main elastic elongation  $\varepsilon_x$  caused by the stretching stresses  $\sigma_x$  (defined by the amount  $a_{11}$ ).

Thus, for example, during stretching at a  $45^\circ$  angle to the fibers, the elastic constants  $a_{16}$  and  $a_{11}$  for wood are close to each other in quantity (fig. 2.3,a). Consequently, the secondary deformation that is determined by the coefficients of mutual influence in this case cannot be ignored.

The size of the coefficient of mutual influence  $\nu_{xy,x} = \frac{a_{16}}{a_{11}}$  is computed in the work of K. V. Zakharov [33] for three types of plywood. For uneven (three- and five-ply) plywoods, the extreme values of this amount are equal to 1.43 and 1.67, and for a two-ply plywood, 1.1. /46

K. K. Turoverov [5] experimentally defined the quantities  $\nu_{xy,x}$  for bakelite 11-ply plywoods 10 mm thick. The greatest amount that he obtained for a  $15^\circ$  angle direction to the fibers of the casing is 1.24.

Thus, for wood anisotropic materials, the secondary elongation that is induced by tangential stresses can even somewhat exceed the main elongation induced by the perpendicular stretching stresses if

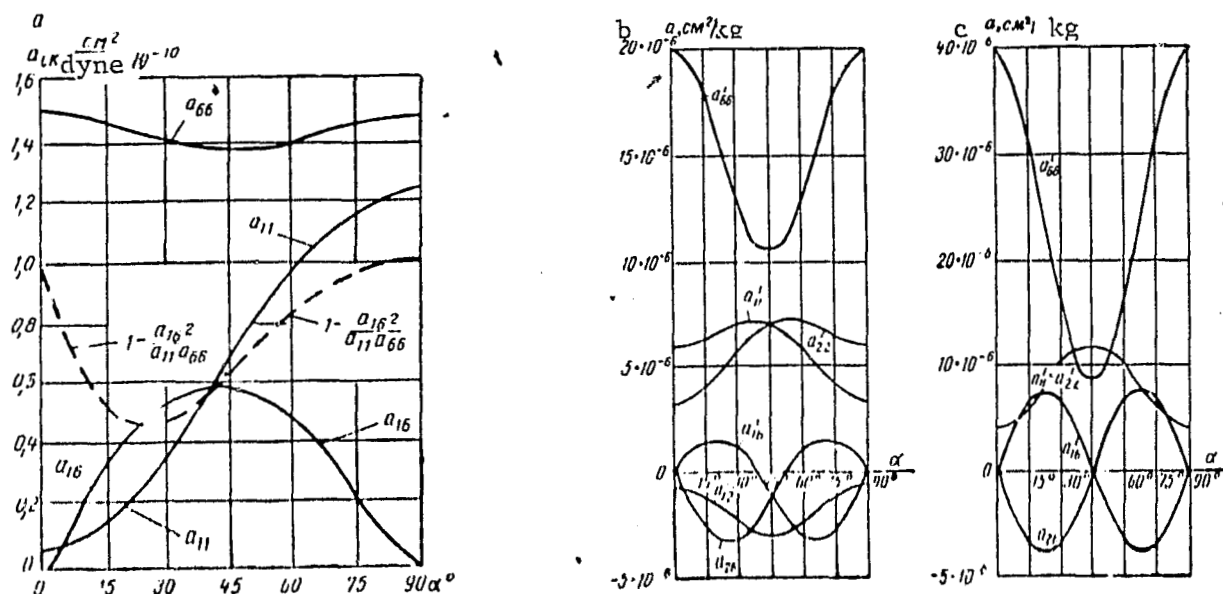


Figure 2.3. Graphs for Change in Physical Elastic Constants Depending on the Direction in Relation to the Fibers  
a--for wood; b--for SVAM fiber glass-reinforced plastic on epoxy-phenol binder with 1:5 fiber ratio; c--for SVAM fiber glass-reinforced plastic on Butvar-phenol binder with 1:1 fiber ratio.

/45

the quantities of these stresses are the same. Figures 2.3 b and 2.3 c present graphs for the change in physical elastic constants for two fiber glass-reinforced plastics of the SVAM type [12].

As is apparent from these figures, for fiber-glass-reinforced plastic on BF-4 binder that has the same properties in the direction of the two symmetry axes ( $a_{11}=a_{22}$ ), the amount  $a_{16}$  is also commensurate with the amount  $a_{11}$ . This is especially displayed in weak resins where the deformability in the diagonal direction is especially great. In this case it is impossible to ignore the shear deformations that are caused by the effect of perpendicular stresses.

Generally in anisotropic materials, the perpendicular stresses that act in a random direction do not only cause longitudinal, but also angular deformations (fig. 2.2.a). The tangential stresses in turn can cause not only angular, but also longitudinal deformations (fig. 2.2, b). It follows from here that the lack of a change in the angle between the two mutually perpendicular areas still does not indicate the lack of tangential stresses on these areas, i.e., the direction of the main deformations in the anisotropic materials does not coincide

with the direction of the main stresses.

M. F. Okatov [54] back in 1865 demonstrated that the axes of the deformation ellipsoid coincide with the axes of the stress ellipsoid in an orthotropic material only in that case where the main stresses act on the axes of elastic symmetry of the material. These ellipsoids are not coaxial with any other orientation.

The angle  $\phi$  between the direction of greatest main deformation  $\epsilon_1$  and the direction of deformation  $\epsilon_x$ , i.e., the stretching stress  $\sigma_x$ , for example, with simple stretching of a plywood sheet at an angle  $\alpha$  to the casing fibers can be found from the equation

$$\operatorname{tg} 2\varphi = \frac{\gamma_{xy}}{\epsilon_y - \epsilon_x}, \quad (2.4)$$

in which deformations are defined by formulas (2.1) with

$$\sigma_y = \tau_{xy} = 0$$

or

$$\operatorname{tg} 2\varphi = \frac{\nu_{xy,x}}{1 + \mu_{yx}}. \quad (2.5)$$

The quantity of greatest deformation  $\epsilon_1$  is determined from the formula

$$\epsilon_1 = \frac{\epsilon_x + \epsilon_y}{2} + \frac{1}{2} \sqrt{(\epsilon_y - \epsilon_x)^2 + \gamma_{xy}^2} \quad (2.6)$$

or

$$\epsilon_1 = \frac{\epsilon_x}{2} \left[ 1 - \mu_{xy} + \sqrt{(1 + \mu_{xy})^2 + (\nu_{xy,x})^2} \right] \quad (2.7)$$

It was assumed in the derivation of all of these formulas that the z axis is perpendicular to the plane of the plywood sheet.

If during simple stretching the direction of the stretching stress does not coincide with the main axes of the material symmetry, and does not lie in the symmetry plane, then in order to determine the direction and quantities of main deformations it is necessary, as in the general case of a spatial problem, to solve a cubic equation whose coefficients are invariants of the tensor of elastic deformations.

The planar problem that can be solved with formulas (2.4)-(2.7) is only obtained with arrangement of the main stresses in one of the planes of material symmetry.

Formulas (2.4) and (2.5) in this case determine the angle between the greatest main stress and the greatest main deformation, i.e., the angle between the large axes of the ellipse of stresses and the ellipse of deformations (see fig. 2.4,a). During simple stretching, the ellipse of stresses becomes a straight line, while the ellipse of deformations obtains an appearance that is presented in fig. 2.4a. If the circle ABCD is drawn on the surface of the plywood sheet, then after elastic stretching of the plywood sheet at angle  $\alpha$  to the fibers, the circle adopts the shape of an ellipse  $A_1B_1C_1D_1$ .

The large axis of the ellipse  $\epsilon_{\max}$  will be inclined to the direction of the stretching stress  $\sigma$  as shown in fig. 2.4,a, at angle  $\phi$ , and to the fiber direction, at angle  $\alpha + \phi$ .

Figure 2.4 b depicts the size of the  $\phi$  angle depending on the  $\alpha$  angle for wood with the following quantities of elastic constants (according to the data of Norris [107])

$$\begin{aligned} E_x = E_0 &= 1,27 \cdot 10^5 \text{ kg/cm}^2; \\ E_y = E_{90} &= 0,063 \cdot 10^5 \text{ kg/cm}^2; \\ G_{xy} = G_0 &= 1,4 \cdot 10^4 \text{ kg/cm}^2; \\ \mu_{yx} = \mu_0 &= 0,4; \\ \mu_{xy} = \mu_{90} &= 0,02. \end{aligned}$$

Figure 2.4c,d and e depict the sizes of angle  $\phi$  depending on  $\alpha$  for plywood of varying design. /48

In figure 2.4 c the plywood is made of 90% longitudinal and 10% transverse layers of veneer sheet (delta wood). In figure 2.4,d half of the plywood layers are longitudinal and half are transverse (even plywood), while in figure 2.4, e the plywood has five layers (uneven) made of 60% longitudinal layers and 40% transverse. All the curves in figure 2.4 b-e were constructed by Norris using Mohr's circle.

In figure 2.4, f, the curves show the change in the  $\phi$  angle depending on  $\alpha$  for aviation (dotted) and for bakelite (solid line) plywood. The curves in figure 2.4 f were constructed by K. K. Turoverov according to formula (2.5). /49

All the curves in figure 2.4 demonstrate that the greatest deviation of the maximum elongation from the direction of stretching forces is obtained when wood is stretched at an angle about 15-20° to the fibers, and for plywood at an angle about 15° and at an angle about 75° to the fibers. This deviation comprises an angle of  $\phi$  from 20° to 50°.

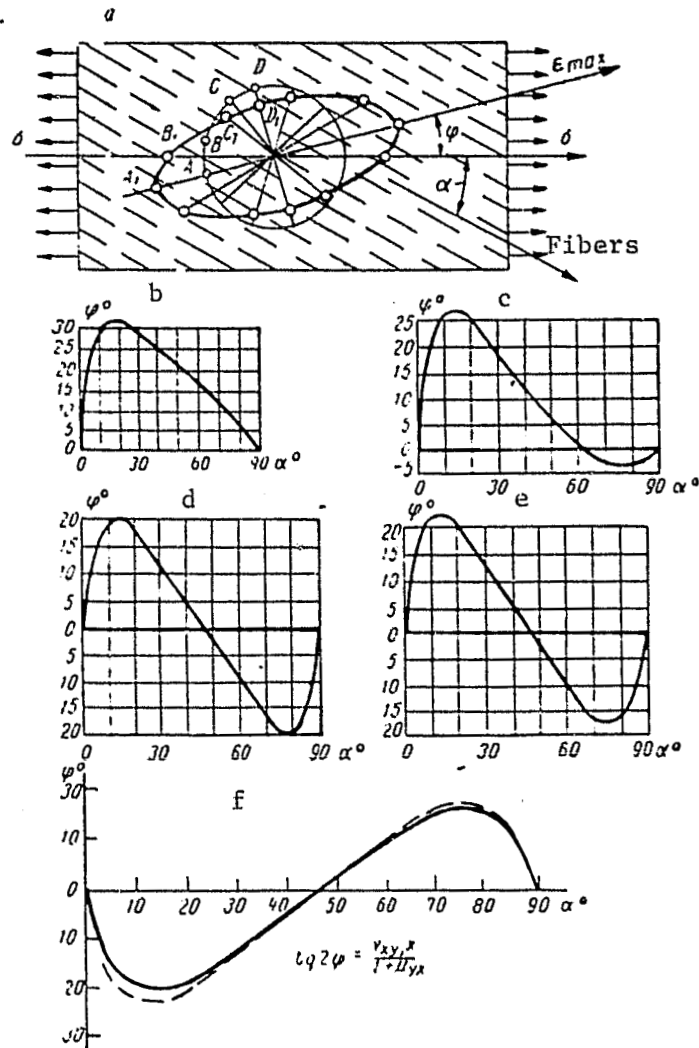


Figure 2.4. Size of Angle between Stretching Stress  $\sigma$  and the Greatest Elongation  $\epsilon_{\max}$ .

Thus, when a wood sample is stretched at an angle about  $15^\circ$  to the fibers, the greatest elongation is an over  $45^\circ$  angle ( $\alpha + \phi$ ) with direction of the fibers. Approximately the same order of angles is obtained for plywood.

## 7. Errors in Experimental Analysis of Strength Characteristics during Stretching and During Compression

During tests of anisotropic materials for stretching and for compression in random directions, additional difficulties and errors develop that are associated with the behavioral features of these

materials during deformation and that are missing in tests on isotropic bodies (for example, metals). During simple free stretching or compression, the anisotropic material receives, as already noted above, not only elongations but also shears: the transverse sections of the sample during stretching must be turned and after deformation will be shifted in relation to each other and turned in relation to the sample's axis.

Absolutely free deformation of the sample is impossible during standard tests for stretching or compression. The end sections of the tested sample generally cannot freely turn in relation to its axis. Rotations of these sections are always restricted to a greater or lesser degree, constrained. As a consequence of the constraint on the angular deformations of the end sections, additional stresses must develop in the sample that are not uniformly distributed over its length and sections. These stresses will diminish from the ends of the sample towards the middle. They will be smaller, the longer and thinner the working part of the sample is. The size of the additional stresses that develop in the constrained stretching or compression depend on the method of transmitting movements to the sample, i.e., on the design of the clamps or support pads of the testing machine.

In addition, during compression, the transverse deformations of the sample's end sections are usually limited by friction. A. K. Kalmanok's article [37] describes a study of stress developing during compression of a parallelepiped of isotropic material between two absolutely rigid stamps. The relative transverse deformations of the end sections of the parallelepiped are assumed to be equal to zero. The epures of stress distribution over the parallelepiped sections show that the stress in it is neither linear nor uniform. During tests of an anisotropic material sample for stretching or compression at an angle to the fibers, the stress can differ even more strongly from the calculated plan of a linear, uniformly stressed state. The resistance indicators that are obtained as a result of these tests therefore cannot be viewed as physical characteristics of the material strength. They are only approximate technical characteristics of its strength. /50

A. A. Kritsuk [39] obtained an approximate solution to the problem of stress distribution during constrained compression of a sample of

anisotropic material (wood). This solution for a planar stress corresponds to the hypothesis that transverse movements are missing on the ends of the sample, while the longitudinal movements are the same over the sample width, i.e., it is assumed that both transverse and angular deformations are missing, not over the entire sample, but only at its ends.<sup>1</sup>

The stress distribution epures for the transverse sections of a wood sample during stretching at a 45° angle to the fibers are presented in figure 2.5,a. The epures were constructed by A. A. Pozdnyakov according to Kritsuk's method with elastic constants taken for a parallel plywood [8]. In figure 2.5 a, the section is taken at the end of the sample. Figure 2.5 b presents stress distribution epures for a cross section located in the middle of the sample length. As is apparent from these epures, the tangential stresses  $\tau_{xy}$  even next to the site of pinching are small as compared to the stress  $\sigma_x$ . Towards the middle of the sample length, the tangential stresses are reduced, while the perpendicular stresses  $\sigma_x$  are somewhat leveled. The law of their distribution approaches the uniform. The perpendicular stresses  $\sigma_y$  that are active in a transverse direction, are very small in all the sections. The epures presented in figure 2.5a and b are constructed for a sample with ratio of length to width equal to 3.

Publication [8] has experimentally verified how significant is the constraint under actual testing conditions, and how strongly it affects the distribution of deformations over the sample section.

Orthogonally anisotropic wood sheet material, parallel plywood /51 (section 10 and table 2.1) was taken as the experimental study material.

Figure 2.5,c presents the deformation distribution epures over the width of the diagonal, long sample. These epures are constructed from the results of measuring longitudinal deformations with wire sensors.

By comparing the elongation distribution epures experimentally obtained (fig. 2.5 c) with the distribution epures of stretching stresses constructed from Kritsuk's formulas (2.5a and b), one can note that the first are distinguished by greater smoothness. The nonuniformity of stress distribution over the sample width that was obtained in the experiment is less significant than follows from Kritsuk's formula.

<sup>1</sup>In Hearmon's work [94], this question is examined on the assumption that the deformations are constrained over the entire sample during a uniform stress.



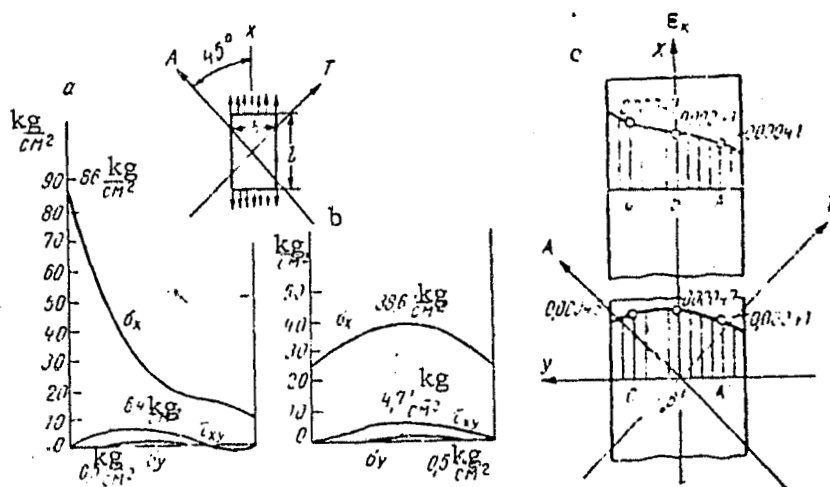


Figure 2.5. Stress Distribution Epures for Sections of Parallel Plywood Sample  
a and b--from calculation results with ratio of sample length to width equal to 3; c--from measurement results with ratio of length of sample to width equal to 13. Points A,B, C--at end; A',B',C'--in middle of sample length.

The following reasons can explain this.

The epures presented in figure 2.5 c were obtained on very long samples (ratio of length to width was 13), while the epures in figure 2.5 a and b were constructed for samples with length to width ratio equal to 3.

A. A. Kirtsuk obtained an approximate theoretical solution and with very stringent boundary conditions. During actual tests they are somewhat smoothed out. The actual stress and deformed states therefore deviate somewhat from this solution and approach the case of free stretching. /52

At those points where the stresses  $\sigma_x$  rise (fig. 2.5), the tangential stresses  $\tau_{xy}$  are comparatively great. The effect of tangential stresses results in a decrease in the elongations. Consequently, due to the effect of tangential stresses  $\tau_{xy}$ , the deformations  $\epsilon_x$  will be somewhat leveled over the rod width. Thus, in the middle section of a fairly long sample, its longitudinal deformations will be roughly constant over the width. The difference between the greatest deformation in the middle of the sample during constrained stretching computed

according to A. A. Kritsuk's method, and the deformation during free stretching is only 7% for  $l:b=13$ . Experience shows that in actuality this difference is even smaller.

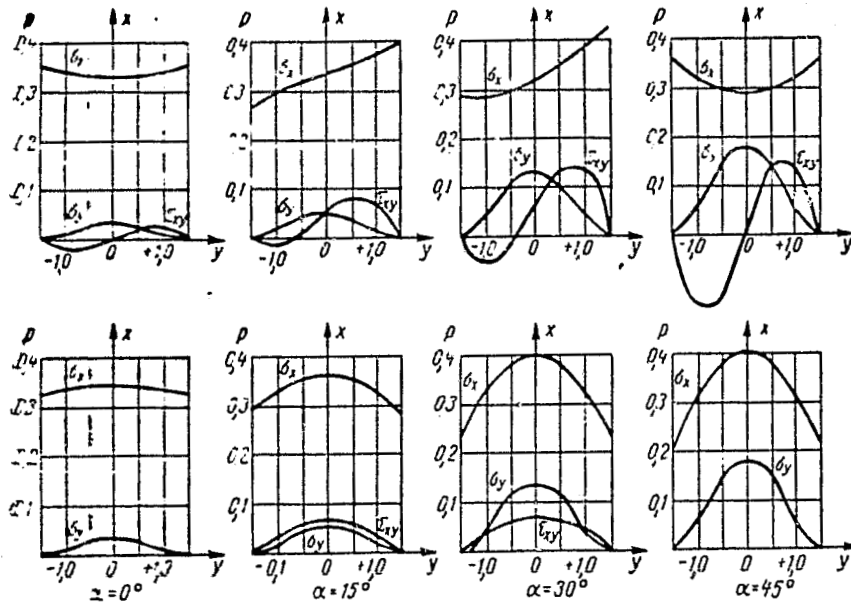


Figure 2.6. Epures of Stress Distribution over Two Sections of Compressed SVAM Sample with Length Equal to Half of Width. Below: for section passing in the middle of the sample length; Above: for section passing at the end;  $\alpha$ --angle between axis of sample and direction of fibers

Even for a material with very pronounced anisotropy of the elastic properties, nonuniformity in distribution of stretching stresses and elongations over the middle section of a fairly long sample (whose length is no smaller than triple the cross dimension) cannot be significant.

In comparatively short samples that are used to avoid loss of stability during compression tests, it is possible for a more noticeable distortion to appear in the stress as a consequence of constraint in the shear deformations on the ends of the sample than during stretching.

If both the transverse and angular deformations are constrained, then, in addition to the perpendicular stresses  $\sigma_x$  that are directed parallel to the compressing force, in a short sample, perpendicular

stresses  $\sigma_y$  also develop which are active in a transverse direction, and additional tangential stresses  $\tau_{xy}$  that are commensurate with the stresses  $\sigma_x$ .

Thus, the stressed state in a compressible sample is not only non-uniform but also nonuniaxial.

Figure 2.6 presents epures for stress distribution over sections of compressed samples of SVAM fiber glass-reinforced plastic that were constructed by A. A. Pozdnyakov [116] according to Kritsuk's method for a ratio of the sample length to width equal to 0.5, i.e., for considerably shorter samples than those studied during stretching of parallel plywood [8], Table 2.1 presents the characteristics of the elastic properties.

TABLE 2.1. CHARACTERISTICS OF ELASTIC PROPERTIES OF STUDIED MATERIALS				
Angle with fiber direction, $\alpha$ deg.	Modulus of elasticity, $E$ kg/cm <sup>2</sup>		Coefficient of transverse deformation $\mu$	
	A	B	A	B
0	207 000	247 000	0.50	0.16
45	18 600	131 000	0.09	0.50
90	9 300	247 000	0.02	0.16

Note: A--parallel plywood; B--SVAM with fiber ratio of 1:1 on epoxy-phenol binder.

The epures illustrated in fig. 2.6 show that the constraint not only of angular but also transverse deformations can have a significant effect. For a diagonal sample whose axis comprises a 45° angle with fiber direction, the constraint of angular deformations for SVAM with 1:1 fiber ratio is lacking since the diagonal axis for this material is the axis of symmetry ( $E_0 = E_{90}$ ). The coefficients of mutual influence in the direction of the diagonal sample axis equal zero. At the same time, the coefficient of transverse deformation  $\mu$  reaches its maximum for this direction (table 2.1). Consequently, strong distortion of the stress is apparently obtained for this case of sample orientation.

Even possessing experimental data on the mechanical properties of fiber glass-reinforced plastic in directions that coincide with the directions of the structural symmetry axis (for example, along and transverse to the direction of fiber laying in the sheet), it is

/54

still impossible to make a complete judgment about the strength of this anisotropic material. We also need tests of samples whose axes are directed at an angle to the axes of symmetry. This is especially important with a  $45^\circ$  angle (diagonal samples). There is no single opinion on the technique for these tests.

The works of certain authors [118, 34] construct the testing technique based on the following main premises.

When planar samples are made with axes oriented at a certain angle to the axes of structural symmetry of an anisotropic (fibrous) material, the fibers are intersected. The strength and elastic characteristics obtained as a result of the testing of these samples for stretching are therefore supposedly underestimated. The effect of the sample width on the testing results is studied here with the a fortiori false assumption that the stress field in the stretched sample always remains uniform and uniaxial regardless of the correlation of dimensions of the working part of the sample. It is considered here that the testing technique will be best in which the diagonal samples yield the highest characteristics of mechanical properties.

Based on these premises, publication [118] for example, suggests that strength and elastic characteristics of sheet fiber glass-reinforced plastics be determined from stretching testing results only of tubular samples since the use of planar samples supposedly results in a significant decrease in the strength characteristics of the fiber glass-reinforced plastics.

Another approach to evaluating the results of tests is more correct. It is based on the application to fiber glass-reinforced plastics of an assumption on a uniform and continuous anisotropic continuum. With this assumption, the testing technique must be considered the optimal if the stress field in the working section of the sample complies in the best possible way with the calculated plan of the uniform and uniaxial stressed state.

Publication [8] showed theoretically and experimentally that in a sample made of very anisotropic wood material whose axis comprises a  $45^\circ$  angle with the fiber direction, the field of stresses does not always conform to this calculated plan. The wider the sample is, the .

more strongly its stressed state is affected by the constraint of angular and transverse deformations that inevitably develop in real testing conditions and that result in the appearance of a nonuniform and nonuniaxial stressed state in the stretched (or compressed) sample. A wide sample that does not have intercepted fibers is under conditions of a nonuniform planar stress. As a result the strength and elastic characteristics of the material are overestimated [116], and are therefore unsuitable for calculating designs. /55

An evaluation of how wide of a plate (in which the fibers pass at an inclined position through the entire length of the plate) is stronger than a narrow and long sample can be made based on the continuum hypothesis. It is necessary to determine the actual stresses in the plate by the methods of the theory of elasticity of anisotropic bodies with regard for the true constraint of deformations in the fastenings. Then for the plate material we need to construct the limit surface or write the condition of strength. We need to verify the strength of the plate by standard methods with regard for the complex (planar) stress developing in it (see chapter IV).

An important feature of anisotropic materials that should be considered in developing a testing technique is the fact that the principle of Saint-Venant is not fulfilled as well for them as for isotropic bodies, even if the sample axis coincides with the axis of symmetry of the anisotropic material. The work of A. S. Kosmodamianskiy [38] has shown that during stretching of an orthotropic square band in the direction of one of the main symmetry axes of the material by loads that are distributed on its ends according to the cosine curve law, the nonuniform distribution of stresses over the middle cross section is considerably greater (41-57%) than during stretching of an isotropic band (3%). Table 2.2 presents Kosmodamianskiy's curves for a band whose length is double its width. In the table, the difference in stresses  $\sigma_{\max} - \sigma_{\min}$  in the middle section is given in percentages in relation to an analogous difference at the sites of band loading. For spruce, the difference in stresses  $\sigma_{\max} - \sigma_{\min}$  in the middle section, as for the isotropic material, will be about 3% of the size of this difference at the loading sites only if the band length is 6 times greater than its width.

TABLE 2.2 DATA OF KOSMODAMIANSKIY'S COMPUTATIONS

Material and direction of stretching	Physical elastic constants				Difference in stretching stresses $\sigma_{\max} - \sigma_{\min}$
	$a_{11}$	$a_{22}$	$a_{66}$	$a_{12}$	
Spruce (Canadian spruce) along fibers	26.8	16.1	423.7	12.9	41
Spruce (Canadian spruce) transverse to fibers	16.1	26.8	423.7	12.9	57
Isotropic	-	-	-	-	3

In the sample of isotropic material, the system of forces that is statically equivalent to zero and is applied to its ends, causes stresses close to zero in the section that is separated from the ends by a distance equal to the width of the sample. In the sample of anisotropic material, this requires at least a three-fold larger separation from the ends.

The poor correspondence of anisotropic bodies to Saint-Venant's principle, and the often increased value of the coefficients of stress concentration as compared to isotropic bodies make very stringent requirements for the shape of the sample. A longer prismatic working section of the sample is necessary and curvilinear shape of the working section is not permitted. It would be preferable to have a prismatic sample whose length is 5-6-fold greater than the width.

The natural dispersion of testing results for stretching and compression that is more significant than for isotropic materials is also a characteristic feature for very anisotropic materials.

If we glance at the graphs for the change in the ultimate strengths of such materials as wood or wood veneer sheets presented in section 10 (fig. 3.1), then it is easy to see that the deviation of the sample axis at an angle about  $5^\circ$  from the fiber direction can result in a decrease in the amount of ultimate strength by almost 10%.\*

When laminated plates are made of very anisotropic veneer sheets, an error in laying them at a  $5^\circ$  angle is very possible. It results in a fairly considerable difference between the strength of individual plates, even with the exact same technology of fabricating them. This unique cross grain that is governed by a small error in the mutual orientation of the anisotropic layers is characteristic to a greater or

\* Consequently, the dispersion of testing results is usually the greatest when the sample axes coincide with the direction of greatest strength [120].

lesser degree not only for plywood and DSP, but also for fiber glass-reinforced plastics of almost all types.

This feature of laminated anisotropic sheet materials requires thorough statistical processing of the testing results. In contrast to metals, only series of similar samples of anisotropic materials should be tested with subsequent monitoring of whether the number of samples in the series is sufficient for reliable testing results.

The simple methods of statistical processing that are used to test wood (GOST 6336-52) have also recently been applied to other anisotropic materials, for example, fiber glass-reinforced plastics [42]. /57

It should be noted that in studying the anisotropy of strength it is necessary to select a testing technique so that the shape of the sample is the same with all orientations of its axis, and at the same time to always guarantee destruction of the sample only in the limits of its working area.

Since the results of an experimental study of anisotropy of strength properties made in 1954-1963 were obtained with samples of different shape and dimensions for different construction materials, chapter III presents these data with a description of the appropriate technique.

The technique of mechanical tests of anisotropic materials, and especially reinforced plastics, is being continually perfected.

Experiments have shown that when fiber glass-reinforced plastics are tested for stretching, the samples of square shape without thickenings (heads) used in Czechoslovakia are the best. Rupture occurs in the working section of the samples if measures are taken to reduce the compression stresses on the area of contact between the sample and the clamp. It is sufficient to increase the length of the sample placed in the clamps and to make the vise cut shallow (or equip it with pads made of emery paper [115]). Long wedge-shaped vise jaws that move over a set of rollers are used to hold the sample in the clamps.

When fiber glass-reinforced plastics are tested, the most convenient are samples without heads,  $10 \times 15 \text{ mm}^2$  in section with length of the clamped section in each clamp about 100 mm and total length 300 mm.

When fiber glass-reinforced plastics are compressed in the attachment [5] it is best to take samples 15 mm wide with length of the

working section 22 mm, since the stress in them is more uniform than in the samples used for studies in 1960-1962 presented in chapter III.

The process of developing methods to obtain the mechanical characteristics of anisotropic materials under conditions of uniform stresses of uniaxial stretching and compression is very complicated and requires further research. The first stage is to analyze the features and errors of the extant technique that allows the grossest errors to be avoided.

#### 8. Testing Methods for Simple Shearing and for Shearing

Simple shearing along fibers. It is very important to test anisotropic synthetic materials (for example, fiber glass-reinforced plastics) for strength in a uniform stress of pure shear.

The testing technique for two-sided shearing of a tightly clamped sample that is stipulated in the OST 10044-38\* standard "Determination of Temporary Shear Resistance" provides exaggerated values for resistance of material to the effect of tangential stresses since on the shear areas additional compressing stresses develop that prevent shearing of the material layers in relation to each other. The results of this test can be viewed in the same way as for steel, as a type of technological test. From these tests one can judge the comparative amount of shear resistance of the material with different orientation of the samples in relation to the glass fiber. But it is difficult to use them to judge the strength of fiber glass-reinforced plastic in pure shear.

In order to examine a possible technique of shear testing of very anisotropic fiber glass-reinforced plastics (SVAM type), it is useful to turn to the accumulated extensive data on the technique for testing wood and plywood.

There are many methods for testing wood for shearing along the fibers. The books of F. P. Belyankin [18] and F. Kollman [102] give a survey and detailed analysis of them. In all methods, the tangential stresses are distributed over the shearing areas more or less non-uniformly, and in addition, additional perpendicular stresses act on these areas. The ultimate strength is usually computed according to

\*Plastic of Organic Origin. Methods of Testing, 1964.



the formula

$$\tau_t = \frac{P_{max}}{F}, \quad (2.8)$$

where  $F$  is the shearing area.

This formula is based on an assumption about the uniform stress of pure shear. Such an assumption does not comply with any of the testing methods either during one-sided or two-sided shearing.

As F. P. Belyankin [18] showed, the load-bearing capacity of a sample under the influence of compressing stresses on the shearing plane is higher than the load-bearing capacity of the sample in which additional stretching stresses act on the shearing plane.

Destruction of such an orthogonally anisotropic material as wood, on areas parallel to the fibers in a stressed state of pure shear could occur even in experiments for torsion of correspondingly oriented samples of square section.

The ultimate shearing strength along the fibers of pine in experiments for torsion is 2.5-3-fold higher (about  $194 \text{ kg/cm}^2$ ) than in the experiments for simple shearing according to GOST 6336-52. /59

This discrepancy can be explained not only by the effect of additional stretching stresses developing on the shearing area in the GOST sample, but also partially by the constraint of torsion deformation during tests.

During torsion there is no complete correspondence between the circumstances of the experiment and the calculated plan. The calculated formulas for stresses that develop during torsion of an orthotropic elastic rod of square section were produced on the assumption that the distribution of these stresses depends only on two coordinates and is not changed along the axis of the rod.

When testing for torsion in standard machines, the end sections of the sample are rigidly clamped in metal clamps and therefore cannot be freely distorted. During such constrained torsion, additional perpendicular and tangential stresses develop along the clamped ends of the sample.

As M. S. Drozd [31] showed, rigid fastening of the ends of a prismatic isotropic rod during torsion causes an additional rotation of the end sections in a direction opposite to the direction of the main

torsion. Here additional tangential stresses develop on the areas that are parallel to the axis of the rod, directed opposite to the main calculated stresses of free torsion active on these areas.

Thus, the tangential stresses that are active on the shearing areas parallel to the axis of the twistable rod near the ends where the crack begins are lower than the calculated stresses of free torsion, while the ultimate strength that can be determined from torsion experiments in this case will be exaggerated.

A quantitative evaluation of this exaggeration has still not been made since the problem of constrained torsion of a prismatic rod has only been solved for an isotropic material.

The actual resistance of wood to shearing along the fibers during pure shear must be lower than that amount that is obtained from the experiments for torsion, but it goes without saying, that they are higher than those yielded by shear tests, for example, according to GOST 6336-52.

Shearing along the fibers can also occur during bending, on the neutral layer of a beam. For this shearing to occur before the greatest perpendicular stresses reach the corresponding limit amounts, the ratio of beam section height to its span must be fairly large.

The effect of all the aforementioned circumstances can be excluded /60 to a certain measure, while the testing technique can be simplified, if in order to determine the resistance of fibrous orthotropic materials to shearing along the fibers one adopts the following method.

It is known that during compression and stretching of samples whose axis comprises a small angle with the direction of the fibers, destruction occurs on inclined areas by shearing of the wood along the fibers. Thus, the shear resistance along the fibers can be defined from results of testing wood for stretching or for compression at an angle to the fibers.<sup>1</sup> The tangential stresses are distributed on inclined sections of long stretched samples relatively uniformly. Although additional perpendicular stresses act on these sections, their effect on shear resistance can be evaluated. This method is presented in detail in publication [11] and in section 14 as applied to wood and to fiber glass-reinforced plastics.

<sup>1</sup>Ye. M. Znamenskiy and V. I. Norovskiy also suggested this approach. A. Jlinen [84] later studied this method as applied to Finnish wood types.

Shear testing. Even greater difficulties arise in studying the resistance of wood or any very anisotropic material to the effect of tangential stresses not along the fibers, but on areas inclined to the fibers. It is apparently impossible in this case to produce a uniform stressed state of pure shear: even the conventional strength specifications that can be defined during shearing along the fibers according to GOST 6336-52 are very complicated to obtain at an angle to the fibers.

None of the methods used in testing wood for shearing along the fibers is suitable for studying resistance at an angle to the fibers since destruction generally occurs by shearing on a weak plane, along the fibers and not in the direction of the tangential stresses or shearing forces.

The only possibility for obtaining an approximate quantity for the ultimate strength of wood under the influence of tangential stresses at an angle to the fibers is to test a tightly clamped sample under conditions of forced shearing in an assigned direction. This method has long been used for steel samples. The stressed state here also does not correspond to the pure shear, but the obtained results can be viewed only as approximate amounts of technical, but not physical strength characteristics of the material during shear. Appropriate attachments were used in different versions by Lange and Kramer [18,5] for shearing wood and plywood along the fibers.

The widespread use of wood and wood materials in aircraft construction made it necessary to study the strength of these materials during shearing in different directions. The Junkers firm attachment [102] is known. It is used for forced shearing on two areas of the sample that is tightly fit on bushings. It is cut by the movement of a punch. This attachment was suggested by R. Keylwerth. With proper fit of the sample, it avoids bending and stretching stresses on the shear areas. The ultimate strength of the wood in the tests on this attachment is therefore considerably higher than on others. However the photographs of the samples that were broken down in this attachment show that the wood experiences considerable crumpling before failure. As a result, a small gap is formed and rupture cracks appear on the convex side of the slightly bent sample [102].

The attachment that has been suggested for testing wood for shearing in different directions [5] differs from Keylwerth's attachment because the sample is not fit to the bushings before testing, but is tightly clamped in the punch and in the matrix by special clamping screws. The sample dimensions are selected so that the crumpling area is significantly greater than the shearing area and therefore, during loads that cause shearing of the sample, the crumpling of its surface is quite insignificant. The sample dimensions are 5 x 20 x 80 mm. The crumpling area is 20 x 40 mm<sup>2</sup> and the shearing area is 2 x 20 x 5 mm<sup>2</sup>.

Crumpling of the surface in the tested samples has only a local nature. It appears near the shearing site during considerable movements of the punch. In the beginning of testing, the stress on the shearing area is relatively uniform and is fairly close to the pure shear scheme.

Experimental determination of the quantities that characterize resistance of plywood to tangential stresses is done in principle by the same method as testing of wood for shearing in different directions.

The attachment for testing plywood and fiber glass-reinforced plastics for shear is given in publications [5] and [12].

The resistance of plywood to tangential stresses can be studied by other methods besides shearing. Another, very popular method is testing for distortion recommended by GOST 1148-41 "Methods of Testing Physical and Mechanical Properties of Aviation Plywood." A hinged frame recommended by GOST for these tests transforms the compression into shear. A stress close to pure shear is attained by simultaneous transmission to the plywood sheet of stretching and compressing stresses that are equal in absolute amount and are directed in two mutually perpendicular directions. The transmission of these stresses from the frame hinges to the sample occurs through the main bosses glued on the edge of the plywood sample. The nature of failure of the plywood samples, as far as one can judge from the photographs given in several studies, does not always correspond, however, to the stress of pure shear. Failure often occurs from the local swelling of the plywood. Thus, testing for distortion makes it possible to verify the properties of plywood under conditions that are close to the operation of plywood casing of the fuselage. But in this form it can hardly characterize

/62

the resistance of plywood to pure shear that passes, for example, on the neutral layer of the plywood beam that can be bent in the layer plane. The last time distortion testing was used fiber glass-reinforced plastic was tested.

A. Jlinen [98] suggested a somewhat different type of hinged frame to determine the shear moduli of wood. The wood in this frame is not secured on four, but only on two edges. Local swelling of the middle of the sheet therefore does not occur.

The study of plywood strength used an attachment that was close in the sample loading plan to the frame of Jlinen [5]. Here the upper and lower halves of the sample can be moved to opposite sides. The sample has a free field (between the attachment plates) 40 mm wide and 180 mm long. The length of the sample edges that are clamped in the plates is 300 mm. The junction from the long edges to the shorter working section (free field) is rounded to reduce local stresses.

Failure in this case usually occurs in the middle of the free field of the sample. It allows the hypothesis that the nature of stress on the failure plane is very close to the uniform stress of pure shear.

If a sample is tested whose axis is perpendicular to the casing fibers, initially the plywood is separated into layers on the areas that are parallel to the casing fibers. The reason for this separation is apparently the shearing of the outer veneer sheet layers along the fibers under the influence of tangential stresses. They develop on these areas during pure shear (according to the law of paired tangential stresses). The beginning of separation into layers in the sample corresponds to the moment the load drops during testing.

When testing samples for distortion whose axes make a  $45^\circ$  angle with the casing fiber direction, failure does not occur by shear, but by rupture of the plywood on the weak plane parallel to the fibers under the influence of the main stretching stresses. At the same time, swelling folds appear that pass perpendicularly to the rupture cracks. They develop under the influence of the main compressing stresses. /63

Thus, failure by shear occurs during distortion only for samples whose shear plane is parallel to the casing fibers, i.e., during so-called parallel shear. Testing for distortion cannot be recommended

to determine the resistance characteristics of plywood to tangential stresses with any orientation in relation to the fibers, judging from the appearance of the samples that were destroyed during diagonal shear, i.e., at a  $45^\circ$  angle to the fibers.

The results of testing plywood for distortion generally proved to be somewhat lower than the shear testing results according to the method previously described.

According to the data presented in the references [16], the ultimate strengths of plywood during shear also exceed its ultimate strengths during distortion. The first explanation for this fact should be sought in the differences among the stressed states that develop on the failure areas during these two types of testing.

The shear testing sample is close to Lange's samples for shearing of wood. F. P. Belyankin [18] used them to study the stress in the failure zone by the optic method. This study shows that despite the two-sided shearing, the epures of tangential stresses represent a single-humped curve. The law of perpendicular stress distribution in Lange's sample is almost the same as in bending. In our sample, the additional splitting of the middle of the sample on its contour reduces the amount of stretching stresses in the lower part of the sample and results in the fact that perpendicular stresses are compressing probably over almost the entire shear plane.

During distortion, the compressing stresses are missing on the failure area, while the stretching stresses can develop when the attachment is incorrectly installed in the machine.

The actual pure shear resistances probably should lie between the testing results for shear and for distortion.

Strictly speaking, it is impossible to experimentally determine the resistance of wood anisotropic material during pure and uniform stresses of stretching, compression, and especially, pure shear at an angle to the fibers. In all types of tests, perpendicular and tangential stresses develop simultaneously on those areas where failure occurs. The stressed state is to a certain measure nonuniform.<sup>1</sup> /64

<sup>1</sup>F. P. Belyankin [18] was the first to study the methods of testing wood for shearing along the fibers by examining the development of the stressed state. He applied the first classic theory of strength to the wood.

The fairly good coincidence in the results of testing wood for compression, stretching and shear in different directions with the calculation results using formulas presented in chapter 1 and derived for resistance to pure shear or stretching and pure shear, is explained by the fact that the strength of anisotropic material in any stress depends on these resistances. This coincidence is better, the more strictly the same type of stress is maintained over the dangerous areas at different angles of incline of the fibers, i.e., the freer and purer the type of testing is. This coincidence indicates the existence of physical strength characteristics in simple stressed states (linear stretching, pure shear) that change depending on the angle of fiber incline according to the laws for transformation of the fourth order tensor components, and that determine the technical strength of an anisotropic material during its testing and during its operation in structures.

#### 9. Evaluating the Structural Strength of Anisotropic Materials from Results of Mechanical Tests

It is fairly complicated to evaluate the structural strength according to the results of mechanical tests even for isotropic metal materials [72] whose properties have been well studied.

This work does not examine those extremely important properties that are characteristic for synthetic and wood materials, such as the strong dependence of mechanical characteristics on the loading time (rate of deformation), temperature, and on the item dimensions.

It is assumed that the temperature-velocity regime is maintained the same for all stress orientations. When the results of this work are used in practice it is necessary to take into account the temperature-velocity regime of loading and the dimensions of the structure.

Anisotropy of mechanical properties in materials has great importance for an analysis of their structural strength. Failure of structural parts in certain cases can be governed by an incorrect approach to evaluating the material anisotropy [22, 74, 119].

In this respect it is most important to select the necessary characteristics of the mechanical properties by which one can judge the strength of the anisotropic material, and how much its anisotropy is

important for operation of the structural part.

This question is important in formulating the specifications for testing and inspection of new synthetic anisotropic materials , and in calculating and designing parts made of reinforced and wood plastics, and sometimes made of metal alloys [22, 119].

One should first note once again that testing of samples whose axes are mutually perpendicular (for example, oriented along and transverse to the rolled metal sheet) is not sufficient to judge the degree of anisotropy of the material's strength properties, since the intermediate-diagonal direction can be weakened. Only a sheet material that has the same quantities of strength characteristics in three directions can be considered isotropic: in the direction of greatest strength and at a 45 and 90° angle to this direction. If the difference between these three amounts lies within the limits of testing results dispersion (whose accuracy indicator does not exceed 5%), then the material can be considered isotropic.

The degree of anisotropy of the material is judged best of all from rupture tests.

One should be very cautious of the results from testing anisotropic materials for transverse bending (static and impact). These results are very dependent on the method of sample loading, the shape of the sample and its dimensions (especially during bending of cantilever samples). The bending testing results can therefore be viewed rather as a technological test than as a method of determining the strength characteristics of a material. The reasons for these results include: inapplicability of the hypothesis on planar sections to the majority of anisotropic bodies that are in a stage close to failure; considerable effect of interlayer shear, even during elastic deformations that result in distortion of the deformability and strength of the laminated samples. As a consequence of these reasons, this work does not examine the results of testing for transverse bending.

An experimental analysis of the following mechanical characteristics is needed for complete judgment on the strength of an isotropic material with randomly oriented stress:

1. From the stretching tests it is necessary to analyze the ultimate strengths in six structural directions: in three directions



of the material's axis of symmetry (direction of greatest strength and two directions in space perpendicular to it) and in three diagonal directions that lie in planes of symmetry and make a  $45^\circ$  angle with the axes of symmetry ( $\sigma_{xy}^{15}$ ,  $\sigma_{yz}^{15}$ ,  $\sigma_{zx}^4$ ). /66

2. Six ultimate strengths for the same directions must be determined from compression tests.

3. Three strength characteristics during pure shear ( $\tau_{xy}$ ,  $\tau_{zx}$  and  $\tau_{yz}$ ) must be determined from shear tests (if more correct tests under conditions of uniform pure shear are not possible). This requires data on the material's strength with six different cases of shear on the material's symmetry planes in the direction of the symmetry axis. In other words, after testing the material, for example, by shear on the plane perpendicular to the symmetry axis  $x$  in direction of the  $y$  axis ( $\tau_{xy}^0$ ) and on the plane perpendicular to the  $y$  axis in direction of the  $x$  axis ( $\tau_{yx}^0$ ), one should take from these two quantities the least as the strength characteristic during pure shear  $\tau_{xy}^0$ , in which the tangential stresses of the same quantity are active on the two examined planes.

In order to avoid using the ratios between the amounts of resistance with different types of testing, it is useful to also define the ultimate strengths for shear on diagonal areas.

Eighteen strength characteristics of the orthotropic material are thus determined in the general case of the volumetric problem: six in stretching, six in compression and six in shear. Based on the 18 quantities, one can compile two tables for the strength tensor components (see table 1.3) separately for stretching and separately for compression. One can also compute the resistance with any orientation of the simple stress of stretching, compression or shear according to formulas (1.20)-(1.25). In shear tests, a fortiori inaccurate characteristics of the material's strength are obtained. It is therefore very desirable to replace these tests with those that reflect more completely the calculated plan of uniform pure shear stress randomly oriented in the material. This plan can be fulfilled with a certain approximation by testing thin-walled pipes for the combined effect of internal pressure, axial compressing force and torque. By changing the correlations between these loads, one can obtain a pure shear stress of different orientation

in relation to the axis of the pipe, parallel to the fibers.

Such tests are fairly complicated. We do not know of any published sources that cover the results of these tests for very anisotropic materials. We therefore have to start from very simplified experiments for shearing and simple shearing that have been used in practice. Only in the first rough approximation do they permit an evaluation of the strength of anisotropic bodies in a uniform pure shear stress. /67

The task of strength verification is simplified for a sheet orthotropic material when it is loaded in the sheet plane. The number of necessary characteristics of the material is reduced.

The ultimate strengths are determined in stretching for the longitudinal, transverse and diagonal directions arranged in the sheet plane, i.e., only three quantities:  $\sigma_0$ ,  $\sigma_{90}$  and  $\sigma_{45}$ .

Three analogous quantities are defined during compression:  $\sigma_0$ ,  $\sigma_{90}$  and  $\sigma_{45}$ . Three types of samples are tested for shear in the sheet plane. They conform to all three directions of tangential stress on areas perpendicular to the sheet plane, longitudinal, transverse and diagonal:  $\tau_0$ ,  $\tau_{90}$  and  $\tau_{45}$ . The least of the quantities  $\tau_0$  and  $\tau_{90}$  is taken into account in the calculations for the effect of tangential stresses.

In order to characterize the sheet orthotropic material when there are forces perpendicular to its plane, one should also determine the ultimate strengths in compression perpendicular to the sheet plane, and mandatorily with shearing in the layer (see fig. 1.1).

It is of practical importance to investigate the quantity and orientation of the possible maximum amount of resistance of an anisotropic material. When new anisotropic materials are created, for example, reinforced plastics, it is useful to be able to predict the direction of the greatest and least strength, if one knows the strength characteristics in the direction of the symmetry axis. One can draw certain conclusions on this question for a sheet material by examining formulas (1.22). The extreme value of the ultimate strength  $\sigma_b$  corresponds to those correlations  $\sigma_0$ ,  $\sigma_{90}$  and  $\sigma_{45}$  in which the first derivative from the denominator of the right side of formula (1.22), taken at angle  $\alpha$ , becomes zero. It follows from this equation that the diagonal

direction ( $\alpha=45^\circ$ ) can be the extreme ( $\sigma_{\max}=\sigma_{45}$ ) only with  $\sigma_0=\sigma_{90}$  ( $c=1$ ).

The maximum value of  $\sigma_b$  with  $\alpha=60^\circ$  ( $\sigma_{\max}=\sigma_{60}$ ) is possible on the condition that  $\sigma_{90}=\sigma_{45}$ , and with  $\alpha=30^\circ$  ( $\sigma_{\max}=\sigma_{30}$ ) with  $\sigma_0=\sigma_{45}$ .

Thus, an oriented plastic that has the same number of fibers laid, for example, in a longitudinal ( $\alpha=0$ ) and in a diagonal ( $\alpha=45^\circ$ ) direction, and where there is no reinforcement in the transverse direction, will have the greatest ultimate strength at a  $30^\circ$  angle to the longitudinal direction. If it is necessary to coordinate the direction of the greatest material strength during stretching with the trajectories of the main stretching stresses, one can thus select the material of optimal anisotropy.

Scattering of the testing results is especially great for materials that are distinguished by strong anisotropy [120]. Even when testing rolled steel of comparatively low anisotropy, lack of attention to the possible scattering of results can result in errors as shown in section 12 and in publication [13]. In turn, a small disorder in orientation, for example, of a glass fiber in a plastic part, can result in a considerable decrease in its strength. /68

The second circumstance that impairs the direct use of testing results is the fact that stress in the samples made of anisotropic materials differs more strongly from the uniform than in metal isotropic samples. The shape of the sample and the method of transmitting the load to it therefore require especially intent attention in selecting the methods of testing anisotropic materials.

For anisotropic materials, it is very important to decide what criterion to use in determining the quantity of the strength characteristics from the results of testing the samples.

It is known that wood undergoes plastic deformation (is pressed) during compression transverse to the fibers in a radial direction, but is easily sheared (brittle failure) if the direction of the compressing force makes a  $45^\circ$  angle with the fiber direction and lies in the radial plane.

The dangerous or limit state is defined differently for these two cases of wood compression. A common characteristic of strength in technical, engineering understanding in both cases is the stress that complies with the transition of the material to a dangerous state.

GOST 6336-52 "Methods of Physical and Mechanical Tests of Wood" and "Standards of Planning Wood Designs SNIIP P-V.4-62" by the terms ultimate strength or resistance mean that general case where this amount for the same directions can comply with strict failure of the sample, and for others, with the explicit transition beyond the limits of application of Hooke's law, but without signs of failure.

These features of very anisotropic materials are so characteristic that there are suggestions [23] that in developing a theory of elastic-plastic deformation of anisotropic bodies, the limits of proportionality and not the yield stress should be taken as the material characteristics. These limits can be approximately defined for each structural direction.

One can assume that all characteristic properties of orthotropic materials that determine the ultimate amounts of stress in the transition from one mechanical state to another must change when the coordinate axes rotate according to the laws of transformation of fourth order tensor components during coordinate axis rotation. This hypothesis is confirmed in fatigue, impact and prolonged tests. /69

There are strongly anisotropic materials that fail without noticeable residual deformations, but with stresses that differ considerably from the amount of ultimate proportionality. These are materials whose deformation comprises elastic and very elastic deformation, while the shape of the stretching pattern depends strongly on the rate of sample deformation.

For these materials, and they include directed fiber glass-reinforced plastics, the amount of ultimate resistance cannot be identified with the ultimate proportionality nor the yield stress.

One can define the amount of ultimate resistance with any orientation of stress in any anisotropic body if one understands by this amount, the stress that corresponds to the transition of the material to a dangerous state in the general engineering sense of this word.

For some cases this can be the yield stresses (for example, during stretching of rolled steel). For others it is the ultimate strength (for example, in the case of stretching films of direction polymers), and in third cases, limits of proportionality and limits of endurance.

The amount of limit resistance should not be linked to any one type of limit state or failure, since for all types of transition of the anisotropic materials from one mechanical state to another, there hypothetically are certain general tensorial laws. It is the main task of this work to explain these laws.

As experience has shown, these general laws are approximately confirmed in those cases where strength anisotropy results in a different type of dangerous state with different orientations of stress in the material, for example, in wood compression.

The book of Dzh. Nay gives a systematic analysis of those properties of crystals for which the rank of the corresponding tensor has been determined. Nay includes among the properties that are not expressed by the tensors the separation stress on the soldering plane and the yield stress during plastic deformation.

Taken separately from each other, these quantities cannot be classified as tensors, if only because they do not exist for all directions in the crystal.

Undergoing brittle failure by separation on the soldering plane, the same crystal can reveal plastic deformation with another orientation of the stress.

The strength characteristics that are experimentally defined in chapter III for anisotropic materials (ultimate resistances) exist for all directions. They conform to the state that is dangerous for the efficiency of the parts of real structures in a short-term static load. /70

Further wise combination of testing samples and parts in the complex problem of evaluating structural strength [72] is necessary for an efficient use of anisotropic materials in engineering.

### Chapter III. Results of Experimental Study on Anisotropy of Mechanical Properties of Structural Materials

#### 10. Wood and Wood Materials

The theoretical conclusions of chapter I are compared in this chapter with the results of mechanical tests on different anisotropic materials, wood, metal and fiber glass.

A large portion of the testing was done in the laboratory of resistance of materials in the Leningrad Forestry Engineering Academy by the author, or with the author's participation. Some results were

taken from published sources.

Publication [5] has described in detail the experimental study of strength properties of pine and plywood.

The assumption on the orthogonal anisotropy of wood that permits tensorial formulas to be applied to it, which were derived in chapter I, makes certain requirements of the material: dimensions and shape of the samples tested for strength of wood.

The assumptions at the basis for the derivation of the tensorial formulas do not take into consideration the curvature of the annual layers, the differences in the properties of the early and late zones of the annual layers, the heterogeneity in the wood trunk along its length and diameter, and the irregularities in the structure and flaws in the wood. Requirements are consequently made for the wood samples that are suitable for the purposes of this study.

The pine wood was purchased in the Lisinsk educational-experimental tree farm of the Leningradskaya Oblast in the fall of 1950. From the two experimental trees, a portion was used that was 6 m long from the base. The trunk (without roots) diameter in this section was from 50 to 60 cm. Such a large trunk diameter was selected to reduce the effect of annual layer curvature on the testing results of the wood samples.

The composition of the felling area plantings according to data of taxation documents was 3Ye30s2B2S with average age of 87 years, fullness 0.6 and II quality index. The pine had a cross section of regular circular structure for the annual layers.

/72

All the samples were cut from the alburnum portion of the wood because the radius of curvature of the middle annual layer remained the same for the variously oriented samples designed for one type of testing. This radius was no less than 20 cm for the stretched samples and about 25 cm for the samples used to determine the elastic constants of wood in compression [1,2].

Each beam was sawed into chocks from 50 to 70 cm long. The ends of the chocks were marked on measuring rods. Their centers were arranged in one growth zone, while the axes of the measuring rod sections with radii of the annual layers made different angles (every 15°).

The measuring rods were punctured on a fiber from each chock, and then processed and marked on the samples so that the edge of each

sample made a certain angle  $\alpha$  with the fiber direction. This angle had seven different values (every  $15^\circ$ ).

In order to make samples for stretching, measuring rods were used with a section of 200 x 30 mm that were oriented at the end at seven different angles to the radii of those annual rings that pass in the middle of the larger measuring rod section. Wood containing a water layer, blue rot or trunk eccentricity was not allowed in the working section of the sample.

The effect of slight cross grain present in the base part of the beam was excluded in the following manner. When the measuring rods were punctured, the true direction of the wood fibers was established that was used for further marking of the samples.

During the tests, the moisture content of the wood for the entire batch of samples was almost constant and comprised from 10 to 12%. The volumetric weight of the wood in the absolutely dry state was about  $0.4 \text{ g/cm}^3$ . The number of annual layers in 1 cm was from 5 to 10. The percentage of the late wood was from 16 to 20. The ultimate strength of the wood in compression along the fibers averaged  $446 \text{ kg/cm}^2$ .

Despite the careful marking and preparation of the pine wood samples from a large diameter log, we did not succeed in completely eliminating the effect of the annual layer curvature in the samples. The orientation of the sample axis in relation to the annual layers changed somewhat in the working section of the long sample designed for stretching. This was especially influential in the samples whose axes had to be arranged in a tangential direction and in directions close to the tangential. In processing the stretching testing results the wood was therefore viewed as a transverse-isotropic material, i.e., only the orientation of the sample axis in relation to the wood fibers was fixed.

The effect of curvature in the annual layers can be considerably reduced if the samples for stretching testing are cut not from natural wood, but from a stripped veneer sheet. In this case, the longitudinal axes of all the samples are arranged fairly accurately in the tangential plane, while the axis of the sample cross section that is perpendicular to the veneer sheet plane is directed to the radii of the annual rings of that wood of which the veneer sheet was made.

/73

A stripped birch veneer sheet of the I sort, from 1.1 to 1.2 mm thick was obtained from the Ust'-Izhora plywood plant. The samples were cut at different angles to the fibers at 15° intervals.

The Ust'-Izhora plywood plant, in addition to the veneer sheet, also provided plywood that was especially glued from the same veneer sheet. The direction of the fibers was the same in all of its layers (parallel). Gluing was done on a 1:1:1:1:1:1:1:1 plan. Thus, for the eight layers of the veneer sheet there were eight glued interlayers (: = interlayer). The thickness of the parallel plywood averaged 8 mm.

The parallel plywood was accepted as the material used to produce large-sized uniform samples that did not contain curvilinear annual layers. By this method one could model the wood as an orthotropic body.

Aviation plywood of I sort BS-1 was also tested (birch, glued bakelite film). It was manufactured according to GOST 102-49 by the Murom, Kostroma and Manturovo plants.

The plywood was 10 and 8 mm thick respectively with 9 and 7 layers of veneer sheet laid mutually perpendicularly with alternating placement.

Bakelite plywood BFS (GOST 1853-51) with the same arrangement of the veneer sheet was 10 and 7 mm thick respectively with 11 and 7 layers of birch veneer sheet.

All the experimental studies published in works [1-8] were done on the wood materials listed above.

The results of the classic study of A. N. Flakserman that are used in some of these works and in this chapter were obtained on pine that was very close in properties to the wood described above. The ultimate compression strengths along the fibers had practically the same value for both woods.

Stretching strength. Figure 3.1 presents the testing results from stretching three very anisotropic wood materials, birch veneer sheet, parallel plywood and pine (see also curve 4 in figure 3.4). For all the angles of fiber incline, the curves constructed from the tensorial formula (1.22) show a fairly close correspondence to the average experimental data. Failure of all three material samples occurred on the plane parallel to the fibers and inclined to the sample axis. Thus,



on the area of stretching failure, not only perpendicular, but also tangential stresses were generally active. For plywood and the veneer sheet samples were used according to GOST 1143-41, and for wood a sample was especially developed ([5], fig. 1.1) whose working section had dimensions of 6 x 20 x 40 mm.

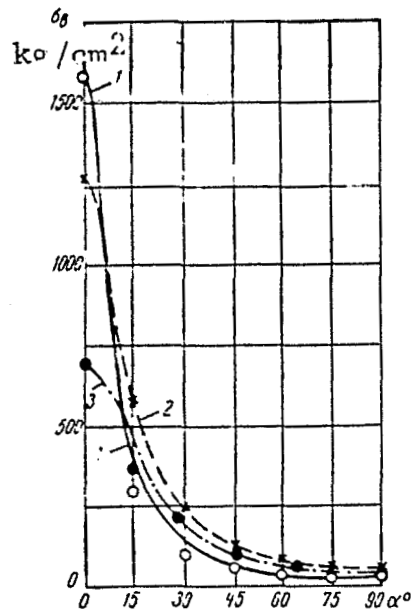


Figure 3.1. Results of Testing Wood Materials for Stretching. Curves constructed from tensorial formula (1.22)  
 1--for birch veneer sheet; 2--for parallel plywood; 3-- for pine. The average values of ultimate strength according to testing results: ○--for veneer sheet; x--for plywood; ●--for pine.

Figure 3.2 presents the results of testing aviation and bakelite plywood for stretching. They were made by G. M. Rubinshteyn [5]. The curves were constructed using formula (1.22).

M. M. Chernetsov [77] tested wood of different kinds for stretching in different directions transverse to the fibers on standard shape samples (GOST 6336-52). He tried (in the same way, for example, as the Italian authors [92] did for anisotropic metals) to express the dependence of ultimate strength on the angle between the direction

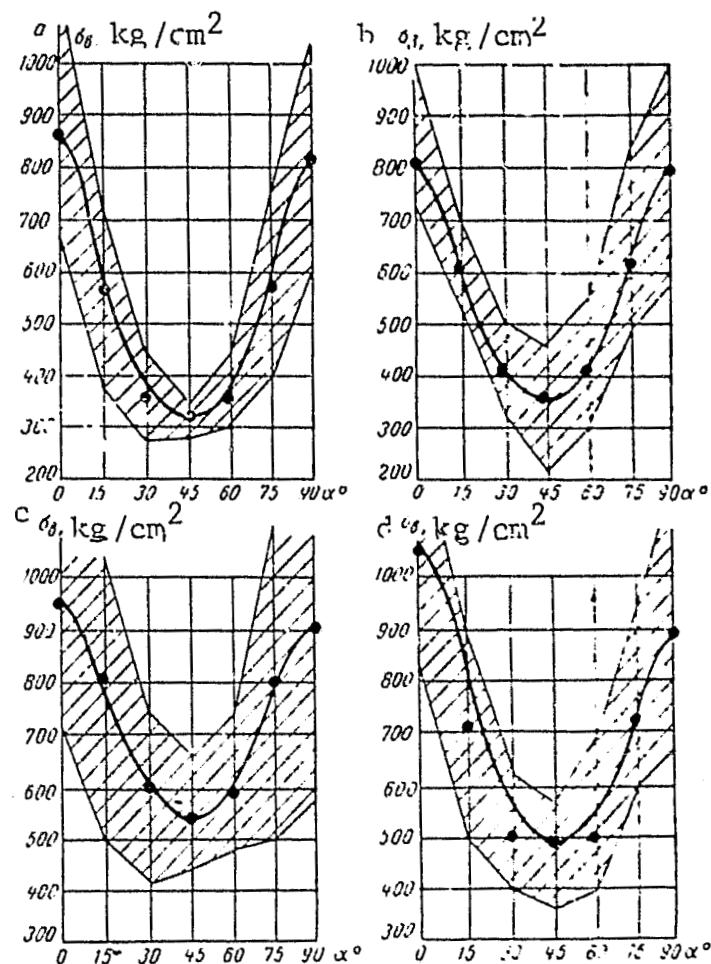


Figure 3.2. Results of Testing Plywood for Stretching  
 a and b--aviation, 8 and 10 mm thick; c and d--bakelite, 10 and 7 mm thick; O--average values of ultimate strengths from experiments. Hatched region is the actual scattering of experimental data.

of stretching and the tangential direction in wood (annual layer) by empirical correlation equations.<sup>1</sup> It is natural that the coefficients in these equations are different for different types of wood and different testing conditions (temperature, moisture content).

<sup>1</sup>Empirical relationships are generally very widespread in wood science. Thus, in the book of F. Kollman ([102], section 415) they are even given to compute the modulus of elasticity of wood in different directions, although the corresponding theoretical formulas have been known since the time of Saint-Venant and Voigt.

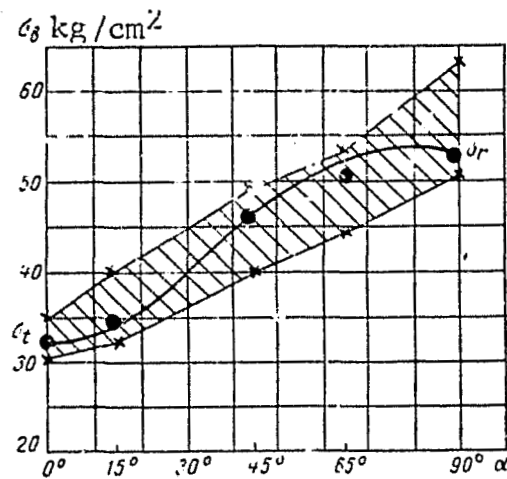


Figure 3.3. Results of Testing Pine for Stretching Transverse to the Fibers [77]. Values of ultimate strength from the experiments:  
 ●--average; X--extreme. Hatched region is the actual dispersion of the results.

Figure 3.3 presents a comparison of the experimental data of Chernetsov for pine with a curve constructed from the tensorial formula (1.22) that shows good agreement with the experiment. /75

Effect of incline of fibers on compression resistance of wood. Compression resistance of wood in different directions has been studied the most completely [71,36,85]. All the researchers tested small pure samples, for the most part in the shape of cubes. On the condition that the curvature of the annual rings was small within the sample, the wood in these studies can be considered an orthotropic material. /76

Chapter I derives formula (1.22) which permits computation of the ultimate strength of wood during compression in a random direction in three different cases of compressive force orientation: in tangential and radial planes, and transverse to the fibers.

Figure 3.4. (curves 5,2 and 3 and the points referring to them) presents the results of experiments by A. N. Flakserman. They are famous for their careful execution and accurate orientation of the tested samples. The spread of the testing results, as the researcher asserts, was comparatively insignificant: the scattering of points usually

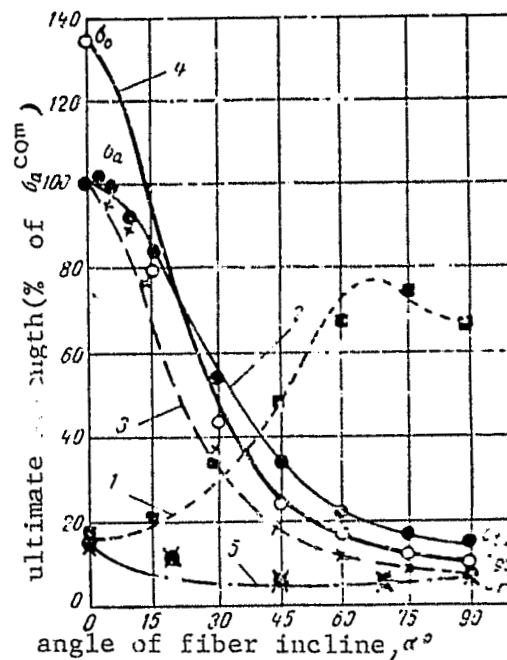


Figure 3.4. Dependence of Pine Strength during Stretching, Compression and Shear on Angle of Incline of Force to Fibers  
 1--shear (with  $\alpha=0$ --shearing along fibers; with  $\alpha=90^\circ$ --intersection of fibers); 2--compression in tangential plane; 3--compression in radial plane; 4--stretching; 5--compression in plane perpendicular to fibers. Curves constructed according to tensorial formulas (1.22) and (1.24). Ultimate strengths expressed in percentages of amount  $\sigma_a^{CO}$  -- ultimate strength in compression along fibers.

found in the wood tests was not observed in his diagrams.

In figure 3.4., curves 2, 3, 4 and 5 were constructed from the tensorial formula (1.22). The points plotted from the experimental data of Flakserman lie fairly close to curves 3 and 2, thus confirming the correctness of the formula for wood compression. The somewhat greater deviation of the experimental data from curve 5 that was constructed for results of compressing wood transverse to the fibers in different directions in relation to the radii of the annual layers is primarily

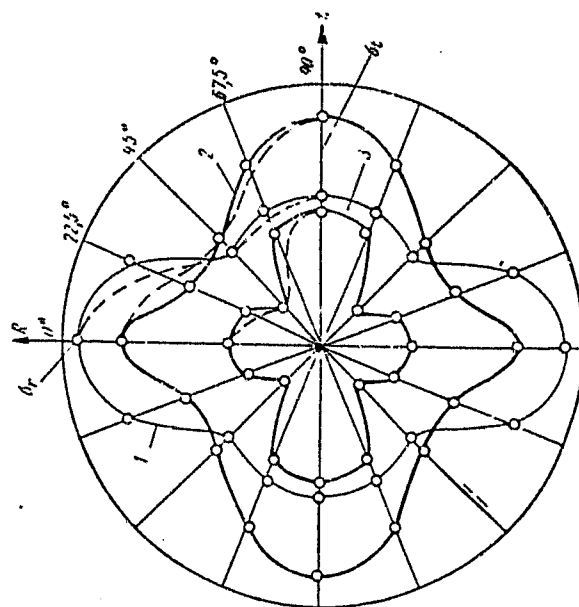


Figure 3.5. Polar Diagrams of Change in Ultimate Strength of Wood during Compression Transverse to Fibers [91]: 1--white beech; 2--pine; 3--spruce.

explained by the fact that the change in wood resistances in these directions is not great. Precise fixation of the angle between the directions of action of the load and the radial direction is very difficult due to the curvature and irregularities in the shape of the annual layers. /77

Gaber [91] made a study of the strength of wood in different directions transverse to the fibers during compression. Figure 3.5 presents the polar diagrams for change in resistance of wood of different types during compression transverse to the fibers. They were constructed according to Gaber's data (solid lines). Curves constructed from the tensorial formula (1.22) are also plotted on this figure in one quarter with a dotted line. The detected discrepancy can apparently be entirely explained by the strong effect of curvature in the annual rings. It is very significant in the samples that Gaber used in his experiments. The samples were large (5 x 5 x 5 cm), therefore there was considerable scattering of the points. /78

Compression of the plywood. During the testing of natural wood for compression, the curvature of the annual layers and the nonparallel

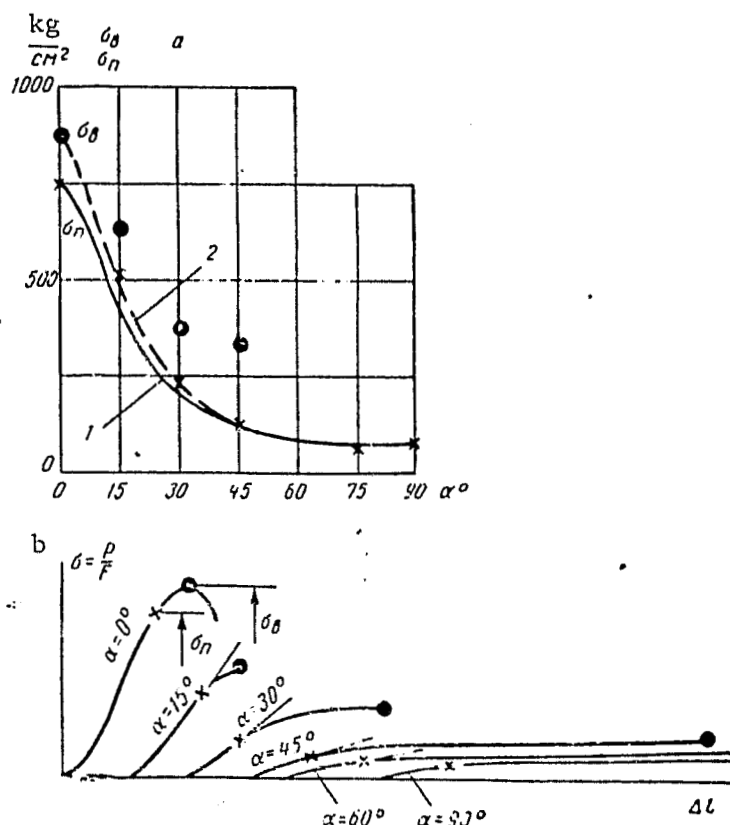


Figure 3.6. Results of Testing Birch Parallel Plywood for Compression  
 a--curves of change in ultimate proportionality (1) and conditional ultimate strength (2) depending on angle of incline of fibers; b--compression diagrams with different angles  $\alpha$  of fiber incline.

nature of the ends of the sample as a consequence of shrinkage inevitable for samples cut at an angle to the fibers can have an especially strong effect. Somewhat better conditions can be obtained by testing parallel plywood for compression in the attachment suggested by I. P. Boksberg [5].

Figure 3.6, a presents the results of testing parallel birch plywood for compression in the attachment. Figure 3.6 b presents a view of the compression diagrams obtained for parallel plywood with different angles of incline of the fibers. During compression along the fibers and at an angle to the fibers of less than  $45^\circ$ , the testing ends with destruction of the sample and dropping of the load. Here failure in compression, in the same way as stretching, occurs on the areas that

are parallel to the fibers. With angles of incline of the fibers exceeding  $45^\circ$ , and during compression transverse to the fibers, the load does not drop and failure of the sample does not strictly occur, i.e., separation of one part from another. Failure here has the nature of a local loss in stability and further pressing of the sample section that is located between the attachment clamps. Thus, with angles of incline of the fibers over  $45^\circ$ , one can only determine the conditional ultimate strength of the parallel plywood during compression, i.e., the stress in which the compression diagram deviates from the initially rectilinear section, or essentially, the ultimate proportionality  $\sigma_p$ . Figure 3.6 b makes note of the loads used to determine the ultimate proportionality  $\sigma_p$ , and what loads are used for the ultimate strength  $\sigma_B$  with different angles of fiber incline.

In figure 3.6a, the crosses mark the average values for the ultimate proportionality. The dark circles mark the average values for the ultimate strength according to experimental data. Formula (1.22) is used to construct two curves for the change in resistances of the parallel plywood depending on the angle of fiber incline. In constructing curve 1, it was assumed that in the formula,  $\sigma_0, \sigma_{90}$  and  $\sigma_{45}$ , i.e., the ultimate resistances to compression with all angles of incline of the fibers, equal the limits of proportionality  $\sigma_p$ . In constructing curve 2 it was assumed that  $\sigma_0 = \sigma_B$ , while  $\sigma_{90} = \sigma_p$  and  $\sigma_{45} = \sigma_p$ , as is usually accepted for natural wood. /80

Both curves pass very close to the average quantities  $\sigma_p$  of the ultimate proportionality experimentally obtained with different angles of incline of the fibers and marked by crosses in fig. 3.6a.

Thus, the indicators for compression resistance of parallel plywood that are accepted as equal to the conditional ultimate strengths, change depending on the angle of incline of the fibers according to the tensorial formula. This thus confirms the correctness of the adopted assumption as applied to compression of a highly anisotropic material.

Tests of parallel plywood for compression in the attachment were made on Gagarin's press. From 10 to 12 samples were tested for each angle of incline of the fibers. The accuracy indicator P was from 1.9% to 3.4%.

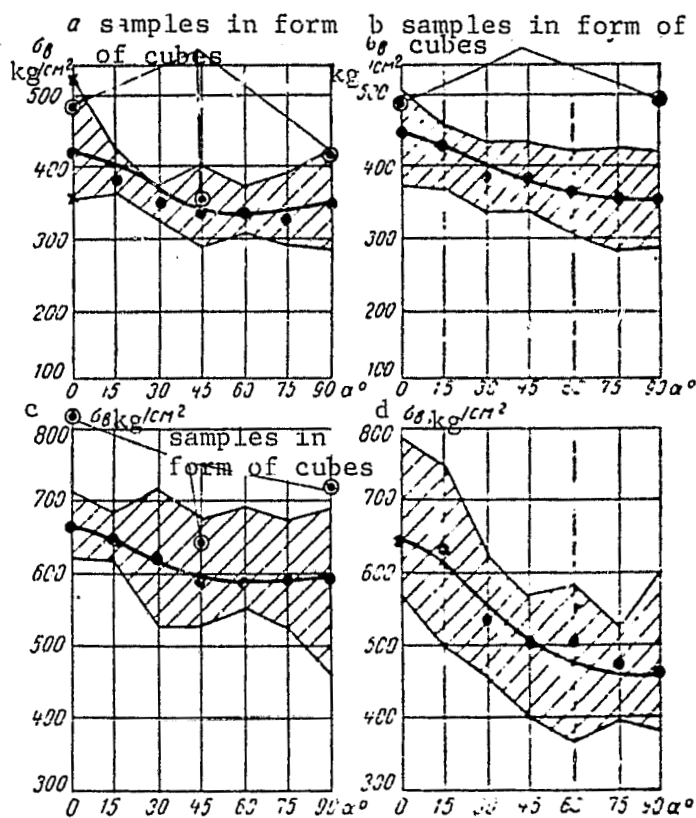


Figure 3.7. Results of Testing Plywood for Compression  
a and b--aviation, thickness of 8 and 10 mm;  
c and d--bakelite, thickness of 10 and 7 mm.

Tests of aviation and bakelite plywood for compression were also made in the device of I. P. Boksverg [5]. Some of the testing results are graphically illustrated in figure 3.7. The accuracy indicator  $P$  was not greater than 5% anywhere, i.e., was in the limits of accuracy indicated in GOST 6336-52 to determine the physical and mechanical properties of wood. The area of actual dispersion of the testing results is hatched on the graphs (fig. 3.7) [5]. The black circles mark the average arithmetical values for the ultimate strengths. In all cases of testing, the destruction of the sample occurred after the greatest weight had been attained.

The ultimate strength with all angles of incline of the fibers was computed by dividing the greatest load by the area of the sample cross section. Cubes were glued from the same plywood. Their testing



results are also plotted on the graphs (fig. 3.7).

On the graphs, the solid line indicates the curves plotted from the tensorial formula (1.22). It is apparent from the graphs that by using the testing results with  $\alpha=0$ ,  $\alpha=45^\circ$  and  $\alpha=90^\circ$  one can use the indicated formula with a great degree of accuracy to compute the ultimate strength of plywood during compression at any angle to the casing fibers.

It is further apparent from the graphs that the ultimate strength in compression along the casing fibers ( $\alpha=0$ ) is higher than the ultimate strength in compression transverse to the fibers ( $\alpha=90^\circ$ ). These graphs were constructed according to experimental data for certain plywood sheets. In the majority of cases the graphs have an analogous appearance for each separate sheet. In order to produce reliable average data, it is necessary to strive to increase the number of tested samples taken from different sheets, but not to increase the number of samples from the same plywood sheet.

The experiments showed the lack of a clearly pronounced link between the thickness of the plywood and the ultimate compression strength. The ultimate compression strength for aviation and for bakelite plywood systematically diminishes with an increase in the angle  $\alpha$ . It reaches the least value with  $\alpha=90^\circ$  (compression transverse to fibers of plywood casing). The formula (1.22) reflects well the laws governing the change in plywood ultimate strength in compression depending on the angle of incline of the casing fibers to the sample axis.

Compression of DSP wood plastics. The book of F. P. Belyankin, V. F. Yatsenko and G. I. Dybenko [19] presents the results of tests on three types of DSP plastic for compression in different directions in relation to the casing fibers.

DSP-B plastic is made of layers of veneer sheet with mutually perpendicular arrangement of the fibers. In the direction of the fiber casing, 20 times more layers of veneer sheet are laid than in the perpendicular direction, i.e., this plastic is similar in structure to parallel plywood. DSP-V plastic is made so that the fibers in all adjacent layers of the veneer sheet are perpendicular to each other, i.e., the number of layers laid longitudinally and transversely is the same (analogous to bakelite plywood).

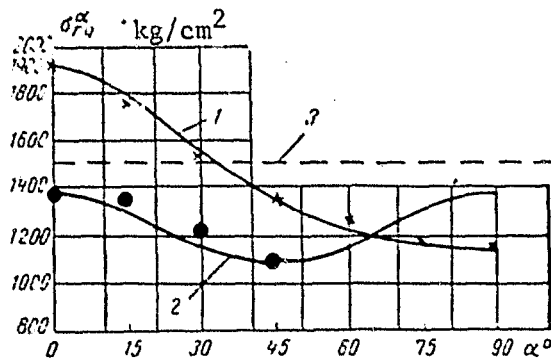


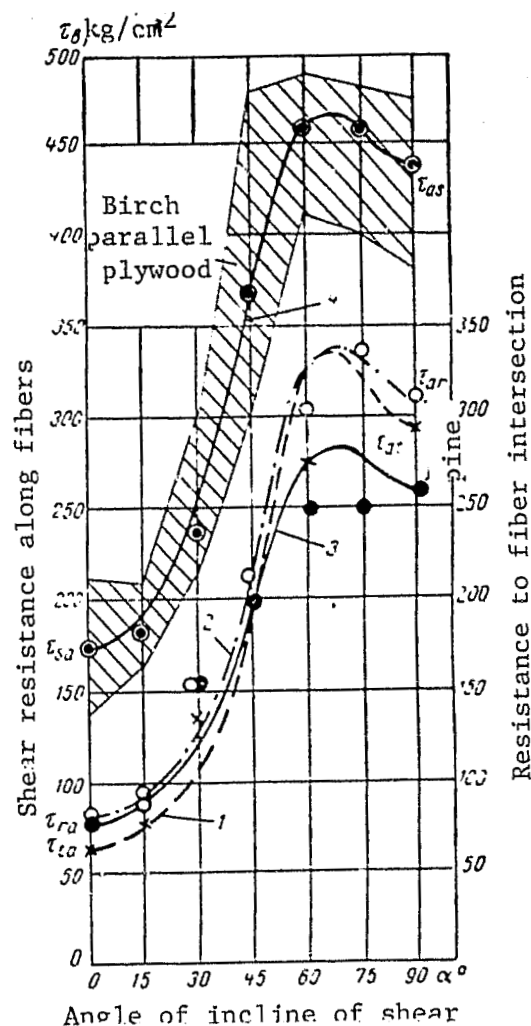
Figure 3.8. Results of Testing Laminated Wood Plastics for Compression [19]  
1--DSP-B; 2--DSP-V; 3--DSP-G.  
Average experimental data: O--for DSP-V; X--for DSP-B

DSP-G plastic has a "stellar" structure with fiber direction in the adjacent veneer sheet layers at a 30° angle to each other.

In figure 3.8, the results of these tests are compared with curves constructed from tensorial formulas. For DSP-B plastic the coincidence of this curve with the experimental data is even better than in the case of constructing the corresponding curve by the correlation equation as done in publication [19].

Testing of wood and plywood for shearing and simple shearing. Pine was tested for shearing in different structural directions in devices described in publication [5]. Measuring rods 200 x 30 and 60 x 80 mm were used to make the samples.

Irregularities in the structure of wood resulted in the fact that despite the careful marking and preparation of the samples, the orientation of the samples far from complied with the assigned in all cases. Therefore not all the samples were used for tests. In figure 3.9, curves 1,2 and 3 were constructed from the testing results from three series of samples. Each point corresponds to the average ultimate strength computed from the testing results from 2 to 20 equally oriented samples. The smooth lines on this figure show the change in ultimate strength with a continuous change in angle  $\alpha$ , computed



area to fibers  
 Figure. 3.9. Results of Testing Pine (1,2,3) and Parallel Birch Plywood (4) for Shear  
 Average values of ultimate strength for pine: X--for curve 1; o--for curve 2; ●--for curve 3; 0--for birch plywood.

according to the formulas derived in chapter I. Curve 1, constructed from the formula (see also 1.24) /84

$$\tau_b = \frac{1}{\cos 2\alpha \left( \frac{\cos^2 \alpha}{\tau_{ta}} - \frac{\sin^2 \alpha}{\tau_{at}} \right) + \frac{\sin^2 2\alpha}{\tau_{at}^{45}(\alpha)}} \quad (3.1)$$

shows the change in wood resistance to tangential stresses directed perpendicularly to the radii of the annual layers (axis r), depending on the position of the plane of action of these stresses, if it is

rotated around the axis  $r$  (this area remains parallel to  $r$ ). Thus, with  $\alpha=0$  on this curve,  $\tau_B=\tau_{ta}$  is the ultimate strength of wood during shearing along fibers in the radial plane. With  $\alpha=90^\circ$ ,  $\tau_B=\tau_{at}$  is the ultimate strength when the fibers are cut in a tangential direction. The average values for the experimental results for seven different angles corresponding to this curve are marked by crosses.

Curve 2 in figure 3.9 and curve 1 in figure 3.4, constructed according to the following formula [see also (1.24)]:

$$\tau_b = \frac{1}{\cos 2\alpha \left( \frac{\cos^2 \alpha}{\tau_{rc}} - \frac{\sin^2 \alpha}{\tau_{ar}} \right) - \frac{\sin^2 2\alpha}{\tau_{(ra)}^{45}}}, \quad (3.2)$$

show the change in wood resistance to the effect of tangential stresses directed perpendicularly to the annual rings ( $t$  axis). The plane of action of these stresses in this case should be turned around the  $t$  axis (the plane remains parallel to  $t$ ). With  $\alpha=0$  on this curve,  $\tau_B=\tau_{ra}$ , i.e., the ultimate strength during shear along the fibers in a tangential plane, and with  $\alpha=90^\circ$ ,  $\tau_B=\tau_{ar}$ , i.e., the ultimate strength when the fibers are intercepted in a radial direction. The corresponding experimental results are marked by circles.

Curve 3 shows the change in wood resistance to tangential stresses perpendicular to the axis that comprises a  $45^\circ$  angle with the radial and tangential directions, if the plane of action of these stresses is turned around the same axis. In this case the experimental results are marked by black circles. They were obtained from testing samples cut from measuring rods forming a  $45^\circ$  angle at the end with the annual ring. The curve that conforms to the latter case should be considered less reliable than the previous two curves, since the orientation of the shear plane here is maintained less accurately, especially at  $\alpha > 45^\circ$ .

Based on experimental data (curves 1, 2 and 3, fig. 3.9), one can draw a conclusion regarding the small difference in the wood resistance to shear in different directions comprising the same angle with the fiber direction, i.e., the relative suitability of the calculated plan of transverse isotropy in this case (see fig. 3.4., curve 1).

It should be noted that curves 1, 2 and 3 have a clearly pronounced maximum with angle of incline of the shear plane to the fibers of  $60-70^\circ$ .

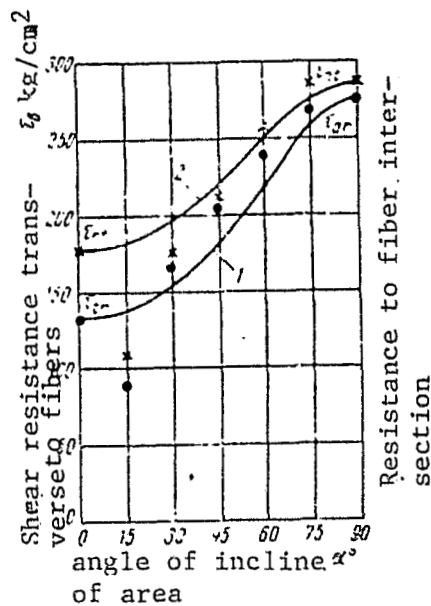


Figure 3.10. Results of Testing Pine for Shear  
Average values of ultimate strength:  
O--for curve 1; X--for curve 2.

Figure 3.10 presents the testing results for another series of samples. Here curve 1, constructed according to the following formula [see also (1.25)]:

$$\tau_b = \frac{1}{\frac{\cos^2 \alpha}{\tau_{tr}} + \frac{\sin^2 \alpha}{\tau_{ar}}}, \quad (3.3)$$

shows the change in wood resistance to tangential stresses directed perpendicularly to the fibers and parallel to the  $r$  axis. The planes of action of these stresses should be rotated around the  $r$  axis, while the planes remain parallel to the  $r$  axis. Curve 2 is constructed from the formula

$$\tau_b = \frac{1}{\frac{\cos^2 \alpha}{\tau_{rt}} + \frac{\sin^2 \alpha}{\tau_{at}}}. \quad (3.4)$$

Thus, with  $\alpha=0^\circ$  on curve 1,  $\tau_b=\tau_{tr}$  is the ultimate strength during simple shearing transverse to the fibers in a radial direction. With  $\alpha=90^\circ$ ,  $\tau_b=\tau_{ar}$  is the ultimate strength with fiber intersection. Here  $\tau_{ar}$  is lower than for the batch of samples used to construct the curves in fig. 3.9. The ultimate shearing strength transverse to the fibers for this series of samples is considerably higher than is usually

obtained in tests according to GOST 6336-52. This can be explained by the features of the device (in the tests there are no stretching stresses on the shearing planes), as well as the possibility of sharp increase in ultimate strength with the slightest deviation of the sample shear area from the plane (with slight cross grain), since in this case intersection of the wood fibers that fall under the punch begins immediately. Among the shortcomings of this testing method one should /86 include the small dimensions of the samples. This always results in a comparatively large spread of the testing results. In fig. 3.10, the circles and crosses show the average quantities of the experimentally obtained ultimate strengths. The average value of the testing results from 3 to 15 samples corresponds to each point.

Figure 3.11 presents the results of G. G. Karlsen's experiments [41], that confirm the tensorial formula (1.25).

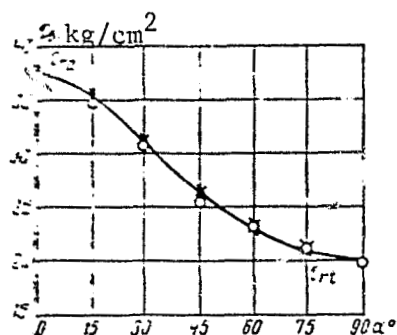


Figure 3.11. Ultimate Strength of Pine to Shearing in Tangential Plane Depending on Angle  $\alpha$  between the Direction of Tangential Stresses and Direction of the Fibers  
 O--average values of 5 experiments according to Karlsen [41]; X--according to formula (1.25).

The experimental data that refer to several not extensively studied cases of change in the strength characteristics of wood under the influence of tangential stresses depending on their angle of incline to the fibers (fig. 3.9 and 3.10) makes it possible to believe that the general formulas (1.21 and 1.24) and the particular formulas (3.1-3.4) given in this paragraph provide a fairly good correspondence to the testing results.

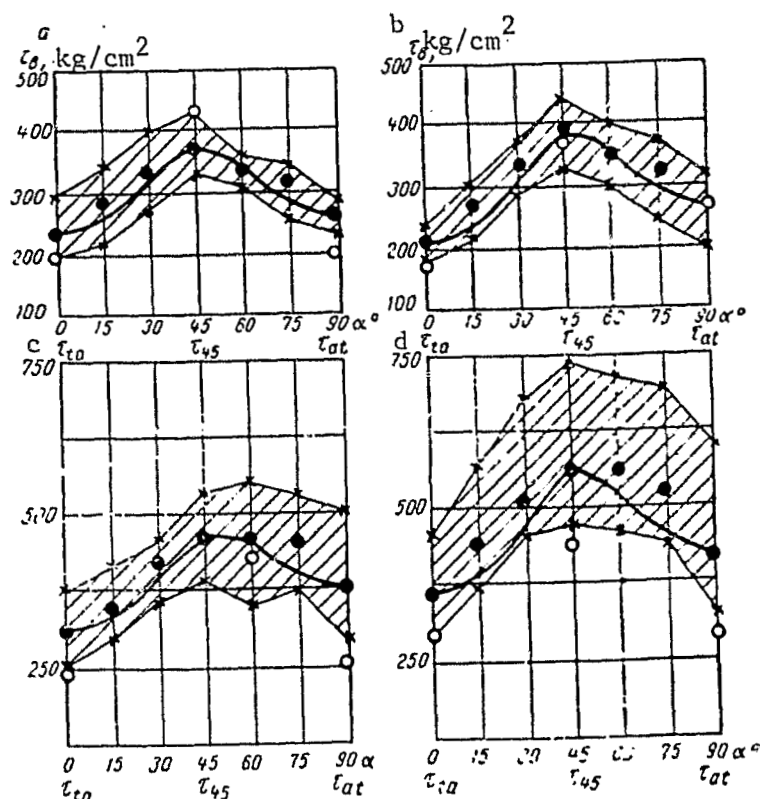


Figure 3.12. Results of Testing Plywood for Shear  
a and b--aviation, thickness of 8 and 10 mm;  
c and d--bakelite, thickness of 7 and 10 mm.  
Experimental values of ultimate strengths in shear: ●--average; X--extreme; o--average during distortion.

Curve 4 is plotted on figure 3.9 for the change in ultimate strength during shear of a parallel plywood. This curve passes higher than the corresponding curves for pine. It shows the good coincidence of the results of computation using the formula and the testing data.

Tests of parallel plywood confirm the existence of a maximum shear resistance for wood with incline of the shear area at roughly a 60-70° angle to the fibers.

The results of testing aviation and bakelite plywood for shear are given in fig. 3.12.. The solid lines indicate the results of calculation using the tensorial formula (1.24). The results of testing plywood for distortion are plotted on fig. 3.12 in the form of individual circles. The hatched regions on this figure represent the limits of

change in the testing results. The circles represent the average ultimate strength values.

The curves for change in ultimate strength in shear for aviation plywood 8 mm thick, and for bakelite plywood 10 mm thick are also presented in fig. 3.13. A comparison of the curves for strength change during stretching, compression and shear is given here for these two types of plywood. /37

For all types of plywood, the curves that are constructed from the tensorial formulas (1.22 and 1.24) pass close to the average experimental results. They do not go beyond the limits of their actual spread anywhere.

One can thus consider that the change in shear resistance for plywood depending on the angle of incline of the shear area to the fibers can be expressed by the tensorial formula (1.24). Consequently, the assumptions that were the basis for the derivation of this formula can be applied to plywood: the assumption regarding the orthogonal anisotropy of plywood and the assumption regarding the tensoriality of the strength specifications of plywood under the influence of tangential stresses.

The spread of results and inaccurate orientation for plywood is somewhat lower than for wood, since in this case large-sized samples were used (12 x 80 mm) and the curvature of the annual layers did not bear any effect. /88

The ultimate shear strengths of plywood were computed in the same way as for wood, by dividing the greatest loads by the shear area. The value of the loads  $P_{\max}$  corresponded to the highest points on the automatically recorded testing diagrams in shear.

The maximum loads used to compute the ultimate strengths, were obtained for all samples with comparatively small deformations, soon after the end of the rectilinear sections of the diagrams. Thus, the stress in the calculated values of the loads cannot differ very strongly from the stress during elastic deformation of the sample in the initial testing moment. Collapse of the plywood sample surfaces during testing in the device was quite insignificant. One can thus consider that the employed testing method of the plywood for shear to a certain degree makes it possible to judge its resistance to tangential stresses with any



orientation in relation to the casing fibers.

Testing of wood plastics for shear (according to data of R. Keylwerth [102]). Kollman's book [102] presents the results of determining the ultimate shear strengths for variously oriented areas for several types of wood materials. Keylwerth did the tests in a device analogous

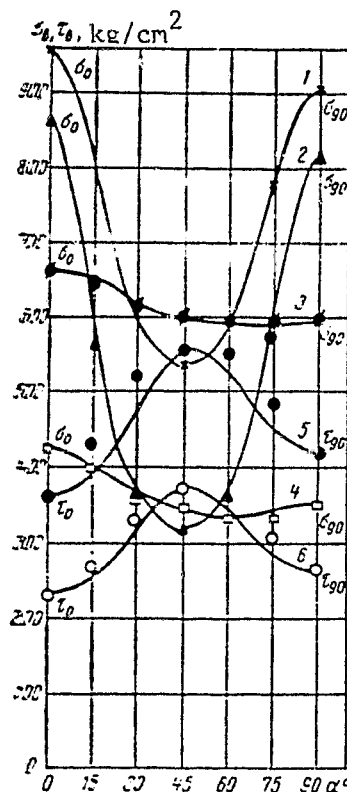


Figure 3.13. Results of Testing Plywood (summary graph)  
1,3,5--bakelite, 10 mm thick; 2,4, 6--aviation, 8 mm thick; 1 and 2--stretching; 3 and 4--compression; 5 and 6--shear.

to that in which steel rods are usually tested for shear. The average testing results of 20 identical samples are plotted on the graph in the form of one dot. Figure 3.14 presents the photographs of Keylwerth's graphs that were constructed from the results of testing beech laminated wood plastic corresponding to the structure of DSP-B plastic, i.e., /89 consisting of 20 veneer sheet layers laid in parallel. (fig. 3.14, a and

b) and a multiple-layer glued plywood (fig. 3.14, c and d) with fibers arranged in the adjacent veneer sheet layers at a 90° angle to each other.

The curves made on Keylwerth's graphs with solid lines were constructed according to the formula enclosed in Kollman's book and easily related to formula (1.22):

$$\sigma_{\gamma} = \frac{1}{\left( \frac{\cos^2 \gamma}{\sigma_0} - \frac{\sin^2 \gamma}{\sigma_{90}} \right) \cos 2\gamma - \frac{\sin^2 2\gamma}{\tau_{45}}}, \quad (3.5)$$

while the dotted lines correspond to the empirical formula also given there

$$\sigma_{\gamma} = \frac{\sigma_0 \tau_{90}^n}{\sigma_0 \sin^n \gamma + \tau_{90} \cos^n \gamma}. \quad (3.6)$$

Formulas (3.5) and (3.6) are given here in Kollman's designations, but since we are concerned with shear, then it can be assumed that the letter  $\sigma$  enters these formulas instead of the letter  $\tau$  because of a misprint. In figure (3.14) the ultimate strengths in shear are designated by Kollman by the letters  $\tau_B$ . The exponent  $n$  in empirical formula (3.6) is assumed to be different and is given in the figures. Kollman adopted the following designation for the wood symmetry axes: the  $y$  axis is directed along the fibers  $a$ , the  $z$  axis on the radial  $r$  and the  $x$  axis on the tangential  $t$  direction. Thus, in our designations

fig. 3.14a should illustrate the results of that rotation of shear areas in which  $\tau_0 = \tau_{rt}$  and  $\tau_{90} = \tau_{at}$ , i.e., must correspond to the case presented for pine in figure 3.10 (curve 2). Formula (3.4) was obtained for this case. In contrast to Keylwerth's formula (3.5), the resistance  $\tau_B$  can be computed even without preliminary experimental determination of the shear resistance on the diagonal area  $\tau_{45}$ . The second case (fig. 3.14b) conforms to the case represented by curves 1 and 4 in figure 3.9, formula (3.1). According to the appearance of the curves photographed in figure 3.14, one can assume that another misprint occurred and that the rotation of the areas in fig. 3.14 a corresponds to the case where  $\tau_0 = \tau_{ta}$  and  $\tau_{90} = \tau_{at}$  (fig. 3.9). The rotation of the areas in fig. 3.14a conforms to the case where  $\tau_0 = \tau_{rt}$  and  $\tau_{90} = \tau_{at}$  (fig. 3.10, 2). The latter hypothesis is confirmed by the fact that in fig. 3.15 b, the curve constructed from empirical formula (3.6) with

$n=2$ , i.e., essentially according to the tensorial formula (3.4), yields a very good coincidence with the testing results. In this case  $\tau_{45}$  does not need experimental determination but can be computed from formula (3.4). Figure 3.14a shows the good coincidence of the testing results with formula (3.5), i.e., with tensorial formula (3.1). Empirical formula (3.6) in this case yields fairly significant deviations. /90  
 The appearance of a maximum in figure 3.9 and 3.14a is apparently explained by the fact that intersection of the fibers of natural wood, parallel plywood and plastic Sch-T-Bu-20 that is close to it in structure, requires the greatest stresses when it occurs not at a right angle, but at an acute angle to the fiber direction. This is also confirmed by the testing results for shear of plywood (fig. 3.11, 3.12, 3.14 d) where the maximum resistances were at an angle about 45-50° to the casing fiber direction. In figure 3.14c, the plywood testing results are the same as in figure 3.10, and in figure 3.14d, the same as in figures 3.11 and 3.12, and correspond to formula (3.1). The appearance /91  
 of these graphs confirms all that has been said above. It once again makes it possible to be convinced of the advantages of the tensorial formulas that always have the same appearance, over the empirical formula (3.6) in which the exponent  $n$  adopts other values in each separate case and requires a selection based on processing experimental data. At the same time, the empirical formula (3.6), even with the special value  $n$  computed for each case, yields a worse correspondence (dotted curves) with the testing results than the tensorial formulas used, essentially, to construct the solid curves on Keylwerth's graphs.

Fatigue of parallel plywood. Testing of variously oriented planar samples of parallel plywood for repeatedly varying pure bending with a symmetrical cycle was carried out in the LTA [Leningrad Forestry Engineering Academy] laboratory by A. A. Pozdnyakov [55-57]. The endurance limits were determined with  $N=10^7$  number of cycles. A. A. Pozdnyakov also studied the stressed state that develops in the sample in which the fibers are not parallel to its axis due to the constraint of the shear deformations by the machine clamps. The maximum stresses  $\sigma_{\max}$  computed by A. A. Pozdnyakov differ fairly significantly from the stresses computed according to the elementary formula

$$\sigma_e = \frac{M}{W}.$$

Figure 3.15 presents the curves constructed by A. A. Pozdnyakov for the dependences of the endurance limits (with  $N=10^7$ ) of parallel plywood on the angle of fiber incline. The curves were constructed according to the tensorial formula (1.22). In figure 3.15a, the curve and the points that conform to the experimental data are plotted in the stresses  $\sigma_e$  computed from the elementary formulas for material resistance. Figure 3.15 b plots them in the maximum stresses  $\sigma_{max}$  determined by the methods of the theory of elasticity of an anisotropic body for the most stressed point of the sample.

The calculated plan used to define the stresses  $\sigma_{max}$  is distinguished from the actual conditions at the ends of the working section of the sample. It does not take into consideration the possible deviations in the sample deformations from Hooke's law. This calculated plan makes it possible to evaluate only in the first approximation the effect of constraint of the shear deformations in the sample on the size of the stresses developing in it.

It is apparent from fig. 3.15 a and b that the endurance limits computed in the maximum stresses  $\sigma_{max}$  agree fairly well with the tensorial formula (1.22). This cannot be said about the endurance limits in the stresses  $\sigma_e$  computed from the formulas for material resistance.

This can be explained by the nature of the fatigue strength: the fatigue crack appears precisely where the maximum stresses are active. The fatigue crack in samples of parallel plywood really always begin at that point in the sample where computations predicted the greatest amount of stresses  $\sigma_{max}$ . /92

Thus, the fatigue strength of parallel plywood is determined not by the stresses  $\sigma_e$ , but by the maximum stresses that can be determined in the first approximation by the methods of the elasticity theory of an anisotropic body.

The correlation equations of fatigue diagrams in the maximum stresses have different angular coefficients with different angles of fiber incline. The limits of (restricted) endurance are computed with a smaller number of cycles, therefore are separated more and more from the tensorial curve. With over 30 million cycles, the points approach

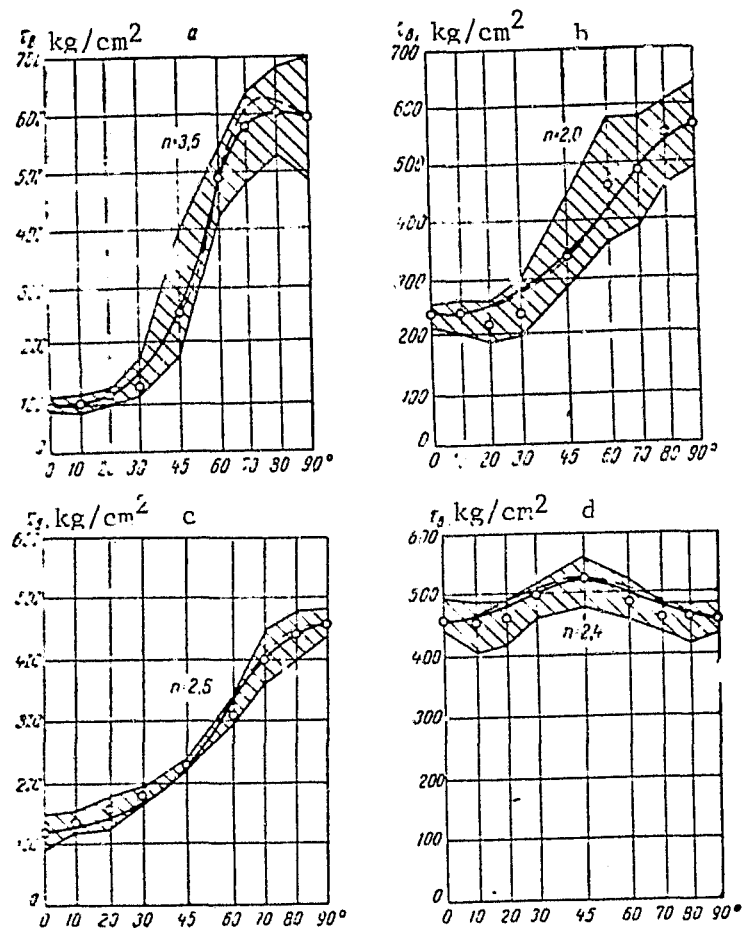


Figure 3.14. Testing Results  
a and b--beech laminated wood sheet Sch-T-Bu-20;  
c and d--multilayer plywood according to Key1-  
werth [102]. Hatched region is actual dispersion  
of experimental data.

the curve. The greatest coincidence is observed when the number of cycles equals 50 million. The points further deviate from the curve to the other side.

The good coincidence of the endurance limits with the tensorial curve with  $N=50$  million permitted A. A. Pozdnyakov to hypothesize that with this base, the true endurance limit of wood appears. In order to verify this hypothesis, four samples from the series with  $\alpha=30^\circ$  were tested with stresses near the suggested endurance limit. These samples were not destroyed even with 100 million cycles. One can thus agree with the hypothesis that the true endurance limit of wood is determined with  $N=50$  million cycles.

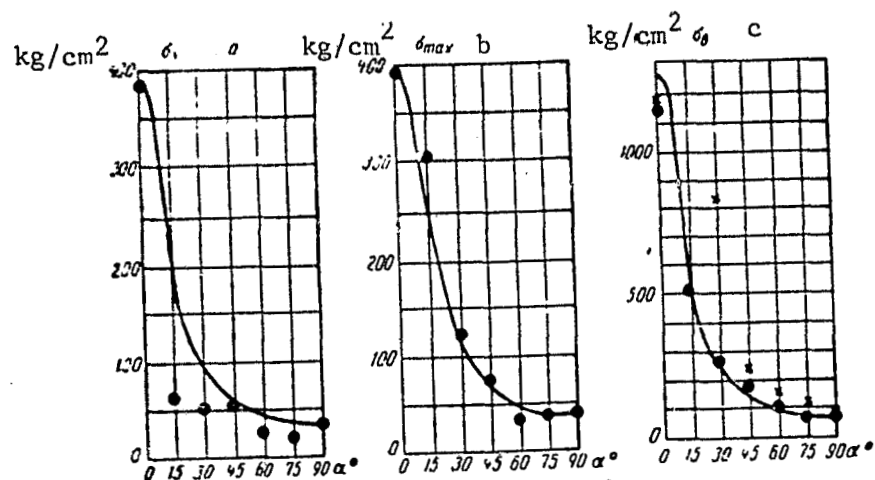


Figure 3.15. Dependence of Endurance Limits of Parallel Plywood on Angle of Fiber Incline  
a and b--with  $N=10^7$  cycles; c--tests for static rupture;  $\bullet$ -- $\sigma_e$ ;  $\times$ -- $\sigma_{max}$

If, in turn, we compute the endurance limits in stresses  $\sigma_e$  with the smallest bases using the correlation equations, then these amounts will approach more and more to the tensorial relationships until  $N=1$  coincides with it. Figure 3.15 c has constructed a curve for change in the ultimate strengths of parallel plywood according to the data of static tests for rupture. It also has the points corresponding to the fatigue strength indicators with  $N=1$  that were computed from the correlation equations. The good coincidence of the fatigue strength indicators with the tensorial curve of ultimate strength is clearly visible in fig. 3.15 c with  $N=1$  in the elementary stresses  $\sigma_e$  (dots). This is understandable since the ultimate strengths are computed in the elementary stresses, based on the assumption of their uniform distribution over the width of the cross section. The fatigue strength indicators with  $N=1$  in the maximum stresses (crosses) deviate significantly from the tensorial curve. For the direction with  $\alpha=15^\circ$ , the point did not even fall within the drawing field. This indicates that the static strength that can be viewed as a particular case of fatigue strength with a single change in the load ( $N=1$ ) is determined for wood not by the maximum stresses, but stresses  $\sigma_e$ .

Testing of wood for impact compression. Wood is often exposed to the effect of short-term impact loads. At the same time, experimental study of the dynamic strength of wood is a very complicated task due

to its anisotropy. This explains the lack of data on the strength of wood in impact compression, shearing and stretching in different directions in relation to the fibers.

Impact tests are presently being conducted only for bending transverse to the fibers.<sup>1</sup> The specific destruction work is used as the characteristic of resistability to impact bending. It is determined with considerable errors governed by the crumpling of the sample on supports and under the impact knife, as well as by friction on the supports, etc.

The amount of impact energy expended strictly for destruction of the sample is unknown. This to a considerable measure depreciates the results of testing wood for impact bending.

It also needs to be noted that tests of wood for bending are generally of lower interest than for compression or stretching. This is due to the indefiniteness in the amount of stress developing in the sections of anisotropic beam beyond the limits of elasticity. /94

In light of what has been said, the impact tests become especially important in which strength characteristics of wood can be obtained in a stressed state that is the closest to the uniform and linear.

Impact testers are adapted the best for determining the dynamic strength characteristics of materials. There is no static force in the loading process.

The impact testers are designed, as is known, to test for impact bending, and in certain cases, for impact stretching. The special device suggested by B. P. Dutov and described in publication [5] permits the tester to be used to test wood for compression.

B. P. Dutov used the impact tester equipped with a photoelectron device to obtain diagrams of impact compression. He studied the strength of wood along the fibers in different regimes of dynamic loading.

The impact resistance of wood, in the same way as in static loads, strongly depends on the orientation of the applied forces in relation to the fibers.

Publication [6] covers a study of this relationship during impact.

The tensorial formula (1.22) describes the dependence of static resistances of wood on the force orientation. The hypothesis on the possible extension of this formula to cover the case of impact compression

<sup>1</sup>See "Methods of Physical and Mechanical Testing of Wood" GOST 6336-52.

was experimentally studied for pine.

The tests were carried out on samples made of the base part of two experimental pine trees of large diameter (about 60 cm) acquired in the Lisinsk educational-experimental forestry farm. The radii of curvature for the measuring rod annual layers (4 x 4 cm) from which the samples for these tests were made, were about 24 cm. With a 2 cm edge of the sample, this makes it possible to consider the annual layers practically rectilinear within the sample.

It was necessary for this study to guarantee the same loading regime in all cases of orientation of the dynamic force in relation to the fibers.

We did not succeed in preserving the same rate of increase in the destructive stress as a parameter determining the loading regime as B. P. Dutov did for the following reasons.

It is known that variously oriented samples have a different nature of deformation. The wood is destroyed along the fibers almost as a brittle material. Compression transverse to the fibers is accompanied by large residual deformations. This peculiarity of wood results in a different rate of increase in the destructive stress. It will be lower the more pliable the sample is. Only by changing the external conditions of impact loading can one maintain this parameter constant for different orientations. The considerable difficulties of this testing technique and the indefiniteness of the practical application of the results force us to give preference to the method of study in which the constant parameters that determine the impact loading regime are the velocity of the striking body at the moment it touches the sample (impact velocity) and the reserve of kinetic energy of the striking body. /95

The tests were done on impact tester PS VO-1000 with a pendulum whose maximum work margin was 5 kq·m with impact velocity of 4 m/s.

The tester equipment permits direct production of an impact compression diagram of the sample in the force-deformation coordinates. The image of the diagram that develops on the screen of the oscillograph double-beam cathode tube is photographed on 9 x 12 cm film.



The block diagram of the photoelectron testing equipment is given in publication [6].

The calibration testing of the impact compression oscillograms consisted of photographing the loading of the piezoquartz testing sensor with a static reference load of 500 kg.

Twelve batches of samples with nine variously oriented samples in each batch were tested for impact compression with the same loading regime. Six batches of samples were made so that the compression forces in testing were in the tangential plane. The axes of the samples in the remaining six batches were arranged in a radial plane. The angle between the direction of the compressing force and the direction of the fibers was 0, 15, 30, 40, 45, 50, 60, 75 and 90°.

In order to obtain comparable results from tests with different orientation, it is necessary to preserve the same dimensions and shape of all the samples, in addition to the same loading regime. GOST 6336-52 stipulates samples of varying length for compression along and transverse to the fibers. The samples tested in the preliminary experiments showed a considerable loss of stability in impact compression transverse to the fibers. The length of these samples was therefore reduced and the dimensions 2 x 2 x 2 cm were adopted for all the samples.

Figure 3.16 shows photographs of the destroyed pine samples in impact compression.

Figure 3.17 presents the characteristic oscillograms of the tests. The scale of the oscillogram differs and is indicated on the y-axis. Figure 3.17 a illustrates the diagrams for tangential, while figure 3.17b illustrates the radial, samples. As the angle changes between the axis of the sample and the fiber direction, the nature of the compression diagram also changes. Corresponding changes were also observed in the form of destruction of the samples. Figure 3.17 c presents a compression oscillogram along the wood fibers ( $\alpha=0$ ). /96

With compression at angles from 0 to 40° (in a tangential plane and at 45° angle) a sharp increase is visible on the oscillograms, and then a drop in the force. These diagrams conform to brittle failure of the samples that are thus separated into several parts. Failure occurred primarily by shearing along the fibers in the areas inclined to the sample axis. In these diagrams, the repeated increase in force



Figure 3.16. Photographs of Pine Samples (Tangential Plane) after Testing for Impact Compression left--along fibers, then at angle of  $15^\circ$ ,  $30^\circ$ ,  $45^\circ$ ,  $60^\circ$ ,  $75^\circ$  and  $90^\circ$  to direction of fibers.

is linked to wedging of parts of the destroyed sample between the support and the striker, and therefore should be ignored.

In this group of oscillograms, the ultimate strength of wood is determined by dividing the maximum force by the area of the sample section measure before it was tested.

The process of impact compression is somewhat more complicated for the remaining directions, and consequently, the processing of the corresponding oscillograms is also. On the oscillograms of this second group, the curves of deformation with definite values of the stresses pass into oscillating, almost horizontal sections. In these cases, the samples generally did not experience strict failure, i.e., were not divided into parts. They merely received significant residual deformations.

The nature of plastic deformation is somewhat different for radial and tangential samples.

The tangential samples experience a loss in stability of the late wood layers. Protruding folds appear on their lateral edges, parallel to the tangential plane. These folds pass parallel to the fibers, usually on the side of swelling of the annual layers. Small cracks are visible in places on the early wood (see fig.3.16).

The radial samples behave differently. Pressing of the wood in the direction of the annual layer radii is noticeable here. The layers of early, weaker wood are seemingly squeezed out, forming wavy projections on the lateral edges of the cubes. These projections are arranged on the edges parallel to the radial plane.

/97

There is another distinguishing feature among the two groups:

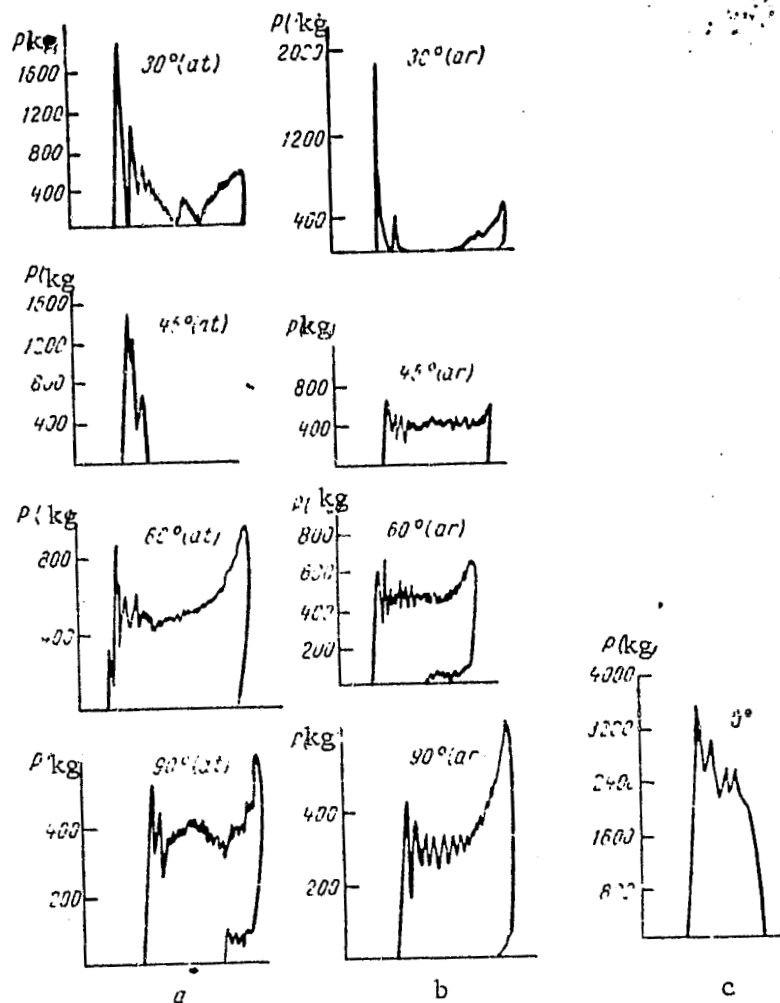


Figure 3.17. Oscillograms of Impact Compression of Pine  
a--tangential plane from top to bottom:  
 $\alpha = 30, 45, 60$  and  $90^\circ$ ; b--radial plane  
from top to bottom:  $\alpha = 30, 45, 60$  and  $90^\circ$ ;  
c--along fibers ( $\alpha = 0$ ).

in those samples that underwent brittle failure, i.e., were divided into parts on impact, the angles between the base and the lateral sides remain right angles after the failure. Apparently, the shear angles that inevitably accompany compression at an angle to the symmetry axes in anisotropic materials, in this case have the nature of elastic deformations. The plastic samples experience fairly significant residual angular deformations. Thus, for example, for a sample whose axis in the radial

plane forms a  $60^\circ$  angle with the fiber direction, the coefficient of mutual influence (ratio of the shear angle to the linear deformation) in impact compression roughly equals 0.6. In the elastic region, this coefficient must comprise 0.4 for pine.

The process of impact compression at an angle over  $45^\circ$ , and in a radial plane, over  $40^\circ$ , is thus reduced to plastic deformation of the sample by its shortening and skewing (shear).

The oscillating parts of the compression diagram can be explained in these cases by the discrete spasmodic nature of the plastic deformation of wood.

The loss of stability and the sudden formation of folds in the tangential samples result in sharp fluctuations in the amount of force on the diagrams. The amplitude of these fluctuations is comparatively great. The number of peaks on the diagrams is generally lower than for radial samples. The alternate "extrusion" of the layers of early wood in the radial samples results in stress fluctuations that lower amplitudes are characteristic for.

It is important to note that the number of fluctuations in the amount of force on the horizontal section of the compression diagram of radial samples is roughly equal to the number of layers of early wood that are alternately squeezed out during impact compression of the sample.

The increase in the ordinates on the last section on certain plastic diagrams can apparently be the same as the third phase of static compression of wood. It is explained by the great strength of the late parts of the annual layers that are involved in the work on this section.

It was shown in the work of B. P. Dutov that the force fluctuations on the deformation curve cannot be caused by changes in the contact force that are linked to the application of natural oscillations in the working organs of the testing unit. The discrete change in the resistance of the sample as it is deformed can therefore serve as a plausible explanation of these fluctuations.

The considerations given above made it possible to adopt the following order for processing oscillograms of the second group ("plastic").

Besides the maximum force that can be measured at the top of the first peak, a force was also noted that equals the ordinate of the average line of the oscillating curve section. The first force during which plastic deformation of the sample apparently begins, is used to compute the ultimate strength of wood. The second force in which one can consider that the plastic deformation continues, is used to compute the characteristics we have conditionally called the yield stress. /99

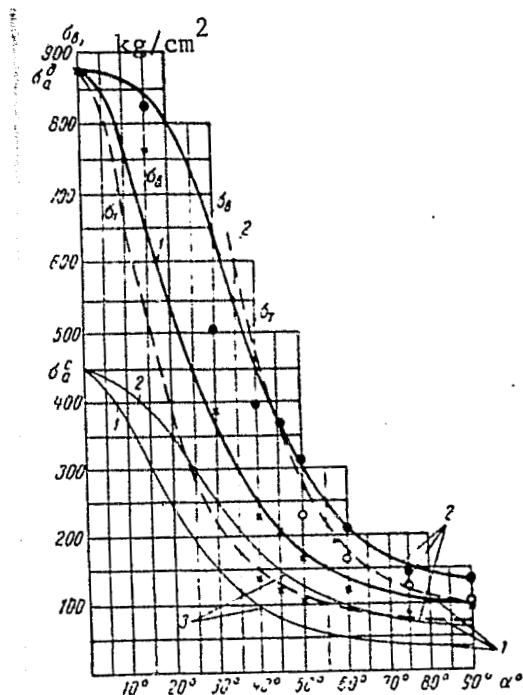


Figure 3.18. Strength of Pine in Impact Compression Depending on Angle of Incline of Fibers.  
Experimental data: ●, ○--in tangential plane; X, +--in radial plane. Curves constructed according to formula (1.22): 1--for radial; 2--for tangential plane; 3--static compression.

Of course, the division of the compression diagram and the nature of sample failure into two groups called brittle and plastic here, in actuality is not so definite. The transition occurs gradually, as the angle of fiber incline rises (fig. 3.17). Compared to the static compression, many features of deformation are less pronounced in impact, and division into two different groups is more noticeable.

Figure 3.18 presents the results of the tests in a graph. The curves were constructed according to formula (1.22). The average values for the strength characteristics obtained from the experiment are plotted as points. The solid lines depict the curves for change in the ultimate strength  $\sigma_B$ , while the dotted lines are constructed for the yield stresses  $\sigma_T$ .

Comparison of the curves with the corresponding points indicates that the tensorial formula (1.22) reflects the laws governing the changes in wood strength in impact compression in different directions.

The tests conducted with impact velocity equal to 4 m/s provide the grounds to assume that even with high velocities, formula (1.22) can conform to reality.

The curves (fig. 3.18) that were constructed from the tensorial /100 formula coincide better with the experimental data in those cases where plastic failure of the material occurs. Thus, the coincidence is best for angles over  $30^\circ$ , and is better for the radial plane (curves 1) than for the tangential (curves 2). The almost ideal coincidence with the experimental results produces a curve for the change in yield stresses of radial samples for angles over  $45^\circ$ .

Figure 3.18 presents curves of the change in pine strength in static compression (curves 3) for comparison. The curves were constructed for roughly the same wood that the present studies were conducted for (see fig. 3.4).

For all angles of fiber incline, the resistance to impact compression averaged 2.45-fold higher for the radial and 2.17-fold higher for the tangential plane than the corresponding resistance of wood to static compression.

If one ignores the difference in the properties of wood in the radial and tangential directions, i.e., accepts the assumption on the transverse isotropy of wood, then formula (1.22) remains unchanged. The effect of the angle of fiber incline is determined by the curve passing between the solid curves for the change in impact strength plotted on fig. 3.18. All the ordinates of this curve will average 2-2.5-fold higher than the ordinates of the curve corresponding to the static loading of wood.

With impact velocity equal to 4 m/s, the curve of standardized

resistances of wood passes higher than in static compression. The ratio of the ordinates can be assumed to be roughly equal to from 2 to 2.5 units.

#### 11. Stretching of Uniaxially Oriented Crystal Polymer Films

Crystal polymer materials acquire considerable anisotropy of mechanical properties after large deformations in uniaxial stretching. The development of a neck during stretching of samples of these polymers is a phase transformation of unfavorably oriented crystal microformations into favorably oriented in relation to the force field of the formation [30]. The new samples cut from the neck reveal very pronounced anisotropy during stretching. During stretching in a direction that coincides with the direction of primary stretching, the sample's deformation is slight, but the strength is increased. The samples cut in a transverse (in relation to the primary stretching) direction reveal great deformation and low strength.

Ordering of the polymer structure during its orientation results in anisotropy of the mechanical properties that has not only a quantitative but also a qualitative nature. During stretching in the orientation direction, the strength is determined by the forces of chemical bonds in the chain molecules. They are arranged more or less in parallel. During stretching in a transverse direction, the strength of the oriented polymer is mainly determined by the forces of intermolecular interaction. These forces are considerably smaller than the first. /101

The work of T. A. Dikareva and G. L. Slonimskiy [30] presents the results of stretching tests to rupture of polymer films that have been uniaxially oriented by preliminary stretching. The authors obtained data on the size of the rupture force depending on the angle between the directions of orientation (preliminary stretching) and the stretching force. In figures 3.19-1,2 and 3 these data are presented in the form of points whose ordinates equal the average amounts of ultimate strength  $\sigma_p$  that refer to the original area of the sample sections. Figure 3.19a (curve 1) depicts the results of testing a technical caprone film of plant manufacture that was oriented by 500% preliminary stretching. Figure 3.19 b illustrates (curve 3) the tests of

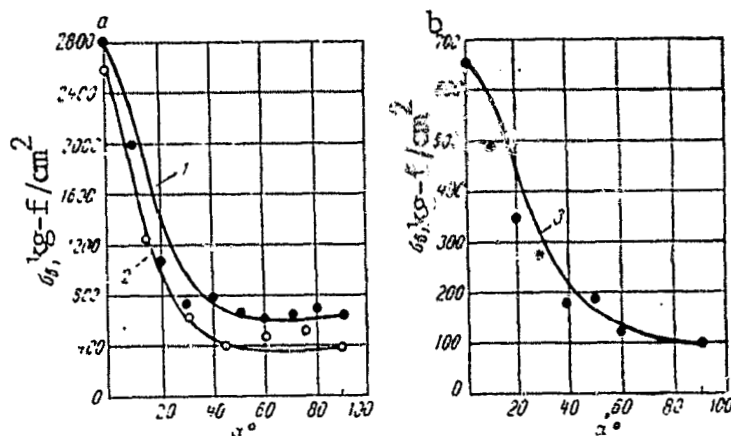


Figure 3.19. Change in Ultimate Strength of Films

1--caprone; 2--polyethylene terephthalate; 3--polyethylene depending on angle  $\alpha$  between direction of stretching and direction of orientation of the film. Experimental average quantities of ultimate strength: ●--for caprone and polyethylene; ○--for lavsan.

high pressure polyethylene film made at the Okhtensk chemical plant and oriented by 300%, and then to 700%. Figure 3.19a (curve 2) illustrates the polyethylene terephthalate (lavsan) films made in the Scientific Research Institute of Plastics by the pressure casting method with rapid cooling and orientation by 700% at 60° temperature. /102 The molecular weight of all three films is 20,000. All the tests were done by the authors of publication [30] in the laboratory of the Institute of Organoelemental Compounds of the USSR Academy of Sciences on samples 1.5 mm wide and 10 mm long with film thickness from 40 to 70  $\mu$ . Tests were done on a Polani instrument at 20° temperature. Each point on the figures complies with the average arithmetical amount of the ultimate strength obtained as a result of testing from 15 to 20 samples. In figure 3.19, the curves were constructed [15] according to formula (1.22). As is apparent from the figures, this formula, based on the assumption on tensoriality of the strength specifications, also conforms to the results of testing anisotropic films of oriented polymers.

## 12. Fiber Glass-Reinforced Plastics

The synthetic high-strength plastics that are reinforced with



glass fiber, spun glass thread or fiber glass fabric possess fairly significant anisotropy.

The author of [12] studied the following fiber glass-reinforced plastics:

1. Fiber glass-reinforced plastic of cold hardening on polyester resin PN-1 made of fiber glass fabric brand T (GOST 8481-57). The sheet consisting of 31 layers of fiber glass fabric containing 50-55% resin, 1000 x 880 x 10 mm in size, was fabricated by the method of contact forming at 23°C. The employed hardener was 3% hyperize and 8% NK accelerator (8% solution of cobalt naphthenate in styrene).

Ten of these sheets were tested. Samples were made from each sheet for all types of tests.

Besides the indicated plates, a plate 5 mm thick, with 30x50 cm format, from the same material was tested for shear.

In order to determine the ultimate strength in compression perpendicular to the layers, samples were made from plates 15 mm thick with 20 x 20 cm format.

2. SVAM\* type fiber glass-reinforced plastic on epoxy-phenol binder No. 64 consisting of 70% epoxy resin ED-6 and 30% phenol aldehyde resin.

SVAM fiber glass-reinforced plastic is made by pressure molding at 130 kg/cm<sup>2</sup> with heating to 160° of sheets of laminated fiber glass sheet crossed structure. The laminated fiber glass sheet was produced by winding fiber drawn from a glass-melting vessel on a rotating drum with simultaneous gluing of the glass fiber with the binding agent. In order to produce the crossed structure of the veneer sheet with ratio of 1:5, after winding seven rows of glass fiber, the drum was stopped and the fiber was cut off on the forming drum. The sheet was then turned and the fiber of the next three rows was wound in a direction /103 perpendicular to the first. The sheet was then turned by 90° and the fiber of the last eight layers was wound in the same direction as the first seven. In the laminated fiber glass sheet that resulted from this winding of the fiber layers, the direction of the three middle layers was perpendicular to the direction of the outer layers. The

---

\*Fiber glass-reinforced anisotropic material [21].

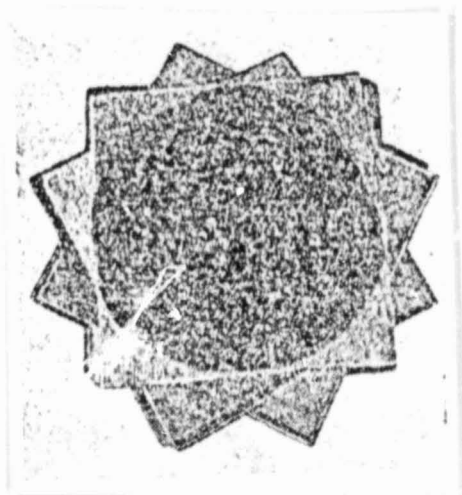


Figure 3.20. Photograph of Plate of Isotropic SVAM with "Stellar" Arrangement of Layers of Anisotropic Glass Laminated Sheet

ORIGINAL PAGE IS  
OF POOR QUALITY

overall structure of 7:3:8 guarantees a ratio of 1:5 in which one-fifth of the fibers are perpendicular to the others.

Several SVAM versions were made on epoxy-phenol resin. They differed in nature of reinforcement, and consequently, in the degree of anisotropy. Two versions of sheets were pressed from the laminated sheet that was reinforced with glass fiber in a ratio of 1:5: with 1:1 laying in which all the laminated sheets were mutually perpendicular, and with 1: 5 laying in which all the laminated sheets had the same fiber direction. The third version of this material was pressed from a laminated sheet with 1:13 glass fiber ratio and laying of the laminated sheets also in a 1:13 ratio. Only one sheet was made of this very anisotropic material. The data on its strength that were obtained in testing a small number of samples therefore are approximate. In addition, two sheets were fabricated with "stellar" laying of the laminated sheet in which the angle between the fiber directions in adjacent layers was  $30^\circ$  (fig. 3.20).

All types of SVAM on epoxy-phenol binder were made in the form of sheets 100 x 500 x 5 mm in size or 1000 x 500 x 10 mm with resin content from 30 to 50%.

All the sheets, except the sheets with fiber ratio of 1:13, were made of laminated glass sheets with a 1:5 fiber ratio. The sheet

molding regime was as follows: heating to 60-70° for 15 min., hold time at 60-70° (compact sheets of mold) for 60 min., elevation of pressure to 200 atmospheres and temperature to 150-160° for 10 min., and hold time at 150-160° with this pressure for 12 minutes.

3. SVAM on binder of Butvar-phenol resin BF-4 with fiber ratio in the sheet of 1:1. The sheets were 1000 x 500 x 5 mm in size. The sheets were made of laminated fiber glass sheet with 1:1 fiber ratio with a structure of 6:9:3. There was a roughly 30% resin content in the sheet. The molding regime was the same as in SVAM on ED-6 binder. /104

The glass fibers in the SVAM were  $15 \pm 2 \mu$  thick. Fibers were made of alkali-free boron-containing glass. The laminated fiber glass sheets were 0.35-0.4 mm thick.

It should be noted that the technology for producing SVAM had still not been completely perfected by the plant when these materials were made. The absolute values of the obtained mechanical characteristics in a number of cases were therefore below the optimal [21]. These absolute values do not have a lot of importance for the purposes of our study since it is quite understandable that all the obtained laws will be suitable for fiber glass-reinforced plastics of any high strength if the latter possess orthogonal anisotropy of the sheet structure. SVAM fiber glass-reinforced plastic in this case is viewed not only as construction material, but also as a model of an anisotropic laminated plastic whose structure and degree of anisotropy are easily modified during manufacture.

Publication [12] presents tables for the statistical processing of all testing results from fiber glass-reinforced plastics. They present the number of samples for each orientation (10-20), variation coefficients (4-12%) and the accuracy indicator not exceeding 5%.

Strength in stretching. The ultimate stretching strength is usually given as the main characteristic of mechanical properties, usually used to judge the advantages of the construction material and its suitability for certain purposes.

Testing of fiber glass-reinforced plastics for stretching is of especial interest because the anisotropy of the material is revealed most strongly from the results of this testing: in different structural directions, the ultimate stretching strengths differ more strongly

than in compression, shear or bending. Thus, testing for stretching with determination of the ultimate strength is one of the most important mechanical tests of fiber glass-reinforced plastics.

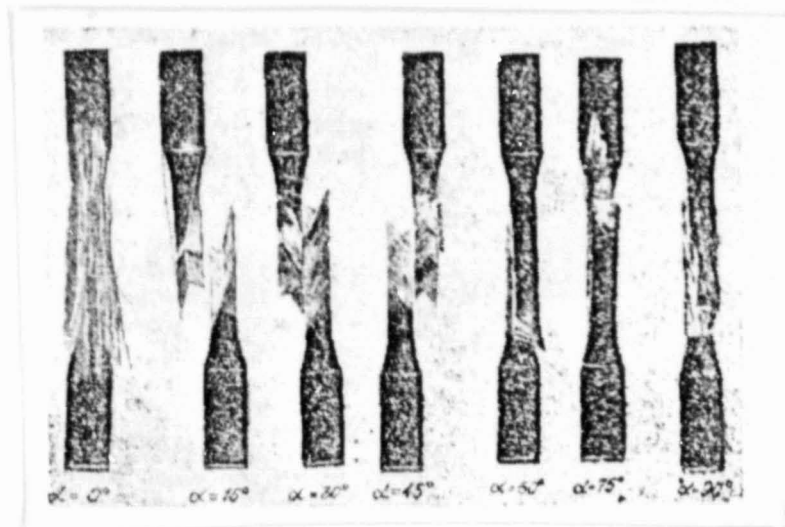


Figure 3.21. Photographs of SVAM Samples Cut at Different Angles  $\alpha$  to the Fibers and Destroyed by Stretching

Samples were taken for testing according to GOST 9-55 to determine the ultimate strength in stretching laminated plastic sheets of organic origin. In addition, samples corresponding to GOST 1143-41 "Methods of Testing Physical and Mechanical Properties of Aviation Plywood and Aviation Veneer Sheets" were used for comparison in testing cold-hardened fiber glass-reinforced plastics on PN-1 binder. These samples were called wide.

/105

Clamps with wedge-shaped clamping jaws that moved on a set of rollers were used for all the stretching tests. These clamps make it possible to increase the clamping force of the sample and hold it reliably in the clamps with a shallow notch of the jaw surface that does not cause a significant concentration of stresses at the clamping sites.

The majority of samples were destroyed in the working section. The testing results from those samples that were destroyed at the clamping sites were not included in the processing of the testing results.

Figure 3.21 presents SVAM samples on epoxy-phenol binder with 1:5 fiber ratio that were cut at different angles to the direction of the glass fiber and were destroyed by stretching.

A characteristic feature of the SVAM type materials is failure on the areas parallel to the fibers for all sizes of angles between the direction of the stretching force and the direction of the fibers.

Fiber glass-reinforced plastic on PN-1 binder made of woven linen fabric was destroyed in a different manner. When the direction of the stretching force coincides with the direction of the threads in the phase or the fabric weft, rupture occurs as for brittle metals, on the area perpendicular to the sample axis. When this fiber-glass-reinforced plastic is stretched at a  $45^\circ$  angle to the direction of the threads in the fabric warp (in a diagonal direction), a drop occurs in the load. It is caused by the appearance of a noticeable neck in the sample. This neck is unique because its appearance is accompanied by a thickening in the direction perpendicular to the sheet plane. The gradual, local thickening of the sheet then results in its stratification. Rupture of individual (initially outer) layers subsequently occurs.

The results of determining the ultimate strength of fiber glass-reinforced plastic of cold hardening made of T fabric on PN-1 binder according to GOST 4649-55 were higher than the results of testing the wide samples.

All the tests were done on the IM-12-R tensile-testing machine designed by TsNIITMASH [Central Scientific Research Institute of Machine Construction Technology]. The movement velocity of the clamps was 16 mm per minute.

Figure 3.22 graphically illustrates the testing results of this fiber glass-reinforced plastic. The curve was constructed from the tensorial formula (1.22). As in all the following figures, the region of actual spread of the experimental data is hatched. The points that correspond to the average ultimate strengths from the tests with  $\alpha=30^\circ$  and  $\alpha=60^\circ$ , as is apparent from the figure, lie very close to the curve. This confirms the applicability of the tensorial formula for this case.

The summary graph in figure 3.23 presents results of testing SVAM on EF-4 binder with 1:1 fiber ratio, according to GOST 4649-55. The

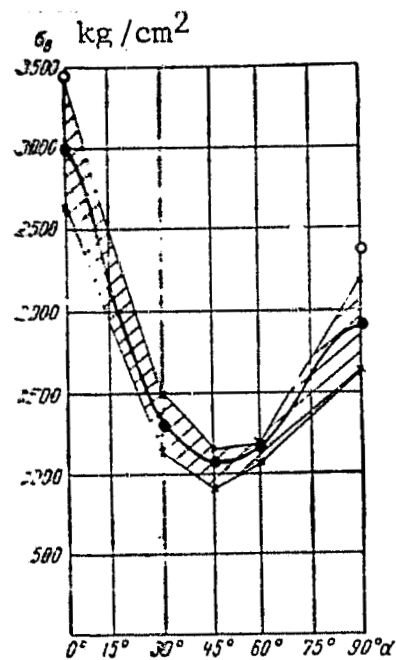


Figure 3.22. Ultimate Strengths in Stretching Fiber Glass-Reinforced Plastic of Cold Hardening ●--average value; X--extreme value from testing wide samples (GOST 1143-41); ○--average from testing samples according to GOST 4549-55. Hatched zones are actual scattering of results.

difference between the ultimate strength values at  $\alpha=0$  and at  $\alpha=90^\circ$  for this material shows that the laying of the laminated sheet did not quite conform to the assigned 1:1 fiber ratio. There were actually more glass fibers arranged in the direction of the casing fibers than in the perpendicular direction.

SVAM with 1:1 fiber ratio on epoxy-phenol binder (fig. 3.23, curve 1 and figure 3.24) was fabricated more carefully. The sheet was 10 mm thick. Here the average value of ultimate strength with  $\alpha=0$  and with  $\alpha=90^\circ$  was the same. Despite the equality of the ultimate strengths along and transverse to the sheet, the anisotropy of these materials was very significant: SVAM on BF-4 binder in the diagonal direction (with  $\alpha=45^\circ$ ) has ultimate strength 4 times lower, and on the epoxy-phenol binder, 3 times lower than the ultimate strength in the

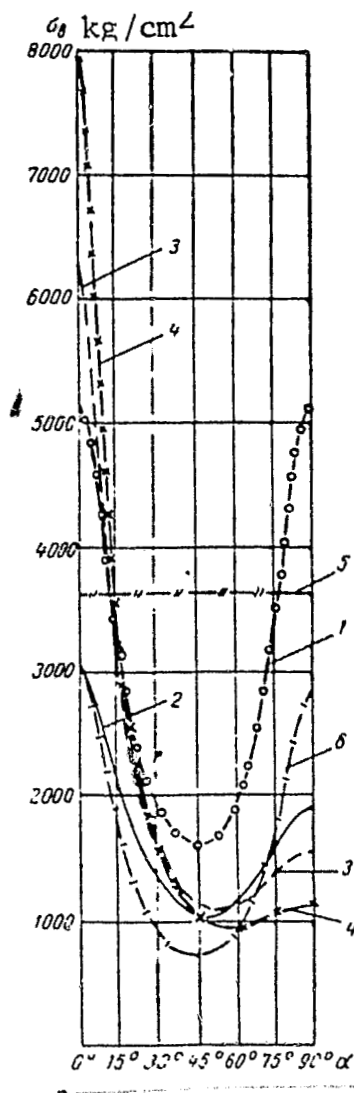


Figure 3.23. Summary Graph of Strength Anisotropy of Fiber Glass-Reinforced Plastics in Stretching

1,3,4,5--SVAM on epoxy-phenol binder (fiber ratios: 1--1:1; 3--1:5; 4--1:13; 5--"stellar" structure); 2--fiber glass-reinforced plastic of cold hardening made of woven linen fabric (T); 6--SVAM on Butvar-phenol binder BF-4 with 1:1 fiber ratio.

longitudinal direction (with  $\alpha=0$ ). It is evident that the epoxy-phenol binder that guarantees higher strength of the material than BF-4, at the same time provides somewhat lower anisotropy. This can be explained by the fact that in a diagonal direction in which the glass fiber has relatively little participation in the absorption of the load, the material strength is mainly determined by the resin mechanical properties.

For SVAM with 1:1 fiber ratio, the diagonal direction coincides with the material's symmetry axis. The strength in this direction is minimal. With another fiber ratio, the least strength occurs with a somewhat larger angle with the fiber direction. Thus with a 1:5 fiber ratio, the minimum strength is obtained with  $\alpha=50^\circ$ , and with fiber ratio of 1:13 with  $\alpha=60^\circ$  (see figure 3.23, curves 3 and 4).

Comparison of the curves constructed according to the tensorial formula (1.22) with the average data of the testing results for variously oriented samples confirms the applicability of this formula to compute the ultimate strengths of all the tested fiber glass-reinforced plastics depending on the orientation of the stretching force [12].

The Madison Laboratory of Forestry Products (United States) used another, more complicated formula [113] for these same purposes. However, the results that were obtained with this formula for the fiber

glass-reinforced plastics are very close to the results of formula (1.22).

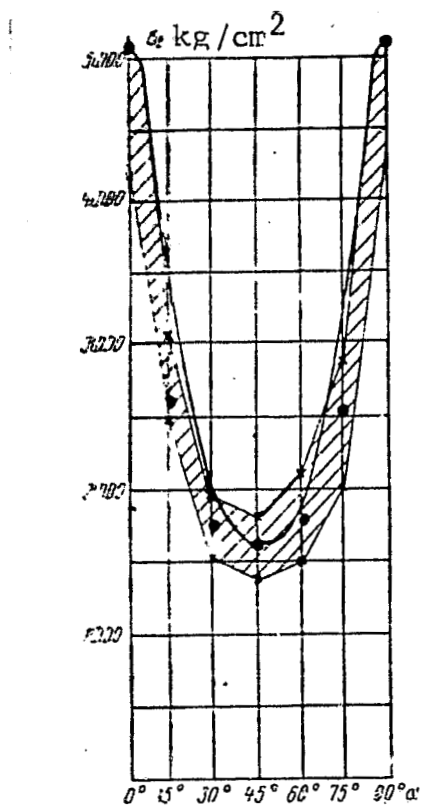


Figure 3.24. Results of Stretching Testing of SVAM 10 mm Thick on Epoxy-Phenol Binder with Fiber Ratio of 1:1  
●--average and X--extreme values of ultimate strength.

Figure 3.25 presents two curves for comparison: curve 1 was constructed according to tensorial formula (1.22), curve 2 used the formula of the Madison Laboratory of Forestry Products, which has the following appearance in our designations:

$$\sigma_b = \frac{1}{\sqrt{\frac{\cos^4 \alpha}{\sigma_0^2} + \frac{\sin^4 \alpha}{\sigma_{90}^2} + \frac{\sin^2 2\alpha}{4\tau_0^2}}} \quad (3.7)$$

Both curves were constructed according to the data obtained in the



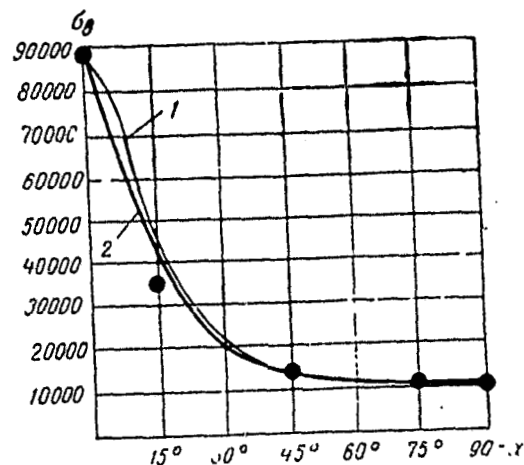


Figure 3.25. Results of Stretching Testing of American Fiber Glass-Reinforced Plastic Fabric [107] 1--curve constructed according to tensorial formula (1.22); 2--curve according to Madison laboratory (3.7); ●--average ultimate strengths in lb per sq. inch.

Madison laboratory for stretching testing of fiber glass-reinforced plastic made of 143-114 fabric on polyester resins. They practically coincide with all force orientations.

The ultimate strengths of this fiber-glass-reinforced plastic are as follows [113]:  $\sigma_0 = 6150 \text{ kg/cm}^2$ ;  $\sigma_{45} = 966 \text{ kg/cm}^2$  and  $\sigma_{90} = 700 \text{ kg/cm}^2$ .

Compression. Cold-hardened fiber glass-reinforced plastic was tested for compression for comparison by two methods, according to GOST 4651-49 and in the device of I. P. Boksberg [5,12].

The samples for testing in the device were made so that the direction of the compressing force with the direction of the fiber glass fabric warp threads comprised the angle  $\alpha$ . It was assumed to be successively equal to 0, 15, 30, 45, 60 and 90°. According to GOST 4651-63, samples were only tested with  $\alpha = 0, 45$  and 90°. All the tests were done on a universal testing machine UIM-50 with movement velocity of the pad 4 mm/min.

The results of testing the fiber glass-reinforced plastic fabric of cold hardening for compression in the device are presented in fig. 3.26. The points correspond to the average values of ultimate strength

of the variously oriented samples. The region of actual scattering of the testing results is hatched. The solid curve was constructed from the tensorial formula (1.22). The dotted curve was constructed from the same formula for the testing results according to GOST 4651-63.

As is apparent from this graph, the tensorial formula agrees well with the experimental data for the examined material.

Comparison of the curves that were computed from the tensorial formula for the two compression testing methods shows that the testing results in the device with all sizes of angle  $\alpha$  are exaggerated as compared to the testing results according to GOST 4651-63.

It is generally known that the ultimate strength increases with a decrease in the dimensions of the tested samples. Something different happens here: the ultimate strengths of the small samples (10 x 10 x 15 mm) are lower than the ultimate strengths of large samples (10 x 30 x 70 mm). This difference, consequently, cannot be explained by the scale factor. It permits the assumption that when samples were tested in the device, their selected width was too great (see section 7).

The type of failure of the cold-hardened fiber glass-reinforced plastic fabric samples during compression depends little on the angle between the direction of the fiber glass fabric warp and the direction of the compressing force. This is characteristic for weakly anisotropic materials.

For a strongly anisotropic SVAM, for all angles between the fiber direction and the direction of the compressive force, the failure plane coincides with the plane that is parallel to the fibers. The external appearance of the destruction is similar to the appearance of crystal destruction. Crystals are also always characterized by failure in the soldering plane.

Figure 3.27 presents a summary graph for the testing results of fiber glass-reinforced plastic for compression. The nature of these curves shows that during compression, anisotropy of SVAM appears. It requires the intent attention of the designer and a special approach in using this material.

Figure 3.28 presents the testing results for stretching (according to GOST 4649-55) and for compression (according to GOST 4651-63) of

cold-hardened fiber glass-reinforced plastic fabric made of AS TT (b) -C- O brand fabric based on polyester resin PN-3. These tests were done by E. V. Ganov [24] under conditions of a spatial problem. The

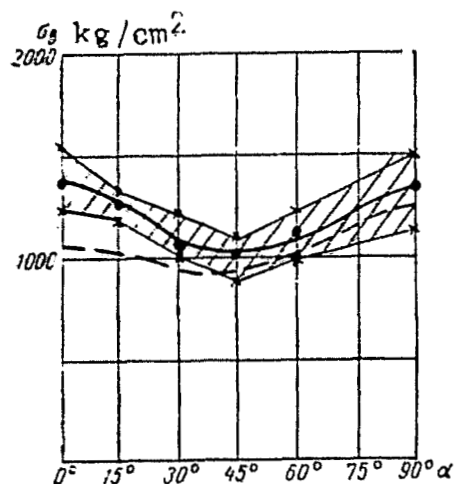


Figure 3.26. Results of Testing Cold-Hardened Fiber Glass-Reinforced Plastic Fabric for Compression in Device  
Dotted curve--for testing results according to GOST 4651-63.

solid lines on this figure show the testing results for stretching, and the dotted for compression. These lines restrict the reflecting surface, while the point vector radii of this surface equal the ultimate strengths in the corresponding direction (including the direction perpendicular to the sheet plane). Both surfaces conform to formula (1.20) and provide an approximate idea about the resistance of the fiber glass-reinforced plastic to the perpendicular stresses in a uniaxial stressed state that is randomly oriented in relation to the three axes of symmetry of the orthotropic fiber glass-reinforced plastic.

Testing for shear and simple shearing. The all-union 1964 standard for methods of testing plastics of organic origin has OST 11044-38 /111 "Determination of Temporary Shear Resistance." It is used to produce double shear of a 10 x 10 mm square section sample that is tightly clamped into a device.

The technique developed for testing plywood [5] is also customarily used to test for double shear a tightly clamped sample, but the device

is equipped with changeable chuck jaws that allow testing of a sample whose thickness equals the sheet thickness and can be smaller or greater than 10 mm. This device can be used to test samples made without disrupting the surface layer of material over 10 mm thick, as well as samples made of material less than 10 mm thick. This is not possible according to OST.

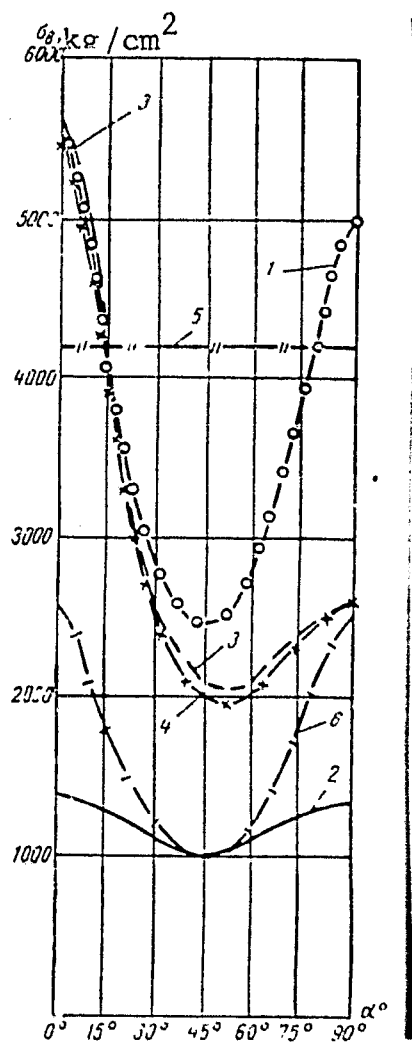


Figure 3.27. Summary graph of Anisotropy of Fiber Glass-Reinforced Plastics in Compression

1,3,4,5--SVAM on epoxy-phenol binder (fiber ratio: 1--1:1; 3--1:5; 4--1:13; 5--"stellar" structure); 2--cold-hardened fiber glass-reinforced plastic fabric; 6--SVAM on BF-4 with 1:1 fiber ratio.

Figure 1.1 shows three possible types of shear testing, i.e., determination of the material's resistance to tangential (shearing) stresses: shear in the sheet plane, shear perpendicular to the sheet plane, and simple shearing in the layer (interlayer shear) (see section 4).

The amount of shear resistance in the sheet plane was experimentally determined for 7 directions.

The tests were conducted on a UIM-50 machine with 5 T on it and movement velocity of the pad about 4 mm/min.

The destructive load was considered the greatest load after which the load-bearing capacity of the sample was exhausted. Usually the subsequent drop in load was accompanied by a snap and sudden shear on the areas where

the shearing forces were active.

Figure 3.29 presents a photograph of the SVAM fiber glass-reinforced samples with 1:13 ratio that were destroyed by shear in the sheet plane with all seven orientations in relation to the fibers.

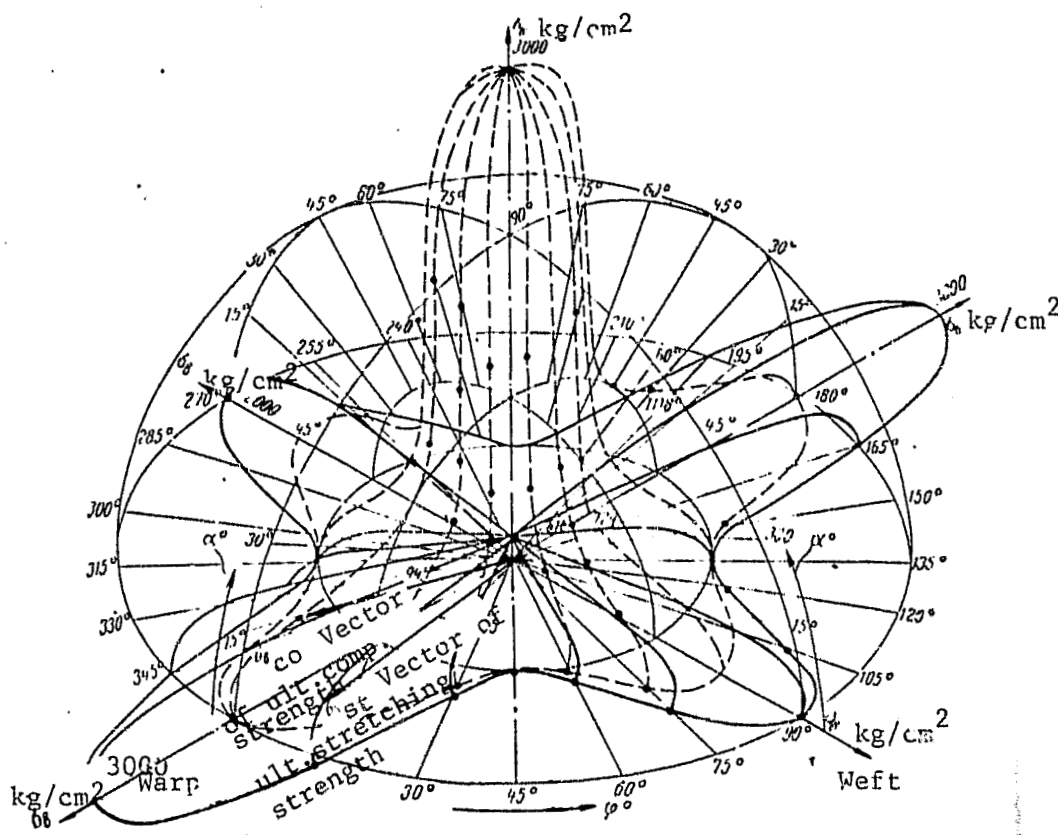


Figure 3.28. Spatial Graph of Testing Results of Cold Hardened Fiber Glass-Reinforced Plastic Fabric for Stretching and Compression (according to E. V. Ganov)

/112

$\alpha$  -- angle between plane of fabric and direction of force;  $\phi$  -- angle between direction of waft and projections of direction of force on fabric plane.

Figure 3.30 presents the results of testing for shear in the sheet plane of fiber glass-reinforced plastic made of T fabric on PH-1 binder. The testing results for 10 mm thick sheets are quite reliable. As is apparent from this figure, the difference in the amount of resistances immediately for sheets 5 mm and 10 mm thick is not great. Almost everywhere it is in the limits of the actual spread of the testing results. The curve that is constructed according to the tensorial formula (1.24), for a 10 mm thick sheet passes with all angles of incline, close to the points that conform to the average testing results.

/113



Figure 3.29. Photographs of SVAM Samples with 1:13 Fiber Ratio That Were Destroyed in the Device by Shear in the Sheet Plane with Seven Different Orientations in Relation to the Fibers

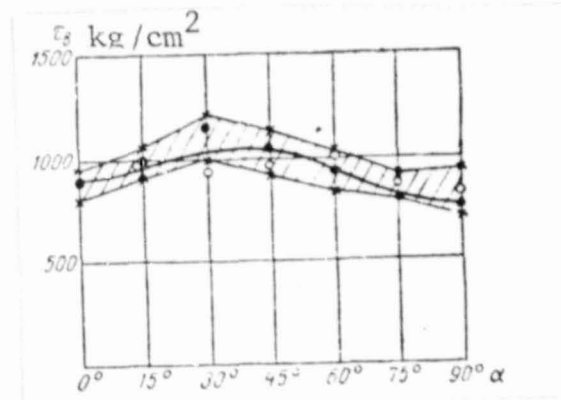


Figure 3.30. Results of Testing for Shear of Cold-Hardened Fiber Glass-Reinforced Plastic Fabric 5 mm Thick (O--average amounts of ultimate strength) and 10 mm (●--average amounts and x--extreme amounts of ultimate strengths).

Figure 3.31a and b present the results of testing for shear in the plane of SVAM layers on epoxy-phenol binder for sheets 5 and 10 mm thick. For this material, especially with 5 mm thickness (the area of crumpling is small), during testing of diagonal samples, there was considerable crumpling of the sample surface preceding shear. As a result of the crumpling, the shear area was considerably reduced. Apparently, this resulted in an underestimation of the ultimate strength /114 referring to the initial shear area. Figure 3.31 a shows two points for the diagonal direction. One conforms to the average ultimate strength  $\tau_{45}$  that is computed as the quotient from dividing the load

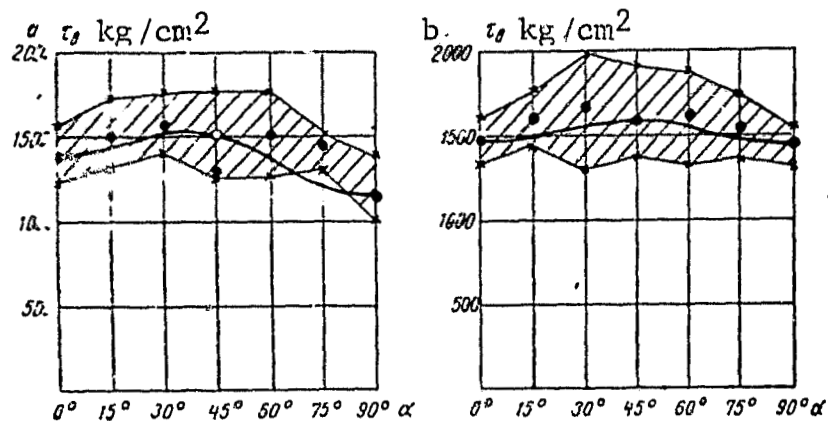


Figure 3.31. Ultimate Strengths in Shear in Plane of SVAM Sheet on Epoxy-Phenol Binder with 1:1 Fiber Ratio and Sheet Thickness  
a--5 mm; b--10 mm.

$P_{\max}$  by the initial shear area, equal to double the initial cross section of the sample. This point that is depicted on the graph by a hatched circle, lies very low. It clearly drops out of the general law governing the change in resistances. The other quantity of ultimate strength  $\tau_{45}$  is computed for  $\alpha=45^\circ$  by dividing  $P_{\max}$  by the doubled area of the sample cross section at the shear site measured after testing. The point illustrated by the circle is used to construct the curve in fig. 3.31a. This correction is not made for SVAM 10 mm thick, since the crumpling here is less significant. It is apparent from fig. 3.31 b that even in this case, if one considers the crumpling at  $\alpha=45^\circ$ , then the curve could be somewhat elevated, approaching the experimental results.

As is apparent from the cited graphs, the shear resistance in the sheet plane has comparatively little anisotropy. It has the maximum values for the directions that are close to the diagonal.

It is evident that under the influence of the transverse forces in the sheet plane, it is efficient to place the reinforcing glass fiber at a  $45^\circ$  angle to the direction of these forces. For the "stellar" fiber glass-reinforced plastic, as should be expected, the shear resistance is higher for all directions than for SVAM of another design (1:1 or 1:5). In figure 3.32, the approximate results of testing fiber glass-reinforced plastic of "stellar" structure are depicted in

the form of a curve that refers to the polar coordinates. Despite the small number of samples, the curve is close to the circle shown by the dotted line.

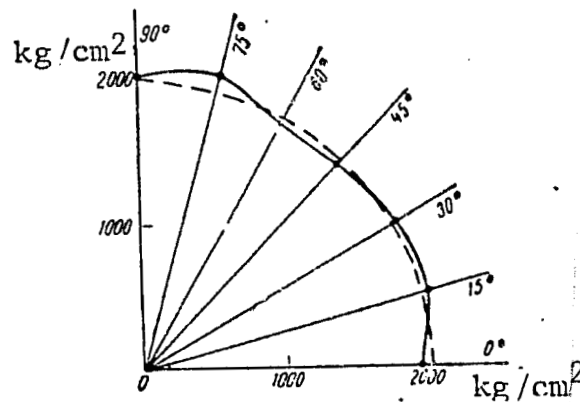


Figure. 3.32. Ultimate Strengths in Shear in SVAM Sheet Plane of "Stellar" Structure Depicted in Polar Coordinates  
 ———according to experimental data;  
 ---- --on the assumption of isotropy.

For a strongly anisotropic material (1:13) the greatest amount of shear resistance approaches the direction in which shear passes on the greatest number of glass fibers. Figure 3.33 shows the tensorial curves of shear resistance for all studied fiber glass-reinforced plastics. Figure 3.34 presents a comparison of the nature of curves for three types of testing for a strongly anisotropic fiber glass-reinforced plastic.

The shear testing results in the device do not yield the true amount of resistance of the anisotropic material to pure shear. At the same time, the method of shear testing in the device permits a judgment regarding the comparative strength of materials with constrained shearing in different directions.

When selecting the permissible tangential stresses to verify the strength of fiber glass-reinforced plastic for shear in the neutral layer during bending in the sheet plane, it is necessary to bear in mind that the absolute quantities of ultimate strength that were obtained from the shear tests in the device are inaccurate.



Another type of device that was suggested by A. L. Rabinovich [64] for shear testing of samples of more complex configuration has the advantage that crumpling of the sample surface is missing; however, the stress there is distinguished from pure shear.

Samples of other dimensions, and consequently, another device [5], are used for shear testing under the influence of forces perpendicular to the sheet plane. This device is designed to test sheets from 4 to 6 mm thick. The sample whose thickness equals the sheet thickness, has the shape of a rectangular parallelepiped whose area equals [illegible] /116 mm. The comparatively great width of the sample is selected to reduce the stress of crumpling on the surface.

In order to compute the ultimate strength in shear perpendicular to the sheet plane depending on the angle between the shear area and the direction of the casing fibers, chapter 1 presents tensorial formula (1.25). In this case, the direction of the shearing force with different values of angle  $\alpha$  coincides with the direction of one of the axes of symmetry, that which is perpendicular to the sheet plane. The

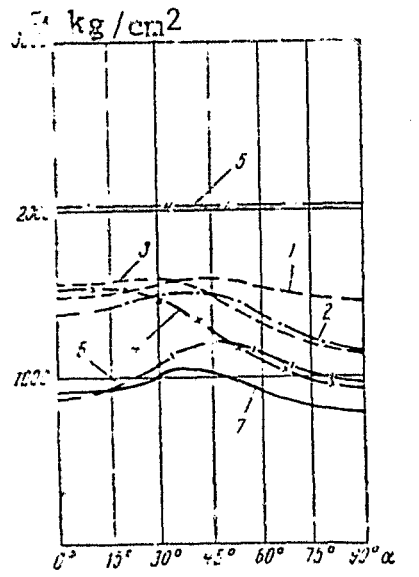


Figure 3.33. Summary Graph of Anisotropy of Fiber Glass-Reinforced Plastic in Shear  
1,2,3,4,5--SVAM on epoxy-phenol binder with sheet thickness 10 mm;  
[continued on next page]

[continued from previous page]  
 fiber ratio: 1--1:1; 3--1:5; 4--1:13;  
 5--"stellar" structure; 2--thickness  
 of sheet 5 mm (1:1 ratio)(inaccurate);  
 6--SVAM on BF-4 (ratio 1:1); 7--cold-  
 hardened fiber glass-reinforced plastic  
 fabric.

censorial formula therefore has another appearance than during shear in the sheet plane where the direction of the shearing force changes depending on the angle  $\alpha$  and continues to lie in the symmetry plane, but only coincides with the direction of the symmetry axis for two values.

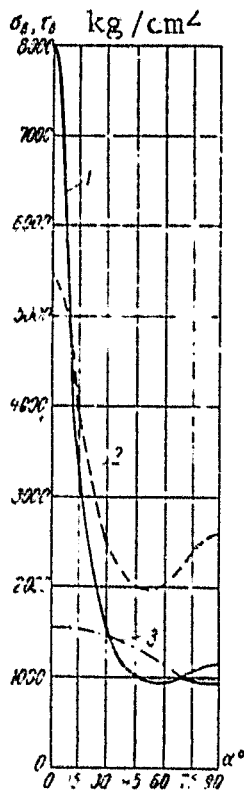


Figure 3.34. Dependence of Ultimate Strength on Orientation of Samples for SVAM with Fiber Ratio 1:13.

1--in stretching; 2--in compression; 3--in shear.

As the experiments showed, the amount of shear resistance in the direction perpendicular to the sheet plane remains almost constant with all orientations of the sample in relation to the glass fiber. Figure 3.35 as an example presents the results of testing SVAM with 1:5 fiber ratio for different orientations. The actual dispersion of results, as is apparent from this graph, significantly exceeds the discrepancy in the amounts of resistances with different angles of  $\alpha$ . The theoretically constructed curve also differs little from the horizontal straight line. Thus, even for fiber glass-reinforced plastic with comparatively high anisotropy, with 1:5 fiber ratio, the shear resistance perpendicular to the layer is a practically constant amount for all orientations in relation to the glass fiber.

/117

The third appearance of fiber glass-reinforced plastic resistance to tangential stresses bears the name of simple shearing in the layer (interlayer shear). Here the tangential stresses act in all cases in one plane that is parallel to the veneer sheet layers. The angle  $\alpha$  between the direction of effect of these stresses and the direction of

the glass fiber is changed. In this case, the tensorial formula acquires the same appearance as in shear perpendicular to the layers (1.25). Experiments show that essentially this resistance does not depend on the size of the  $\alpha$  angle [12].

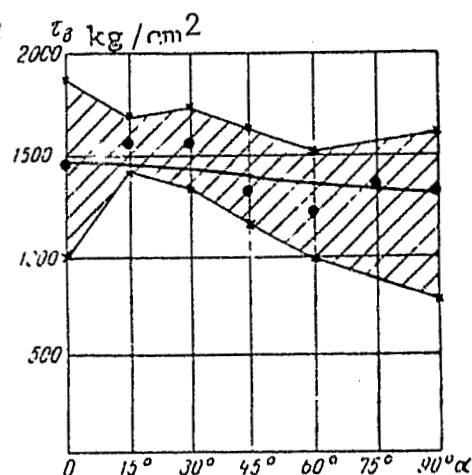


Figure 3.35. Ultimate Strengths in Shear Perpendicular to Plane of Sheet for SVAM on Epoxy-Phenol Binder with 1:5 Fiber Ratio. Hatched region is actual dispersion of testing results.

The amount of resistance to simple shearing in the layer for these fiber glass-reinforced plastics is very low. It is from 100 to 200  $\text{kg/cm}^2$ . This is the only resistance in which the reinforcing effect of the glass fiber is essentially lacking and only one binding agent operates. In the structural materials one should therefore try to avoid that transmission of loads in which the fiber glass-reinforced plastic operates on simple shearing in the layer.

Results of fatigue testing. The anisotropy of fatigue strength of fiber glass-reinforced plastics during bending according to fig. 3.37 a is considerably lower than its anisotropy during static stretching. Fig. 3.36 presents the curves for change in the endurance limits of the tested /118 fiber glass-reinforced plastics depending on the angle  $\alpha$  between the sample bending plane and the fiber direction (or threads of the fabric warp). The curves are constructed according to the tensorial formula (1.22) and according to the quantities of ultimate endurance obtained

experimentally in publication [12].

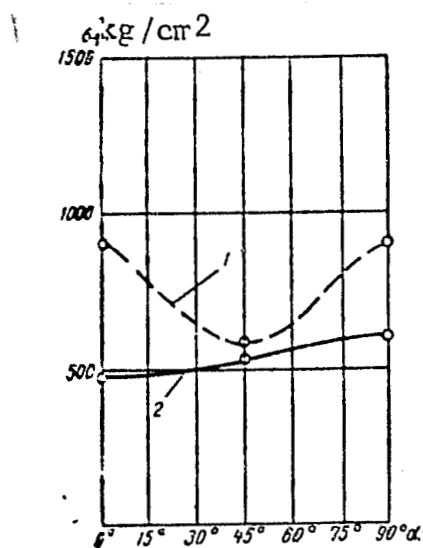


Figure 3.36. Endurance Limits in Pure Planar Bending  
1--for SVAM on epoxy-phenol binder with 1:1 fiber ratio; 2--for fiber glass-reinforced plastic fiber of cold hardening (on PN-1).

The fatigue strength of glass textolite made of T fabric on PN-1 binder, as is apparent from fig. 3.36, in this case practically does not depend on the orientation of stress in relation to the fabric warp.

The anisotropy is more significant for SVAM. The endurance limits were defined on the basis of  $10^7$  cycles with pure bending of flat samples according to tests with assigned amplitude of deformation (angles of rotation of the end sample sections) in the machine designed by I. P. Boksberg. The bending plane passed perpendicularly to the plane of the fiber glass-reinforced plastic sheet. The samples had the shape of a blade with openings of the clamping bolts [12]. In the tests of SVAM with 1:13 fiber ratio, there were cases of cracks appearing from these openings parallel to the direction of greatest material strength. In subsequent experiments, the clamps were redesigned. A square shape of the samples "without heads" was adopted. Their failure occurred in the middle of the length.

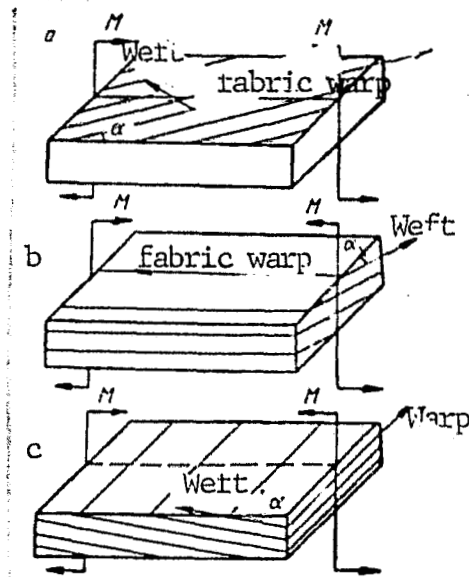


Figure 3.37. Schematic Illustration of Sample Bending during Fatigue Testing in Three Different Cross Grain Cases a--cross grain in sheet plane; b--during bending onwarp ; c--during bending on weft.

In many machine parts and designs, fiber glass-reinforced plastic is used under such conditions in which fabrication inaccuracies, and sometimes the design features of the item (site of connection of elements by molding on), result in the appearance of a type of cross grain, i.e., slight noncoincidence of the material symmetry plane with the plane of action of the external forces. In contrast to the biologically governed cross grain of wood, this cross grain of fiber glass-reinforced plastics can be simulated by the corresponding orientation of the samples. The effect of cross grain on the static strength of fiber glass-reinforced plastics can be easily evaluated from the curves given above (fig. 3.22-3.34). The effect of cross grain on the fatigue strength during bending of one type of fiber glass-reinforced plastic was studied in publication [83]. Figure 3.37 presents three possible cases of cross grain in a fiber glass-reinforced plastic fabric during pure bending perpendicular to the sheet plane. Case a corresponds to the testing results presented in fig. 3.36. With small values of the angle  $\alpha$ , the effect of cross grain here is not great: curve 2 in fig. 3.36 travels

/119

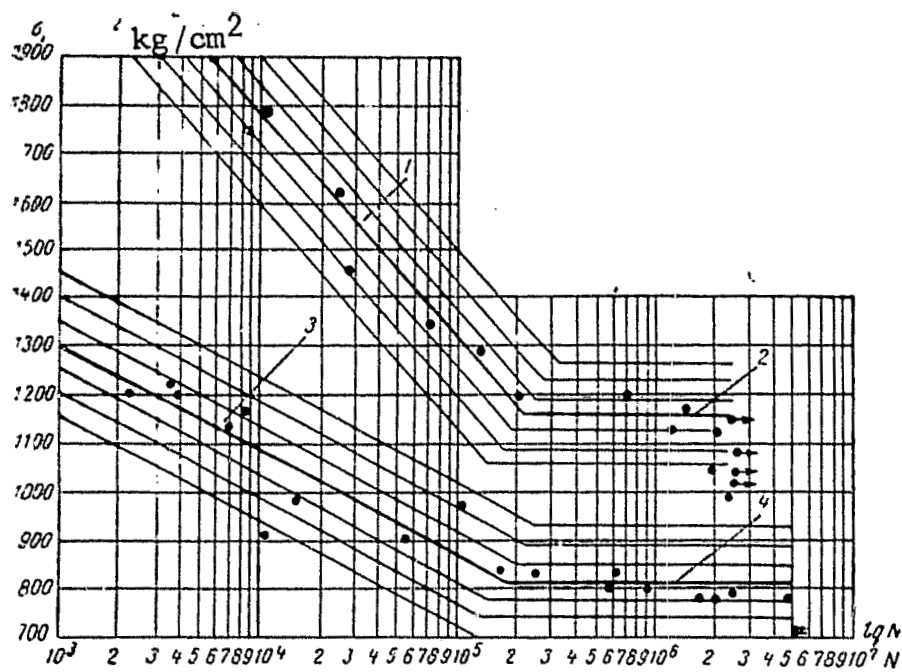


Figure 3.38. Fatigue Diagrams for Cross Grain Series of Samples  
 1 and 2--cross layer on warp; 3 and 4--cross layer on weft; — --according to correlation equations; --- --dispersion bands; → --intact samples.

in limits from  $\alpha=0$  to  $\alpha=15^\circ$  almost horizontally. Cases b and c were experimentally studied in publication [83] with small values of the angle (about  $1^\circ$ ).

Figure 3.38 presents in semilogarithmic coordinates the results of testing two series of cross grain samples that conform to cases b and c in fig. 3.37.

In figure 3.38, the points mark the results of testing individual samples. The ordinates are the amounts of stresses  $\sigma$  that were computed from the sample deflection and the modulus of elasticity of the material determined before the beginning of the tests.

The logarithm is plotted on the x-axis in fig. 3.38 for the number of cycles  $N$  (durability) that the sample withstood before failure.

The correlation straight lines were constructed according to A. K. Mitropol'skiy's method [55] for processing results of a small number of observations, with the assumption of M. Ya. Shashin on the independence

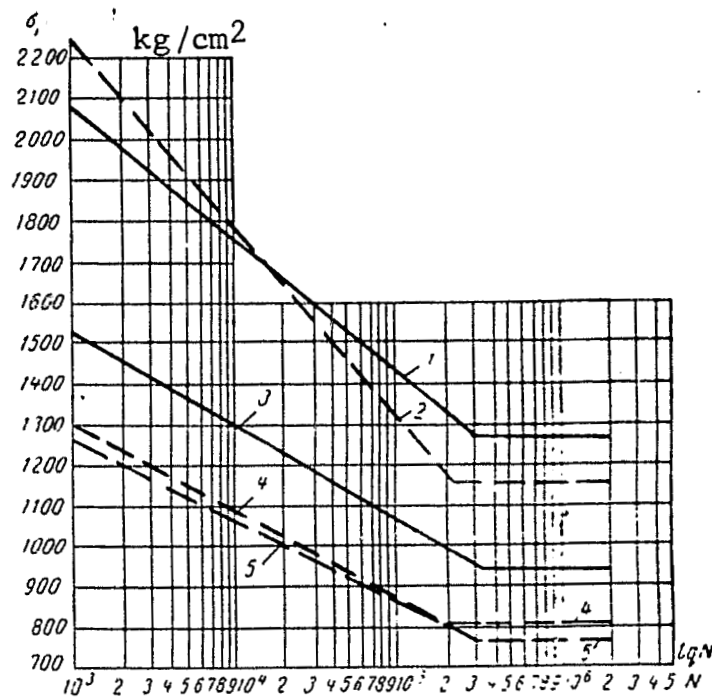


Figure 3.39. Fatigue Diagrams for Series of Samples during Bending on Warp 1--non-cross grain (fig. 3.37, b with  $\alpha=0$ ); 2--cross grain (fig. 3.37, b with  $\alpha=1^\circ$ ) and on weft; 3--non-cross grain (fig. 3.37, c with  $\alpha=0$ ); 4--cross-grain (fig. 3.37, c with  $\alpha=1^\circ$ ); 5--cross-grain unprotected (fig. 3.37, c with  $\alpha=1^\circ$ ).

of the measure of individual dispersion from the amount of stress, and the assumption on the linear link between the amplitude of deformations and the logarithm of sample durability.

The presence on the fatigue diagram of points that are arranged on one level with the points that correspond to the intact sample made it possible to approximately construct horizontal sections of the diagram (straight lines 2 and 4 on fig. 3.38). Continuation of the tests on individual samples resulted in their destruction at  $5 \cdot 10^6$  cycles. This provides the grounds to hypothesize that the straight lines 2 and 4 must actually be slightly inclined to the horizontal, and do not conform to the true endurance limit. With a base of  $2 \cdot 10^6$  cycles, /12/ one can assume that these straight lines are almost horizontal.

Figure 3.38 shows the dispersion bands that pass at a distance of

one, two and three measures of individual dispersion from the correlation straight lines. Figure 3.39 and table 3.1 present the results of determining the endurance limits for five series of the studied fiber glass-reinforced plastic. The fifth series of samples was distinguished by the fact that the material lacked a protective layer of fabric laid parallel to the sheet plane on its upper and lower surfaces as in the material of the second and fourth series. The greatest decrease in fatigue strength is found in the fifth case in which the stretching stress acts during sample bending on the layer of the binder at the site where the fabric emerges onto the sheet surface.

Table 3.1 presents the quantities of the coefficients  $a$  and  $k$  that characterize the fatigue strength of the tested series of samples. The coefficient  $a$  shows what percentage the endurance limit  $\sigma_{-1}$  is of the ultimate strength in static bending  $\sigma_b$ . /121

$$a = \frac{\sigma_{-1}}{\sigma_b}.$$

The coefficient  $k$  shows the ratio between the endurance limits of cross grain  $\sigma_{-1}^k$  and non-cross grain  $\sigma_{-1}$  material, i.e., evaluates the effect of slight cross grain on the fatigue strength of fiber glass-reinforced plastic.

$$k = \frac{\sigma_{-1}^k}{\sigma_{-1}}.$$

As is apparent from the data of fig. 3.39 and table 3.1, even very slight cross grain during bending in the weft plane (fig. 3.37, c) results in a decrease of the endurance limit for the unprotected material by an average of 19%.

Thus, even for a comparatively weakly anisotropic fiber glass-reinforced plastic fabric, slight deviations in the direction of the stress effect on the material's symmetry plane (only by  $1^\circ$ ) result in certain cases (fig. 3.37 c) in a considerable decrease in the fatigue strength in contrast to the case in fig. 3.37 a. It should be noted [83] that the static strength of samples for the fourth and fifth series is 5% lower than for the third, i.e., this case of cross grain (on the weft) has a considerably stronger effect on the amount of endurance limit than on the ultimate strength of the material. Thus, the /122



anisotropy of fatigue strength can sometimes be more pronounced than in static tests.

TABLE 3.1. TABLE 3.1. VALUES OF a AND k COEFFICIENTS

Number of diagram on fig. 3.39	Series of samples	$a = \frac{\sigma_{-1}}{\sigma_b}$	$k = \frac{\sigma_{-1}}{\sigma_{-1}}$	Type of cross grain in fig. 3.37
1	Non-cross grain during bending on warp	0.316	1	b
2	Cross grain during bending on warp	0.296	0.915	
3	Non-cross grain during bending on weft	0.348	1	c
4	Cross grain during bending on weft	0.312	0.86	
5	Cross grain, unprotected during bending on weft	0.290	0.81	c

### 13. Metals

The data on strength of metal anisotropic materials are given in this work mainly from published data.

The author tested one sheet of cold-rolled steel 0.8 KP for stretching in seven different directions in relation to the rolling [13].

The steel had 75% shrinkage in cold rolling. The chemical composition of the steel was: C--0.9%, Si--traces, Mn--0.45%, S--0.020%, P--0.024%, Cr--0.03%, Ni--0.09%. The initial sheet thickness was 2, the final was 0.5 mm. The tested steel sheet was not thermally treated.

E. I. Braynin (ZhTF, Vol. 30, No. 8, 1960) for this cold-rolled steel compared the experimentally obtained values of ultimate strength  $\sigma_b$  in rupture of variously oriented samples with the calculated curves constructed from the tensorial formula (1.22). /124

E. I. Braynin tested one-two samples 130 x 18 x 0.5 mm in size with each of the seven different orientations ( $\alpha=0,15,30,45,60,75,90^\circ$ ) for four different conditions of steel. In three out of the four states he obtained considerable discrepancies between the results computed from tensorial formula (1.22) and the experimental data. The greatest discrepancy was obtained for steel in condition a, after cold rolling with 75% shrinkage. For this condition of steel, the curve for change in  $\sigma_b$  depending on  $\alpha$ , according to E. I. Braynin's data, had a maximum at  $\alpha=15^\circ$  and minimum at  $\alpha=50^\circ$ .

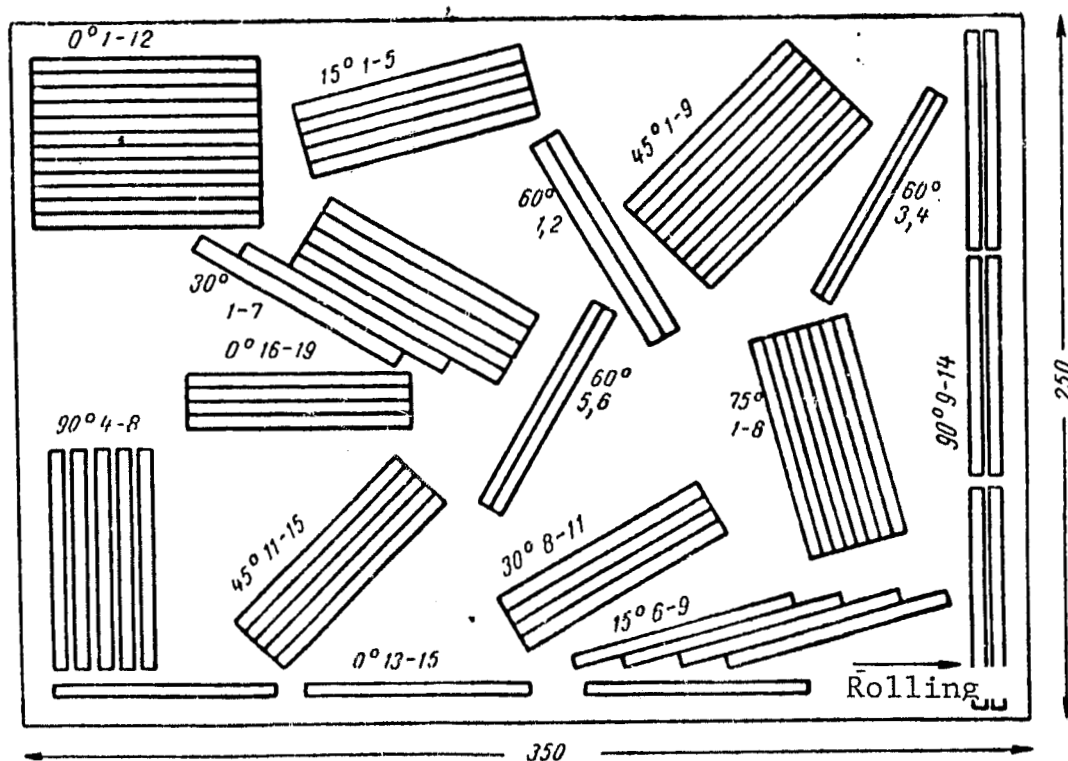


Figure 3.40. Arrangement of Samples on Sheet of Cold Rolled Steel. Angles designated between axes of samples and direction of rolling and number of samples.

/123

A steel sheet 250x260x0.5 mm in size made of the same batch in condition a was supplied by E. I. Braynin to repeat the experiments. For the repeated experiments, smaller dimensions of the samples were taken in order to check the degree of uniformity of the material in the sheet and to obtain reliable average data of the tests on a large number of samples.

Samples 80 x 5 x 0.5 mm in size were cut according to the mark presented in figure 3.40. The samples that were cut perpendicularly to the direction of rolling ( $\alpha=90^\circ$ ) from the left and right side of the sheet (fig. 3.40) yielded the same average quantities of ultimate strength. The samples that were cut parallel to the direction of rolling had varying strength depending on their site of arrangement on the sheet. Samples cut from the middle of the sheet had the greatest ultimate strength, and those cut from the lower part of the sheet had the least.

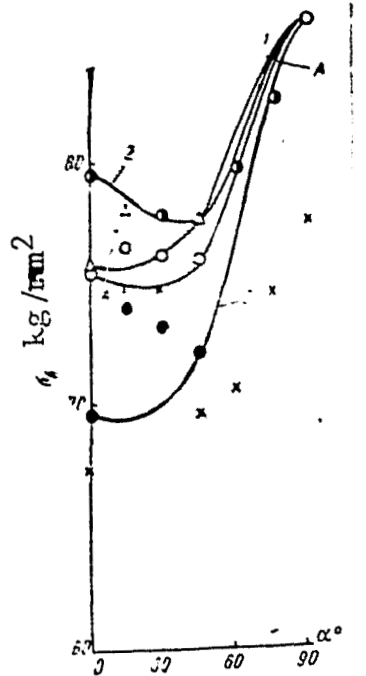


Figure 3.41. Change in Steel Ultimate Strengths in Rupture Depending on the Angle between the Sample Axis and the Rolling Direction (Curves constructed from tensorial formula (1.22): A--average for sheet; 1--on upper sheet; 2--in middle; 3--on lower sheet. Average ultimate strengths according to our data: O--average for sheet; ●--for lower part; Δ--for upper; ⊙--for middle; X--according to Braynin's experiments.

Here the differences in the ultimate strengths of the samples cut from different parts of the sheet with the same orientation exceed the differences between the ultimate strengths of the samples cut from one part of the sheet, but with different orientation.

Figure 3.41 presents the ultimate strengths experimentally obtained /125 by E. I. Braynin (designated x) in addition to our data. Along and transverse to the rolling direction they are considerably lower than our average data. With  $\alpha=0$ , only two samples from the total number of 19 tested samples showed such low strength. These were the samples that were arranged in fig. 3.40 in the lower part of the sheet. A

certain increase in strength with  $\alpha=15^\circ$  as compared to the strength along rolling (with  $\alpha=0$ ) is also apparent according to the results of our tests, but they only average 1.3% for the sheet, while the difference in strength with  $\alpha=0$ , depending only on the site of arrangement of the sample, reaches 14%.

Thus, the existence of maximum strength with  $\alpha=15^\circ$  is doubtful, and the values of ultimate strength obtained with  $\alpha=15^\circ$  that were increased as compared to  $\alpha=0$  can be explained by the heterogeneity of the material.

Figure 3.41 presents the curves that were constructed from the tensorial formula separately for different parts of the sheet and average for the entire sheet.

As far as can be judged from the cited data and the data of publication [119], tensorial formula (1.22) correctly describes the laws governing the change in characteristics of resistance to plastic deformation and failure of metal alloys depending on the angle between the direction of force and the direction of rolling.

H. Hoover [95] tested rolled steel in different directions in relation to the rolling.

A number of the steel bands (first) were rolled only in a longitudinal direction. The length of the rolled band was 210 times greater than the length of the casting. The second group of bands was initially rolled in a longitudinal direction (length of the slab was 13 times greater than the length of the casting), and then in a perpendicular direction. The slab was rolled in this direction so that its length was increased 19-fold. No damages or defects were found on the surface of the bands. The thickness of the bands was from 0.145 to 0.154 in. The strength anisotropy of this steel was not great and according to the amount of temporary resistance on standard samples it was:

$$\frac{\sigma_0}{\sigma_{90}} = 1.1.$$

H. Hoover made tests of an anisotropic steel band on samples that were plates with a deep notch and drilling at the end of the notch. These samples were tested for stretching with different angles of incline of the destructive force to the direction of band rolling. The notch always remained perpendicular to the rupture force. Two types of /126

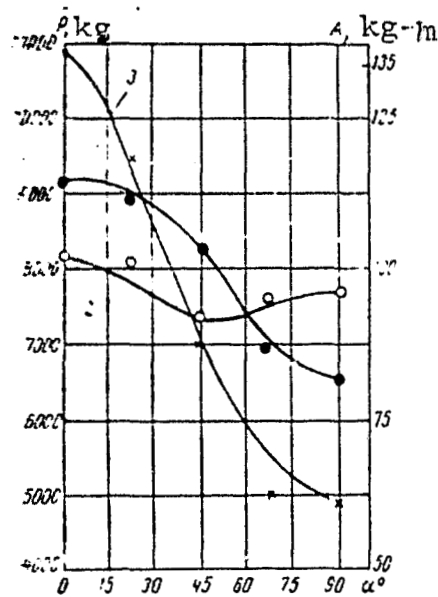


Figure 3.42. Dependence of Ultimate Strength of Rolled Steel on Angle of Incline  $\alpha$  of Force to Direction of Rolling according to Data of H. Hoover 1,2,--rupture forces for steel St.1 and St. 2; 3--rupture work for steel St.1.

material were tested: steel 1 was exposed before testing to preliminary rolling in one direction, while steel 2 differed from steel 1 only in the fact that it was rolled in two mutually perpendicular directions. Figure 3.42 shows curves for the change in rupture force (1,2) and the rupture work (3) for these two materials. The ordinates of the curves were computed from tensorial formula (1.22). A fairly close correspondence was obtained between the data of the calculation and the experiment.

Apparently as a consequence of the slight anisotropy of the elastic properties of the rolled steel, differences in the stressed states of variously oriented samples were negligible in these experiments. The coefficient of stress concentration (that changes depending on the direction of the stretching force more strongly, the greater the difference is in the moduli of elasticity  $E$  along and transverse to the rolled product) in this case remained almost constant. It therefore happened that formula (1.22) that was derived for the strength characteristics

with uniform simple stresses is approximately correct for complex stresses that almost do not change depending on the orientation of the sample.<sup>1</sup>

It should be noted that with the same nature of mathematical relationships, the type of curves that define the resistance of materials to perpendicular and tangential stresses is quite different. The diagonal direction often conforms to the greatest shear resistance, but the least rupture resistance (see fig. 3.13 and 3.34). If the strength characteristics along and transverse to the fibers (or rolled product) differ little among themselves, then the diagonal direction generally corresponds to extreme quantities of resistances: maximum shear resistance and minimum rupture resistance. /127

This rule was confirmed in the fatigue tests of the metals.

Findley and Mathur [88] in studying the fatigue strength of weakly anisotropic metals (steel and aluminum alloys) during bending and torsion noticed the same law. During bending, the least endurance limit was found in the samples that were cut at a 45° angle to the direction of greatest strength of the material (longitudinal). During torsion these (diagonal) samples possessed the greatest fatigue strength exceeding the strength in longitudinal and transverse directions. Here the strength in the longitudinal and transverse directions differed little for these materials both in tests for repeatedly changed bending, and for torsion.

With an increase in the degree of anisotropy of the material, the extreme values no longer coincide with the diagonal direction (curves in fig. 3.34), but as before, the resistance to the perpendicular stresses is the minimum, while the resistance to the perpendicular stresses is the maximum. With a very great degree of anisotropy, the extremum coincides with the longitudinal or transverse direction.

The mathematical relationships make it possible, as shown in section 9, to establish the direction of least or greatest strength of the anisotropic material, in contrast to the purely empirical approach to the question that does not afford such a possibility. Here the same, or almost the same characteristics of strength in the

<sup>1</sup>A more detailed study of anisotropy in the characteristics of sensitivity of the metals to the notch was made in the candidate dissertation of P. G. Miklyayev "Study of Anisotropy of Mechanical Properties of Intermediate Products Made of High-Strength Light Alloys," VILS [All-Union Institute of Light Alloys], 1965.

longitudinal and transverse directions are still not an indicator of the material's isotropy. Its strength in any other direction (for example, diagonal) can prove to be considerably reduced and have an unfavorable effect on the overall strength of the design.

The aluminum alloys<sup>1</sup> studied by Gatto and Mori [92] had considerably greater anisotropy than the rolled steel. They studied two alloys, ergal and avional of the following chemical composition: Ergal 65: Zn--7.7%, Cu--1.7%, Mg--2.62%, Mn--0.18%, Fe--0.15%, Si--0.09% and Cr--0.15%.

Avional 24: Cu--4.85%, Mg--1.45%, Mn--0.63%, Fe--0.32%, Si--0.36%.

Both alloys were tested in the rolled state and after annealing.

Figure 3.43 presents curves for the change in characteristics of plastic deformation resistance during rupture and impact strength of two aluminum alloys, ergal and avional. The experimental data were taken from the work of Gatto and Mori [92]. The tests for static stretching were done on samples 10 mm in diameter (curves 1, 2 and 3). During stretching, an analysis was made of the ultimate strengths  $\sigma_b$  and conditional yield stresses  $\sigma_{0.2}$ . The ordinates of all curves were computed from the tensorial formula (1.22). The same relationship is accepted for the impact strength (curve 4). /128

With a difference in the ultimate strengths for rupture along and transverse to the rolled product not exceeding 2%, the ultimate strengths of these alloys in a diagonal direction (i.e. at a 45° angle to the direction of the rolled product) were lower by 11.6% for avional and by 5% for ergal. The difference in the amount of yield stress along and transverse to the direction of rolling was more significant. And finally, the impact strength showed the greatest anisotropy.

Strictly speaking, the impact strength cannot be computed from the tensorial formulas, since it neither conforms to the material's resistance to the effect of perpendicular stresses in simple stretching, nor its resistance to tangential stresses under pure shear conditions. At the same time, the impact strength is undoubtedly an indicator of the material's resistance with a certain complex stressed state and under the dynamic effect of loads.

<sup>1</sup>More complete and newer data are presented in publication [119] and in the dissertation of P. G. Miklyayev (see p. 134).

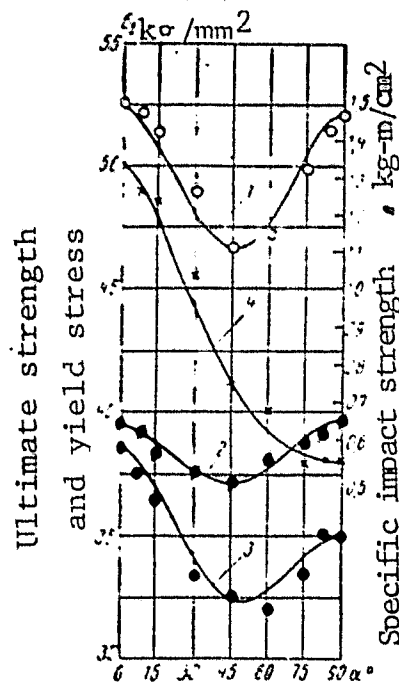


Figure 3.43. Dependence of Characteristics of Plastic Deformation Resistance during Rupture and Impact Strength  $\alpha$  of Aluminum Alloys on the Angle of Incline of the Force to the Direction of Rolling (according to data of Gatto and Mori):  
 1, 3-- $\sigma_B$  and  $\sigma_{0.2}$  for avional; 2, 4-- $\sigma_B$  and  $\sigma_{0.2}$  for ergal.

Formula (1.22) can conform to the change in impact strength if the nature of the stress changes little with the change in orientation of the sample. The dynamic nature of load application does not contradict the assumptions that are the basis for the derivation of this formula. They are therefore applicable in impact tests in which the loading regime does not change with a change in the sample orientation.

#### 14. Determination of Ultimate Strengths for Simple Shearing from Results of Testing for Stretching or Compression of Wood Samples and Directed Fiber Glass-Reinforced Plastics.

During stretching of a sample whose axis forms angle  $\alpha$  with the direction of the fibers (fig. 3.44, a), destruction often occurs on areas parallel to the fiber. Perpendicular  $\sigma_y$  and tangential  $\tau_{xy}$



stresses simultaneously act on these weak areas. The quantity of these stresses changes depending on the ultimate strength of the sample  $\sigma_b$  and the angle  $\alpha$ . If one constructs (fig. 3.44,b) a curve of the mutual relationship of stresses  $\tau_{xy}$  and  $\sigma_y$  that are active at the moment of destruction on the areas parallel to the fibers, then one can make an approximate estimate of which of these stresses was the primary cause of destruction of the material, i.e., does separation or simple shearing occur on the weak interlayer. Those points on the curve for which the perpendicular stress  $\sigma_y$  will be variable, and the amount of  $\tau_{xy}$  constant, must evidently correspond to the destruction by shearing. Consequently, one can judge the material's resistance to shearing along the fibers from the size of the ordinates of these points  $\tau_{xy}$ .

These curves, called limiting, are constructed in fig. 3.44,b for pine.

Figure 3.44b presents the limiting curves that were constructed from the experimental data on strength of pine: for static stretching curve 1 (from the author's experiments [5]), in static compression, curves 2 and 3 (from the experiments of A. N. Flakserman [71]) and in impact compression, curves 4 and 5 (from the data given in section 10). The amount of perpendicular stress  $\sigma_y$  that acts on the area parallel to the fibers is plotted on the x-axis in figure 3.44b. During rupture of the sample whose axis comprises angle  $\alpha$  with the fiber direction (see fig. 3.44,a), the amount of stress  $\sigma_y$  is computed according to the formula

$$\sigma_y = \sigma_b \sin^2 \alpha, \quad (3.8)$$

where  $\sigma_b$ --ultimate strength during stretching at an angle  $\alpha$  to the fibers.

During compression of variously oriented samples, the amount  $\sigma_y$  that conforms to the ultimate strength  $\sigma_b$  will be considered negative and will be computed according to formula (3.8).

The amount of tangential stress  $\tau_{xy}$  that acts on the areas parallel to the fibers of wood, is computed according to the following formula in the stretched or compressed sample

$$\tau_{xy} = \frac{\sigma_b \sin 2\alpha}{2}. \quad (3.9)$$

The stresses  $\sigma_y$  and  $\tau_{xy}$  act simultaneously on the same "weak" areas of the samples at the moment they are destroyed. Each point of the curves depicted in fig. 3.44 b conforms to the results of testing a series of samples oriented in the same way in relation to the fibers.

Curve 1 was constructed according to the results of tests for stretching in which the orientation of the samples in relation to the annual wood rings was not fixed. (As a consequence of the heterogeneous structure and considerable length of the samples [5], it was difficult to maintain this orientation constant over the entire length even in the case where the orientation of the sample axis in relation to the fibers was fixed fairly accurately). Thus, data were used for curve 1 that present the average amounts of resistance that occur with the same incline of the fibers.

Curve 2 was constructed from the results of compression testing of samples whose axes are arranged in a radial plane with all angles of fiber incline. Curve 3 is constructed according to the results of compression tests on samples whose axes are arranged in the tangential plane. Curves 1, 2 and 3 were constructed from experimental data obtained by different authors, but the pine had almost the same ultimate strength for compression along the fibers, comprising about  $450 \text{ kg/cm}^2$ .

Curves 4 and 5 were constructed similarly to curves 2, and 3. respectively for the radial and tangential planes, but for impact compression.

All the curves in figure 3.44 b have a clearly pronounced section for which  $\tau_{xy}$  changes little. This section has a maximum that corresponds to the angles of fiber incline from  $20^\circ$  to  $25^\circ$  to the sample axis. The greatest amount of tangential stress  $\tau_{xy}$  that is active on the area parallel to the fibers is obtained with  $\alpha=20-25^\circ$ .

If one compares the amount  $(\tau_{xy})_{\max}$  during stretching (curve 1) with the average amount  $(\tau_{xy})_{\max}$  obtained in compression (curves 2 and 3), then one can note that they do not differ strongly. Thus, not only angle  $\alpha$  that conforms to the maximum amount of shearing stress, but the actual amount  $(\tau_{xy})_{\max}$  is roughly the same during stretching and during compression. Consequently,  $(\tau_{xy})_{\max}$  depends little on whether

additional stretching or additional compressing stresses are acting on the area parallel to the fibers. Failure of the samples with these angles of incline of the fibers occurs by simple shearing along the fibers. This is confirmed by the external appearance of the failure during stretching and compression. Consequently, the amount  $(\tau_{xy})_{\max}$  approximately conforms to the ultimate strength of the material for simple shearing along the fibers  $\tau_b$ .

This nature of failure is possible only with a certain correlation /131 between the quantities of perpendicular and tangential stresses acting on the areas parallel to the fibers. This correlation, in turn, depends on the angle  $\alpha$  between the axis of the sample and the direction of the wood fiber. The effect of additional perpendicular stresses  $\sigma_y$  is small only for those angles  $\alpha$  that correspond to the tops of the curves illustrated in fig. 3.44.

With large angles of incline of the fibers, the effect of perpendicular stresses  $\sigma_y$  that act on the areas parallel to the fibers, becomes more significant, and even definitive, since the curves here travel almost vertically, and the amount  $\sigma_y$  is close to the amount of the ultimate stretching strength (or correspondingly the compression strength) transverse to the fibers.

When tangential and stretching stresses act simultaneously on the areas parallel to the fibers, the wood failure occurs by rupture if the amount of stretching stresses exceed the amount of tangential (almost vertical section of curve 1). One can draw the conclusion from here that failure of the samples for shearing along the fibers according to GOST 6336-52 occurs primarily by rupture of the wood transverse to the fibers.

As shown by the studies done by F. P. Belyankin [18] on isotropic models by the optic method, the amount of the greatest stretching stress that is active on the shearing plane in the OST-NKLes-250 samples, is 1.6-fold greater than the average tangential stresses that are active on this plane.

According to GOST 6336-52, the sample differs slightly from the sample studied by F. P. Belyankin. It has the same shortcomings. V. Ye. Moskalev [47] also showed that the destruction of samples according to

GOST 6336-52 is accompanied by rupture of the tracheid walls, i.e., occurs not by shearing.

The method suggested here for determining the resistance of wood to shearing along the fibers by constructing limiting curves illustrated in fig. 3.44 b from the results of testing for stretching or compression, makes it possible to correctly approach an evaluation of the amount of corresponding resistance.

As for the actual amount of ultimate strength for static shearing along the fibers, according to this method it is somewhat higher than when it is determined according to GOST 6336-52. According to fig. 3.44  $(\tau_{xy})_{\max} = \tau_b''$  averages about  $110 \text{ kg/cm}^2$ , while according to GOST 4631-49 for pine  $\tau_b''$  is from 60 to  $82 \text{ kg/cm}^2$  (see GOST 4631-49 "Indicators of Physical and Mechanical Properties of Wood").

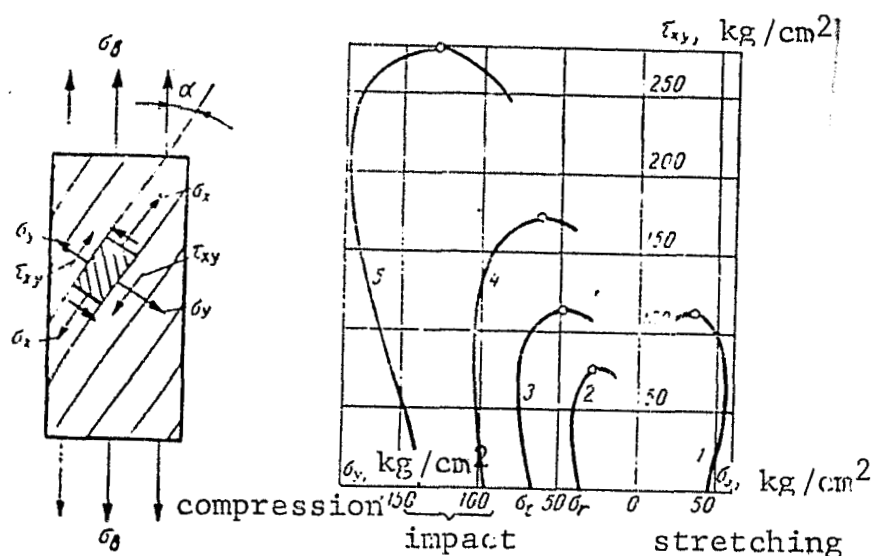


Figure 3.44. Limiting Curves for Pine  
a--stress in stretched sample; b--limiting  
curves; 1--for stretching; 2 and 3--for com-  
pression; 4 and 5--for impact compression.

/132

Comparison of curves 2 and 4, as well as curves 3 and 5 on figure 3.44 b shows that the ultimate strength in impact shearing is increased in relation to its amount with static loading roughly 2.2-2.5-fold.

It should be noted that during impact compression at an angle from 10 to  $40^\circ$  to the direction of the fibers, the destruction of the samples,

judging from their external appearance, occurs by simple shearing along the fibers. The compression oscillograms (fig. 3.17) of these samples have a clearly pronounced brittle nature: after the sharp increase there is a drop in the force in the same way as on the diagrams of static compression [71] with these angles of fiber incline.<sup>1</sup>

A complete graph for the change in ultimate strength during stretching or compression of an orthotropic material depending on the angle of fiber incline can be constructed using the tensorial formula. Here it is necessary to experimentally determine the ultimate strengths of only three directions: along and transverse to the fibers, and at a 45° angle to the fiber direction. This allows us to construct graphs to determine the shear resistance along the fibers that are similar to those depicted in fig. 3.44b. The graphs are constructed on the basis of three experimentally defined quantities of ultimate strength  $\sigma_b$  for stretching or compression:  $\sigma_0$  along the fibers,  $\sigma_{90}$  transverse to the fibers, and  $\sigma_{45}$  in a diagonal direction. All three directions must be arranged in one symmetry plane of the material structure. /133

The method suggested [11] for determining shear resistance of wood along the fibers is significantly simpler than all the extant methods because it does not require any special devices. The quantity of ultimate strength in shear along the fibers is determined based on tests for normal compression (or stretching) of three types of samples: parallel to the fibers, perpendicular to them and diagonal. Here the shape and dimensions of all three types of samples must be the same. The angle in relation to the fibers must be held as carefully as possible.

This method also has the same advantage as the method accepted in GOST 6336-52 for determining the shear modulus of wood according to the compression of samples whose axes form a 45° angle with the direction of the fibers.<sup>2</sup> Testing of diagonal samples determines not only the characteristics of the elastic properties in shear, but also the

<sup>1</sup>Publication [55] presents the limiting curve that was constructed from fatigue testing results of variously oriented samples made of birch. Judging from this curve and from the data of GOST 4631-49, the resistance to repeatedly changing shear along the fibers is roughly two times lower than the resistance to static shearing.

<sup>2</sup>The shear modulus of plywood is determined analogously according to GOST 1143-41.

strength characteristics of wood in shear along the fibers.<sup>1</sup>

The use of the suggested method to evaluate the resistance of SVAM type directed fiber glass-reinforced plastics to the effect of tangential stresses on a plane parallel to the direction of the greatest reinforcement is shown in publication [11]. The ultimate strengths in shear on an area parallel to the fibers can be determined for these materials with the help of limiting curves constructed without consideration for the stress  $\sigma_x$  only in the case of unidirectional reinforcement (see section 17).

In a stretched sample, the stress field is usually more uniform than in a compressed sample. One should therefore prefer the limiting curves that are constructed from the results of stretching tests.

For practical purposes, one can employ the results from stretching tests and approximately define the lower limit of the resistance of any anisotropic fiber glass-reinforced plastic to the effect of tangential stresses by using the limiting curves. The upper limit of this resistance can be defined by shear testing according to GOST 10044-38 when the shear areas are superposed with the direction of the greatest fiber glass-reinforced plastic reinforcement.

#### 15. Experiments on Biaxial Compression

/134

Figure 3.45 presents a plan of a reverser that is known by the name "Fepply's cross". It permits production of biaxial compression of samples by equal stresses on a normal press. The dimensions of the samples were 20x20x20 mm. The tests were made on Gagarin's press with recording of the compression diagram. The tests were continued either until the samples were destroyed (decrease in load on the diagram), or until a clearly pronounced break occurred in the curve, after which the sample was not destroyed.

When the samples were carefully fabricated and accurately installed in the reverser, the stress field was fairly uniform. In the sample made of optically active (isotropic) material, during biaxial compression in the reverser, the stress field, judging from the color pattern of the bands, was uniform to roughly the same measure as in

<sup>1</sup>In publication [84], A. Jlinen used an analogous method to determine the shear resistance of Finnish species of wood. The ultimate strengths  $\sigma_B$  were experimentally determined for all sample orientations.

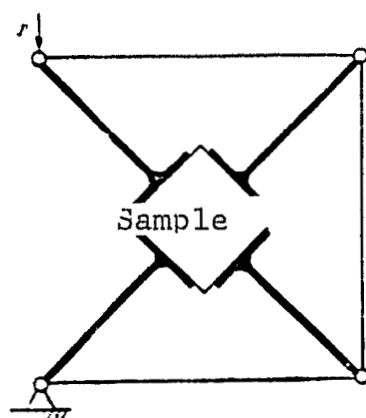


Figure 3.45. Plan of "Fepply's Cross" Reverser

the same sample that was compressed in one direction between two parallel pads.

Of course, the results of testing samples of anisotropic materials for biaxial compression in this reverser make no pretense of accuracy or high degree of uniformity of the stressed state in the tests.

For an anisotropic sample, even when it is tested in the direction of two axes of symmetry, the stress field undoubtedly differs from the calculated scheme of a uniform biaxial compression to the same degree as uniaxial compression.

The results of these tests can be viewed only as an attempt to obtain certain, very approximate data on strength in biaxial stress for those materials used to study anisotropy of mechanical properties in this chapter.

Table 3.2 presents the results of testing pine for bi- and uniaxial compression. The first line gives the average values of  $M$  for ultimate resistances that were obtained in testing  $n$  samples. The table presents the standard deviations  $\sigma$ , variation coefficients  $v$ , average errors  $m$  and index of accuracy  $p$  for these tests.

The following average results were obtained when nine-layer aviation plywood, 10 mm thick was tested.

The ultimate resistance in one-sided compression along the casing fibers was  $\sigma_a = 640 \text{ kg/cm}^2$ , transverse to the casing fibers  $\sigma_t = 450 \text{ kg/cm}^2$ . During biaxial compression in the same directions,  $\sigma_{at} = 438 \text{ kg/cm}^2$ .

TABLE 3.2. RESULTS OF COMPRESSION EXPERIMENTS ON WOOD

Indices	Biaxial compression			Uniaxial compression		
	$\sigma_{at}$	$\sigma_{tr}$	$\sigma_{ar}$	$\sigma_t$	$\sigma_r$	$\sigma_a$
$M, \text{kg/cm}^2$ . . . . .	65,48	41,65	44,64	66,56	42,76	420,10
$n$ , items . . . . .	10	9	10	10	10	10
$\sigma$ , $\text{kg/cm}^2$ . . . . .	13,52	3,77	8,48	8,67	4,66	14,59
$\sigma_v$ , $\text{kg/cm}^2$ . . . . .	20,70	9,06	19,65	13,01	10,90	3,47
$m$ , $\text{kg/cm}^2$ . . . . .	4,26	1,26	2,68	2,74	1,47	1,60
$p$ , $\pm \%$ . . . . .	6,54	3,01	6,01	4,11	3,44	1,09

The uniaxial compression testing results are distinguished for plywood from those previously cited (section 10), because the shape of the samples and the testing method differ. Section 10 presents the results of testing samples whose dimensions were larger. They were tested in a different device.

As is apparent from an analysis of the results, the strength in biaxial compression for plywood, in the same way as for wood, is determined by the amount of ultimate resistance in the weaker direction.

Table 3.3 presents the results of testing cold-hardened fiber glass-reinforced plastic made of T fabric on PN-1 binder and SVAM on epoxy-phenol binder with 1:1 fiber ratio. The tests were done in the same reverser for biaxial compression. The samples were 10 mm thick, equal to the thickness of the material itself. They were cut from the fiber glass-reinforced plastic sheet in such a way that their 20 mm edges were oriented either parallel to the warp threads ( $\alpha=0$ ) and the weft ( $\alpha=90^\circ$ ) of the fabric, or at a  $45^\circ$  angle to these threads ( $\alpha=45^\circ$ ).

The strength in biaxial compression of the fabric plastic in the direction of the symmetry axis was intermediate in relation to the strength characteristics in uniaxial compression in the direction of these axes. The strength of the diagonal ( $\alpha=45^\circ$ ) samples was slightly higher in biaxial compression as compared to uniaxial. Thus, for strongly anisotropic wood, the effect of biaxiality was the most pronounced. The strength of a weakly anisotropic fiber glass-reinforced plastic fabric is practically the same in biaxial and uniaxial compression.

The anisotropy of SVAM fiber glass-reinforced plastic is stronger and its strength in biaxial compression is somewhat lower than in uniaxial.



TABLE 3.3. RESULTS OF COMPRESSION EXPERIMENTS ON  
FIBER GLASS-REINFORCED PLASTICS

/136

Indices	Biaxial compression		Uniaxial compression		
	$\sigma_{0-90}$	$\sigma_{45}$	$\sigma_0$	$\sigma_{90}$	$\sigma_{45}$
Plastic made of glass fabric T on PN-1 resin:					
M, kg/cm <sup>2</sup>	800	826	900	650	725
n, items	15	11	16	14	8
$\sigma$ , kg/cm <sup>2</sup>	134	158	154	91.5	88.5
$\nu$ , %	16.8	19.2	17.1	14	12.2
m, kg/cm <sup>2</sup>	34.6	47.7	38.5	24.5	31.3
p, %	4.3	5.8	4.3	3.8	4.3
SVAM on epoxy-phenol binder (1:1 fiber ratio)					
M, kg/cm <sup>2</sup>	2775	-	3620	-	-
n, items	11		23		
$\sigma$ , kg/cm <sup>2</sup>	184		374		
$\nu$ , %	6.6		10.3		
m, kg/cm <sup>2</sup>	55		78		
p, %	2.0		2.2		

The testing results from uniaxial compression here, as above, differ from those previously obtained in tests according to GOST since the samples have different dimensions and shape.

#### Chapter IV. Strength Anisotropy in Complex Stresses

/137

##### 16. Study of Applicability of Mises' Plasticity Conditions as Strength Conditions of Anisotropic Materials

The strength criteria or the theories of ultimate stresses are one of the most controversial, and at the same time, important problems in material resistance. This problem is even more complicated for anisotropic bodies.

The main problem is to establish the function that determines the equally dangerous stresses. Uniform complex stresses are examined that are characterized by the quantity of main stresses. In order to solve the problem of equally dangerous stresses for isotropic bodies, it is sufficient to know the equation that links the amount of the three main stresses with the one strength characteristic of the material. This equation does not solve the problem for anisotropic materials, since in themselves the main stresses do not determine the mechanical condition of the material. It is also necessary to know the orientation

of the stress in relation to the structural axes of material symmetry.

The equation of equally dangerous states for orthotropic material must thus contain not three, but six quantities that characterize the stress. These can be, for example, the three main directions and the three directing cosines that fix the orientation of one of the stresses in relation to the axes of symmetry of the material.

The equations of equally dangerous states for orthotropic bodies have a simpler and more symmetrical appearance if they include not the main stresses, but the stresses that are active on the areas perpendicular to the axes of symmetry of the material further designated (as in chapter 1) by the letters  $x$ ,  $y$  and  $z$ , since the material characteristics that are included in the equation can then be defined for the directions that correspond to the main axes of symmetry. /138

In 1928, Mises in his classic work [106] suggested the condition of plasticity that links six stress components with the yield stresses in a uniaxial stress state and in pure shear in different crystallographic directions.

Hill's work [75] applies Mises condition to weakly anisotropic plastic materials (rolled steel).

The condition of plasticity can be viewed as a particular case of the equation of equally dangerous states. The plasticity function suggested by Mises as applied to strongly anisotropic materials should be studied in the sense of its suitability as a general condition for equally dangerous states (strength condition) since these materials do not always reveal plastic deformations.

Bearing in mind only the materials that equally resist stretching and compression, Mises suggested the function of plasticity in the form of a uniform second degree polynomial that he conditionally called the plastic potential.

The plasticity function was first written by Mises in a general form without introducing an assumption regarding the independence of the crystal yield stress from the amount of hydrostatic pressure. For a material that possesses general anisotropy, Mises' condition [106] has the following form in our designations:

$$\begin{aligned}
& A_{1111}\sigma_x^2 + A_{2222}\sigma_y^2 + A_{3333}\sigma_z^2 + 4A_{3322}\tau_{zy}^2 + 4A_{1313}\tau_{xz}^2 + \\
& + 4A_{2121}\tau_{yx}^2 + 2A_{1122}\tau_{xy}\sigma_x + 2A_{2233}\tau_{yz}\sigma_z + 2A_{2311}\tau_{zx}\sigma_x + \\
& + 2A_{1132}\tau_{xz}\sigma_y + 2A_{1113}\tau_{xy}\sigma_z + 2A_{1112}\tau_{xy}\sigma_z + 2A_{2223}\tau_{yz}\sigma_z + \\
& + 2A_{2213}\tau_{yz}\sigma_z + 2A_{2212}\tau_{yz}\sigma_z + 2A_{3332}\tau_{zy}\sigma_z + 2A_{3313}\tau_{zx}\sigma_x + \\
& + 2A_{3312}\tau_{zx}\sigma_x + 4A_{3313}\tau_{zx}\sigma_x + 4A_{3112}\tau_{xy}\sigma_z + 4A_{1223}\tau_{yz}\sigma_z = F. \quad (4.1)
\end{aligned}$$

In equation (4.1), the coefficients  $A_{ikop}$  are constants of the material whose number equals 21 in the general case of anisotropy.

If axes  $x, y$  and  $z$  are superposed with the axes of symmetry of the orthotropic material, then one should discard from the symmetry considerations all the components that contain tangential stresses in the first degree and the products of different tangential stresses since these components can change their sign when reflected in the plane of symmetry of the material.

In the axes of symmetry of the orthotropic material, equation (4.1) will contain 9 constants  $A_{ikop}$  and adopt the following appearance: /139

$$\begin{aligned}
& A_{1111}\sigma_x^2 + A_{2222}\sigma_y^2 + A_{3333}\sigma_z^2 + 2A_{1122}\tau_{xy}\sigma_x + 2A_{2233}\tau_{yz}\sigma_z + \\
& + 2A_{3311}\tau_{zx}\sigma_x + 4A_{1313}\tau_{xz}^2 + 4A_{3332}\tau_{zy}^2 + 4A_{2121}\tau_{yx}^2 = F. \quad (4.2)
\end{aligned}$$

In this expression one can select the correlations between the coefficients  $A_{ikop}$  so that the addition of the spherical portion of the stress tensor does not change the size of the  $F$  function. Then the equation loses generality and conforms to Mises' particular assumption regarding the invariability of function  $F$  when the spherical stress tensor is added.

By using the designations of I. I. Gol'denblat [25,26], one can write Mises' plasticity function as a condition of constancy of the second joint invariant of the stress tensor  $\sigma_{ik}$  and the transformed stress tensor  $A_{ikop}\sigma_{op}$ , where  $A_{ikop}$  is the tensor that characterizes the material's resistance to plastic deformations

$$I = A_{ikop}\sigma_{ik}\sigma_{op} = 1 \quad (4.3)$$

It is easy to show that the plasticity tensor  $A_{ikop}$  in this case has a fourth order.

The condition of constancy of the plastic potential results in an assumption regarding the existence of a fourth rank (order) tensor whose components characterize the plastic properties (yield stresses) of anisotropic material.

It follows from equation (4.2) that, for example, the component  $A_{1111}$  is determined from the experiment for uniaxial stretching on the x axis of symmetry, whereupon

$$A_{1111} = \frac{1}{\sigma_{1111}^2} = \frac{1}{(\sigma_x^0)^2}, \quad (4.4)$$

where  $\sigma_{1111} = \sigma_x^0$  is the yield stress of orthotropic material during stretching in the direction of the x axis.

We correspondingly obtain

$$A_{1212} = \frac{1}{\sigma_{1212}^2} = \frac{1}{(\tau_{xy}^0)^2}, \quad (4.5)$$

where  $\sigma_{1212} = \tau_{xy}^0$  is the yield stress in pure shear under the influence of stresses  $\tau_{xy}$ .

Or in general

$$A_{ikop} = \frac{1}{(\sigma_{ikop}^0)^2}. \quad (4.6)$$

Thus, the components of the plasticity tensor according to Mises have another dimensionality than the components of the tensor of elastic deformation constants and the components of the strength tensor. /140 The assumption regarding its existence is substantiated in section 3.

By using Mises' condition as a function of the equally dangerous states, one can understand by the amount  $\sigma_{ikop}$  in formula (4.6) the corresponding ultimate resistance (ultimate strength) in the previously stated general sense.

Thus, the use of Mises' plasticity condition as a condition of strength results in a conclusion about the existence of a fourth rank strength tensor, but the physical dimensionality of the size of this tensor's components is different than assumed in section 3, where

$$a_{ikop} = \frac{1}{\sigma_{ikop}}.$$

Mises' condition of plasticity should be viewed for anisotropic materials from the aspect of its suitability as a condition that determines the equally dangerous stresses (strength conditions). For this purpose it is necessary to solve three main problems.

1. Is this condition experimentally confirmed. This can be verified by comparing it to the results of tests even for simple stretching of variously oriented samples of strongly anisotropic materials (Mises in the mentioned work indicates this possibility which is characteristic only for anisotropic materials).

2. Should ratios be introduced between the constants  $A_{ikop}$  that follow from Mises' assumption on the independence of the  $F$  function from the spherical stress tensor.<sup>1</sup>

3. Can Mises' equation that he wrote for material that equally resists stretching and compression, be applied to those anisotropic materials where these resistances differ.

We will examine the first question. The function (4.2) can be written as follows for planar stress as conveniently oriented in the symmetry plane of an orthotropic material

$$A_{1111}\sigma_x^2 + \sigma_y^2 A_{2222} + 2A_{1122}\sigma_x\sigma_y + 4A_{1212}\tau_{xy}^2 = 1. \quad (4.7)$$

In order to define the four constants, we use four particular stress states: 1) stretching on the symmetry axis  $x$  of the material in which the ultimate resistance  $\sigma_x^0$  equals  $\sigma_0$ ; 2) stretching on another axis of symmetry (lower strength)  $y$ , where the ultimate resistance is designated  $\sigma_y^0 = \sigma_{90}$ ; 3) stretching in a diagonal direction, i.e., at a  $45^\circ$  angle to the  $x$  axis in the plane  $xy$  -  $\sigma_{45}$ , and 4) pure shear in the  $xy$  plane on areas parallel to the symmetry axes in which the ultimate resistance correspondingly  $\tau_{xy}^0 = \tau_0$ . Then equation (4.7) after determination of the constants will adopt the following appearance [117]:

$$\frac{\sigma_x^2}{\sigma_0^2} + \frac{\sigma_y^2}{\sigma_{90}^2} + \frac{\tau_{xy}^2}{\tau_0^2} + \left( \frac{4}{\sigma_{45}^2} - \frac{1}{\sigma_0^2} - \frac{1}{\sigma_{90}^2} - \frac{1}{\tau_0^2} \right) \sigma_x \sigma_y = 1. \quad (4.8)$$

If one assumes that in equation (4.8)

<sup>1</sup>Bridgman's experiments [123] on quartz compression contradict this assumption. 149

$$\left. \begin{aligned} \sigma_x &= \sigma_b \cos^2 \alpha; \\ \sigma_y &= \sigma_b \sin^2 \alpha; \\ \tau_{xy} &= \sigma_b \frac{\sin 2\alpha}{2} \end{aligned} \right\}, \quad (4.9)$$

then the following expression is obtained for the ultimate resistance  $\sigma_{ikop} = \sigma_b$  of the sample whose axis forms angle  $\alpha$  and lies in the xy plane (see fig. 344,a).

$$\sigma_b = \frac{\sigma_0}{\sqrt{\cos^4 \alpha + B \sin^2 2\alpha - c^2 \sin^4 \alpha}}, \quad (4.10)$$

where

$$c = \frac{\sigma_0}{\sigma_{90}}; \quad a = \frac{\sigma_0}{\sigma_{45}}; \quad B = a^2 - \frac{1+c^2}{4}.$$

After substituting into equation (4.8) the quantities

$$\begin{aligned} \sigma_x &= \tau_b \sin 2\alpha = -\sigma_y; \\ \tau_{xy} &= \tau_b \cos 2\alpha, \end{aligned} \quad (4.11)$$

we obtain a formula that expresses the relationship of ultimate strength  $\sigma_{ikik} = \tau_b$  in pure shear depending on the angle  $\alpha$  between the x axis and the perpendicular to one of the areas of action of tangential stresses

$$\tau_b = \frac{\tau_0}{\sqrt{\cos^2 2\alpha - \left(\frac{\tau_0}{\tau_{45}}\right)^2 \sin^2 2\alpha}}, \quad (4.12)$$

where  $\tau_0$  and  $\tau_{45}$ --ultimate strengths in shear in plane of symmetry xy respectively with  $\alpha=0$  and  $\alpha=45^\circ$ . It was assumed in chapter 1

$$a_{ikop} = \frac{1}{\sigma_{ikop}}. \quad (4.13)$$

where  $\sigma_{ikop}$  is the ultimate resistance.

Instead of formulas (4.10) and (4.12), chapter 1 respectively obtained tensorial formulas (1.22) and (1.24) that differ only in the exponent of the ultimate strengths.

From correlation (4.6) one can obtain a formula for  $\sigma_b = \sigma_{ikop}$  and in the general case of random orientation of this quantity in space. This formula will differ from formula (1.20) only in the higher (second) /142

exponent of the constants.

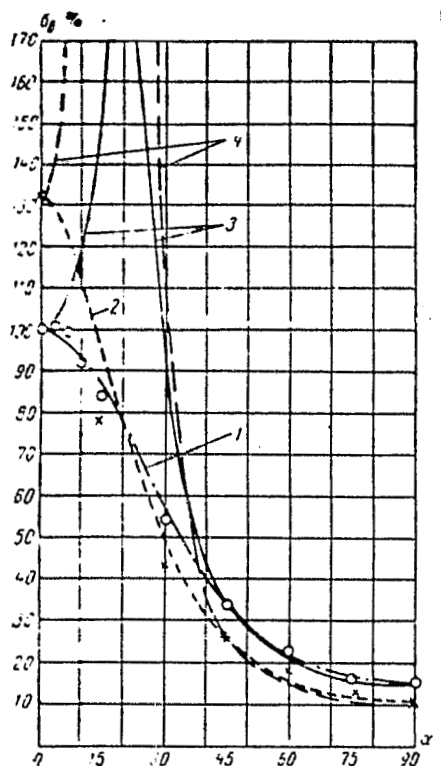


Figure 4.1. Comparison of Curves 1 and 2 Constructed according to Formula (1.22) (1 for compression and 2 for stretching) and Curves 3 and 4 Constructed according to Formula (4.10) (3 for compression and 4 for stretching) with Results of Testing Pine for Compression (o) and for Stretching (x).

Formula (1.22) was verified in chapter III by comparison with experimental data for different anisotropic materials. A verification of the suitability of Mises' function as a strength condition will be, for example, a comparison of formula (4.10) with the experimental data of chapter III.

One should note first of all that formula (4.10) for certain materials (mainly wood) that are distinguished by a high degree of anisotropy, yields a break in the continuity on curve  $\sigma_b = f(\alpha)$  [117].

With certain ratios between the strength characteristics of the

material  $\sigma_0, \sigma_{90}$  and  $\sigma_{45}$ , the size of the coefficient B in formula (4.10) becomes negative, and namely with

$$\sigma_{45} > \frac{2\sigma_0\sigma_{90}}{1 - \sigma_0^2 - \sigma_{90}^2}. \quad (4.14)$$

In this case, with certain values of the angle (close to  $\alpha=15-20^\circ$ ), the curve that illustrates the change in  $\sigma_b$  depending on the size of  $\alpha$ , undergoes a break in continuity ( $\sigma_b \rightarrow \infty$ ), which contradicts the experimental data. For weakly anisotropic bodies, usually  $B > 0$  and formula (4.10) is confirmed by experiment.

Figure 4.1 shows curves 3 and 4 for the change in the quantity  $\sigma_b$  depending on  $\alpha$ , constructed from formula (4.10) for such a strongly anisotropic material as pine in compression and stretching. The curves have a break in continuity.

Thus, for strongly anisotropic materials, condition (4.2) contradicts the experimental data. /144

Table 4.1 presents the data showing in which case a break in continuity is possible during computation with formulas (4.10) and (1.22). As is apparent from the data of these tables, the following is obtained for all tested materials (column 5 and 6):

$$\sigma_{45} < \frac{4\sigma_0\sigma_{90}}{\sigma_0 - \sigma_{90}}$$

and tensorial formula (1.22), derived from ratio (4.13) does not yield the values  $\sigma_b \rightarrow \infty$ .

Formula (4.10) does not yield a break in continuity only in the case of weakly pronounced anisotropy, and for wood materials in four cases (table 4.1) results in  $\sigma_b \rightarrow \infty$  (columns 8 and 7 in table 4.1).

Section 15 describes experiments on biaxial compression of certain anisotropic materials. For this case, we obtain the following from equation (4.8), if we designate  $\sigma_d$  as the amount of resistance to biaxial compression:

$$\sigma_d = \frac{\sigma_{45}\tau_0}{1 - \frac{\sigma_0^2}{4} - \sigma_{45}^2}.$$

For aviation plywood, this formula yields a quite satisfactory coincidence ( $\sigma_d = 428.5 \text{ kg/cm}^2$ ) with experimental results ( $438 \text{ kg/cm}^2$ ), but for wood the formula results in imaginary quantities, since  $\sigma_{45} > 2\tau_0$ .



TABLE 4.1.

Material	Type of testing							Is there break in continuity in calculation by formula (4.10)	Published source
		$\sigma_{11}$ kg/cm <sup>2</sup>	$\sigma_{22}$ kg/cm <sup>2</sup>	$\frac{\sigma_{11} \sigma_{22}}{\sigma_{10} \sigma_{20}}$	$\sigma_{11}$ kg/cm <sup>2</sup>	$\frac{\sigma_{11}^2}{\sigma_{10}^2}$	$\sigma_{15}$		
1	2	3	4	5	6	7	8	9	10
Pine	Compression	443	66	198,3	151	17 045	22 801	Yes	[71]
"	Stretching	593	48	178,0	114	9 156	12 996	Yes	[75]
Birch veneer sheet	"	1400	35	136,6	72	4 896	5 184	Yes	[5]
7 mm bakelite plywood	"	1050	865	1898,7	477	1 785 650	227 529	No	[5]
Aluminum alloy Avional		3850	3500	7333	3250	26 828 053	10 562 500	"	[92]
Cold-hardened fiber glass-reinforced plastic on PN-1		2990	1900	4647	1060	10 286 376	1 123 600	"	[12]
SVAM on epoxy-phenol resin 1:5		5878	2400	6817,7	1154	19 748 825	1 331 716	"	[12]
SVAM on epoxy-phenol resin 1:13		7900	1140	3985	1020	5 092 358	1 562 500	"	[12]
Parallel plywood	Compression	865	81	306,3	130	27 963	16 900	"	[5]
"	Stretching	1260	59	225,5	121	13 893	15 376	Yes	[5]

Thus, the experiments on biaxial compression also confirm that the strength condition (4.8) cannot be applied to strongly anisotropic wood materials whose strength in pure shear on the symmetry areas  $\tau_0$  is considerably lower than the strength of uniaxial stresses.

Figures 4.2 and 4.3 show that formulas (4.10) and (1.22) conform equally well to the results of testing weakly anisotropic materials: bakelite plywood and aluminum alloy.

Figure 1.2 a presented a comparison of the calculation results using different formulas with the results of testing SVAM fiber glass-reinforced plastic. This comparison referred to the polar coordinates.

For SVAM with 1:3 fiber ratio, the solid line (curve 1) is constructed from formula (1.22) (fig. 1.2). With  $\alpha=15^\circ$ , this formula yields the amount  $\sigma_b$  which is greater than the experiment (black dots). In this case, curve 3 (dot-dash) that is constructed from formula (4.10) yields amounts that are smaller than the experiment, based on an assumption regarding the fourth order tensor whose components are quantities that are inverse to the ultimate strength taken not in the first, but in the second degree.

For SVAM with 1:1 fiber ratio, the computation results from formula (4.10) yield curve 6 that conforms somewhat better to the experimental data (circles in fig. 1.2a) than curve 4 that was constructed from formula (1.22).

Figure 4.4 presents the results of compression tests on pine in which the amounts  $\sigma_{pf}$  of the limit of plastic flow [36] were defined by Yu. M. Ivanov using the same technique with all sample orientations. In this case, curve 2 for change in  $\sigma_{pf}$  that was constructed from formula (4.10) has a break in continuity, while curve 1, constructed from formula (1.22) does not.

Since the material's anisotropy has a stronger effect in determining the ultimate strengths for stretching than for compression, then a case is possible where formula (4.10), conforming to the compression experiments, will yield a break in continuity during stretching. The parallel birch plywood (table 4.1 and fig. 4.5) is an example of this material.

Thus, a break in the continuity of the curve in calculation by formula (4.10) is not linked to the different physical nature of the

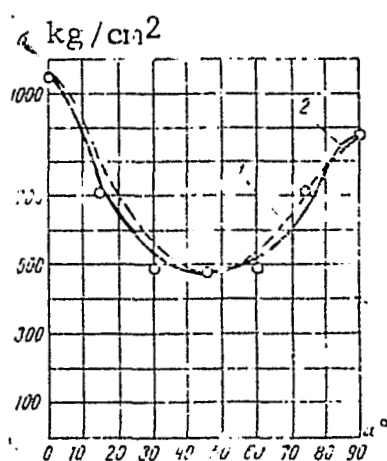


Figure 4.2. Comparison of Curve 1 Constructed from Formula (1.22) and Curve 2 Constructed from Formula (4.10) with Results of Testing Bakelite Plywood for Stretching  
Dots show average testing results

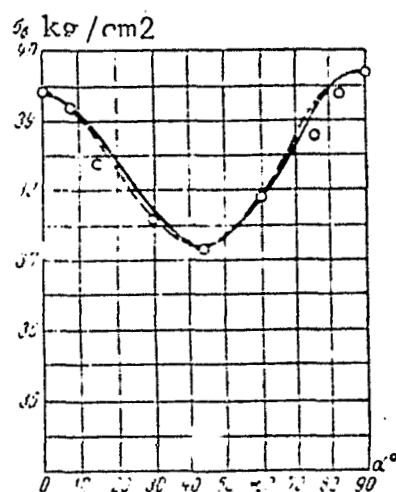


Figure 4.3. Comparison of Curves Constructed from Formula (1.22) (dotted) and Formula (4.10) (solid line) with Results of Testing Aluminum Alloy Ergal for Stretching [92].  
Dots show average testing results

dangerous state of the material with different values of angle  $\alpha$ , and perhaps, can apparently be explained by the unsuitability of formula (4.2) for strongly anisotropic materials. However, for a number of fiber glass-reinforced plastic fabrics, metals and certain other weakly anisotropic materials, Mises' function (4.7) that was adopted as the strength condition, permits a good approximation of the testing results.

Passing to the second question, one should stipulate that the correlations between the material constants that follow from the hypothesis on the invariability of the F function when the spherical stress tensor is added and which result in "rariconstancy," i.e., decrease in the number of constants, were not included in formula (4.10), since the coefficients of equation (4.8) were determined experimentally for the particular cases of stress states.

The correlations between the constants  $A_{ikop}$  in equation (4.2) that follow from the rariconstant assumption of Mises were studied by Hill [75].

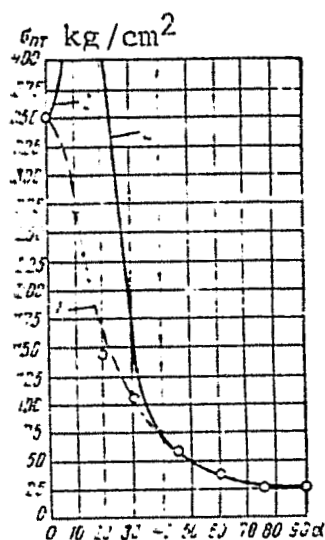


Figure 4.4. Comparison of Curve 1 Constructed from Formula (1.22) and Curve 2 Constructed from Formula (4.10) with Results of Determining Limit of Plastic Flow [36] of Pine in Compression

For strongly anisotropic wood where the ultimate strength in stretching (and compression) along the fibers is much greater than the resistance to simple shearing transverse to the fibers, this correlation is not confirmed even approximately. It is apparently better to take Mises' condition of plasticity in its original form, without introducing hypotheses that artificially reduce the number of independent constants in equation (4.2).

By introducing an assumption on the independence of the yield stress of crystals from the amount of hydrostatic pressure, Mises modifies the plasticity condition (4.1). This results in ratios that are formulated in detail in chapter XII of Hill's book Mathematical Theory of Plasticity as applied to rolled steel. Mises' assumption results in a decrease in the number of independent components of tensor  $A_{ikop}$  in the general case of anisotropy from 21 to 15, and in the symmetry axes of orthotropic material, from 9 to 6.

This assumption is analogous to the known correlations of Cauchy that were suggested as the basis for the rariconstant theory of elastic

constants of anisotropic bodies, and also because these correlations do not have experimental confirmation for strongly anisotropic bodies.

The erroneous nature of Mises' assumption as applied to the strength of strongly anisotropic bodies even in such a comparatively plastic form of testing as compression of wood, can be substantiated by the following simple comparison.

/147

The assumption that Mises [106] introduced and that is used in several modern works on strength of anisotropic bodies, assumes the limit state of the anisotropic body to be unchanged when hydrostatic pressure understood as an algebraic quantity is added to the stress.

This assumption leads to a requirement for equality of the ultimate resistance of the material in biaxial equal compression in the sheet plane and uniaxial stretching in a direction perpendicular to the sheet plane. This is because the addition of triaxial equal stretching should not alter the amount of resistance to biaxial compression. This requirement can be fulfilled, for example, for an isotropic material that resists stretching and compression equally, if biaxial compression under equal conditions yields the same amount of ultimate resistance as uniaxial stretching.

The results of testing anisotropic materials under conditions of biaxial compression demonstrate that this assumption does not conform to reality for strongly anisotropic pine.

The strength of wood in biaxial compression (see section 15) in two directions that are perpendicular to the fibers is considerably lower than its strength during stretching along the fibers. Consequently, the addition of a positive spherical tensor of stresses significantly affects the wood resistance. One can draw a conclusion from here that Mises' assumption is doubtful as applied to the ultimate strengths of strongly anisotropic wood materials. For fiber glass-reinforced plastic made of T fabric on PN-1 resin, the strength in biaxial compression in the sheet plane (see section 15) is roughly 8 times higher than its strength in stretching in a direction perpendicular to the sheet plane.

/148

Passing to Mises' third case, equality of ultimate resistances to stretching and compression of the material, one can note that for many

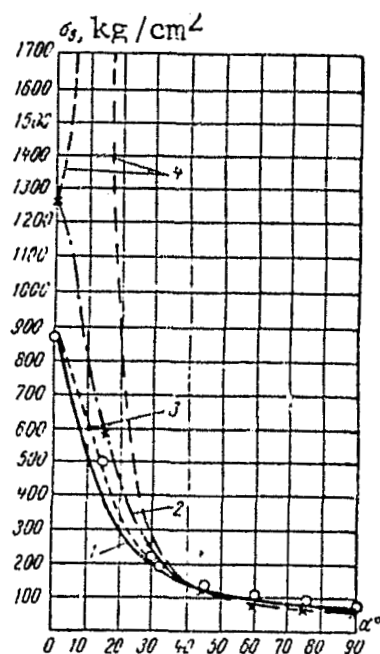


Figure 4.5. Comparison of Curves 1 and 2 Constructed from Formula (1.22). (1--for Compression and 2--for stretching) and Curves 3 and 4 Constructed from Formula (4.10) (3 for compression and 4 for stretching) with Results of Testing Parallel Birch Plywood for Compression (o) and for Stretching (x)

materials whose anisotropy is considerable (wood, fiber glass-reinforced plastic), the difference between the amount of resistance to stretching in different structural directions exceeds the difference between the resistances to stretching and compression in the same direction. Mises' equation can therefore be generalized for a planar stress, for example: for all stresses in which the areas of symmetry are only affected by stretching stresses  $\sigma_x$  and  $\sigma_y$ , or one of the compressing that in absolute amount is smaller than the second, stretching, one should consider that the coefficients  $A_{ikop}$  are determined by stretching and shear.

For those planar stresses in which both stresses  $\sigma_x$  and  $\sigma_y$  are compressing or compressing more than stretching, the coefficients

$A_{ikop}$  are determined according, to compression and shear. This statement of the question becomes clear with a graphic illustration of the surface of equally dangerous planar stresses in the coordinate axes  $\sigma_x, \sigma_y, \tau_y$  that is examined in section 17 of this chapter and that represents the application of the method of piecewise approximation.

Thus, Mises' condition of plasticity in the suggested formulation (4.8), adopted as the phenomenological strength theory for planar stresses, does not contradict the experiments described in chapter III, including for materials that have varying resistance to stretching and compression. This is on the condition that the following correlation is fulfilled between the ultimate strengths of the orthotropic sheet material along ( $\sigma_0$ ), transverse ( $\sigma_{90}$ ) and at a  $45^\circ$  angle ( $\sigma_{45}$ ) to the axis of symmetry.

$$\sigma_{45}^2 \leq \frac{4\sigma_0^2\sigma_{90}^2}{\sigma_0^2 + \sigma_{90}^2}. \quad (4.15)$$

#### 17. Approximate Structure of Surface of Equally Dangerous Planar Stresses from Experimental Data

We hypothesize that the anisotropic material can be viewed as a homogeneous continuum and that a certain surface exists that can be expressed by the equation

$$F_0(\sigma_x, \sigma_y, \tau_{xy}) = 0, \quad (4.16)$$

All of its points conform to the equally dangerous planar stresses /149 variously oriented in the symmetry plane of this (orthotropic) material. The letters  $\sigma_x, \sigma_y$  and  $\tau_{xy}$  here, as in the previous paragraph, designate the stresses that are active in the dangerous state on the material's symmetry areas. The axes  $x, y$  and  $z$  are superposed with its symmetry axes.

The anisotropic materials have features that permit approximate construction of the surface (4.16) from the results of testing variously oriented samples for uniaxial stretching, compression and shearing. With simple (uniform) stretching (or compression) of the samples whose axes lie in the plane  $xy$  and form the angle  $\alpha$  with the  $x$  axis, one can write the correlation (4.9), where  $\sigma_b$  is the

experimentally determined ultimate strength of the sample.

All the points with coordinates computed from formula (4.9) must lie on surface (4.16) if this surface exists. In order to construct the surface of equally dangerous stresses, we will reserve the stresses  $\sigma_x$ ,  $\sigma_y$  and  $\tau_{xy}$  on the coordinate axes. Figures 4.6a, 4.7a, 4.8a and 4.9a construct points with coordinates  $\sigma_x$ ,  $\sigma_y$  and  $\tau_{xy}$  computed from formulas 4.9 for the average testing results of variously oriented samples of cold-hardened fiber glass-reinforced fabric plastic (fig. 4.6a), aviation plywood (4.7a), pine (4.8,a) and SVAM fiber glass-reinforced plastic with 1:1 fiber ratio (fig. 4.9a). All the experimental data were taken from chapter III. The testing results for stretching conform to the points with positive abscissas  $\sigma_x$  and  $\sigma_y$ , and for compression to the negative.

The corresponding points are united into curves in figures 4.6b, 4.7b, 4.8b and 4.9b. The curves that conform to the stretching testing results of variously oriented samples are designated by the letter P on all three figures, and C for compression.

The points whose abscissas  $\sigma_x$  and  $\sigma_y$  have different signs, were constructed from the shear testing results of variously oriented samples made of the same materials. The shear testing results were used to construct the points in an a fortiori inaccurate hypothesis that a uniform stress of pure shear exists in the sample of any orientation at the moment of failure. With this hypothesis, the stresses  $\sigma_x$ ,  $\sigma_y$  and  $\tau_{xy}$  can be computed depending on the amount  $\tau_b$  of ultimate shear resistance on the area that comprises angle  $\alpha$  with the x axis and is perpendicular to the xy plane according to formulas (4.11).

The points with coordinates that are computed from formulas (4.11) are plotted on fig. 4.6a and b, 4.7 a and b, 4.8 a and b and 4.9 a and b. They are united by curves that are designated by the letter T on the figures.

Points on the coordinate plane  $\tau_{xy}=0$  are also plotted in the region of negative abscissas. These points coorespond to the testing results for biaxial compression of square samples  $2 \times 2 \text{ cm}^2$  with the same quantity of main stresses acting on the direction of x and y symmetry axes of the material. These tests were carried out on a special "Fepply's cross" type reverser (see section 15). /153



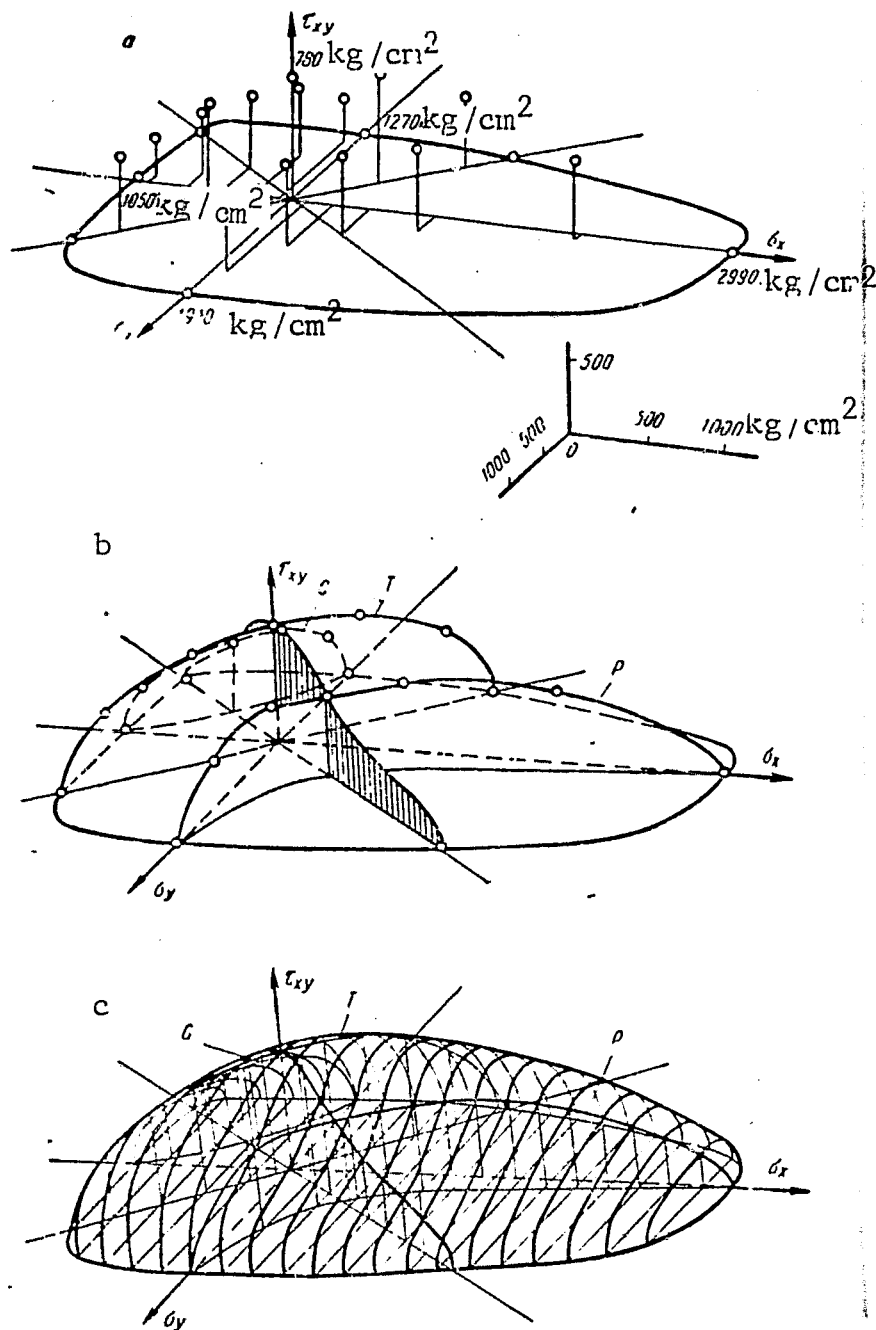


Figure 4.6. Surface of Equally Dangerous Planar Stresses for Fiber Glass-Reinforced Fabric Plastic of Cold Hardening.

/150

On the coordinate plane  $\tau_{xy} = 0$  that conforms to those planar stresses in which the main stresses act in the direction of the material's axis of symmetry, we arranged only seven points for each material. The

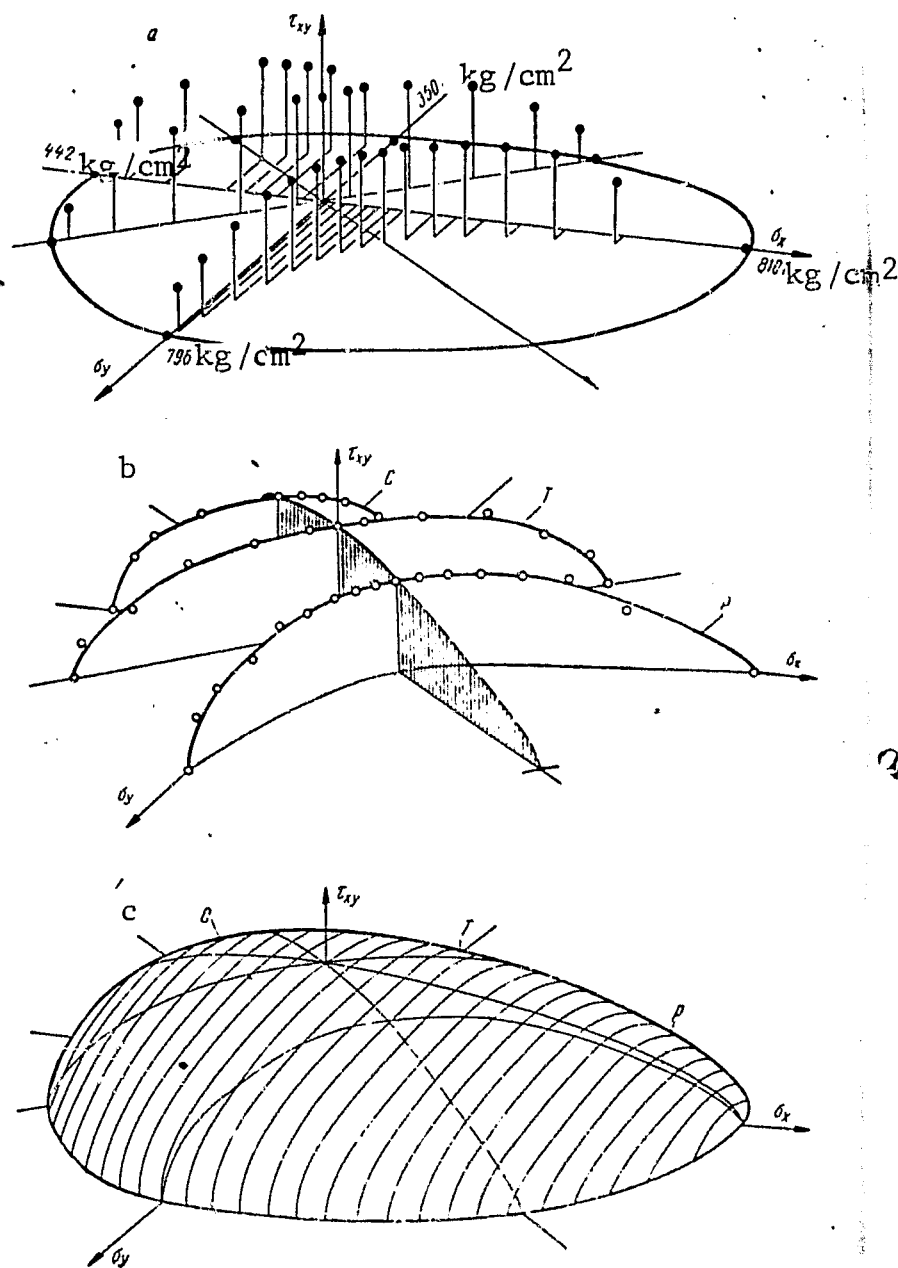


Figure 4.7. Surface of Equally Dangerous Planar Stresses for Aviation Plywood 10 mm Thick.

/151

entire curve for intersection of the limiting surface with this coordinate plane was constructed approximately by extrapolation of experimental data.<sup>1</sup>

<sup>1</sup>The eighth point is plotted on figure 4.6b according to published data [124] for biaxial stretching.

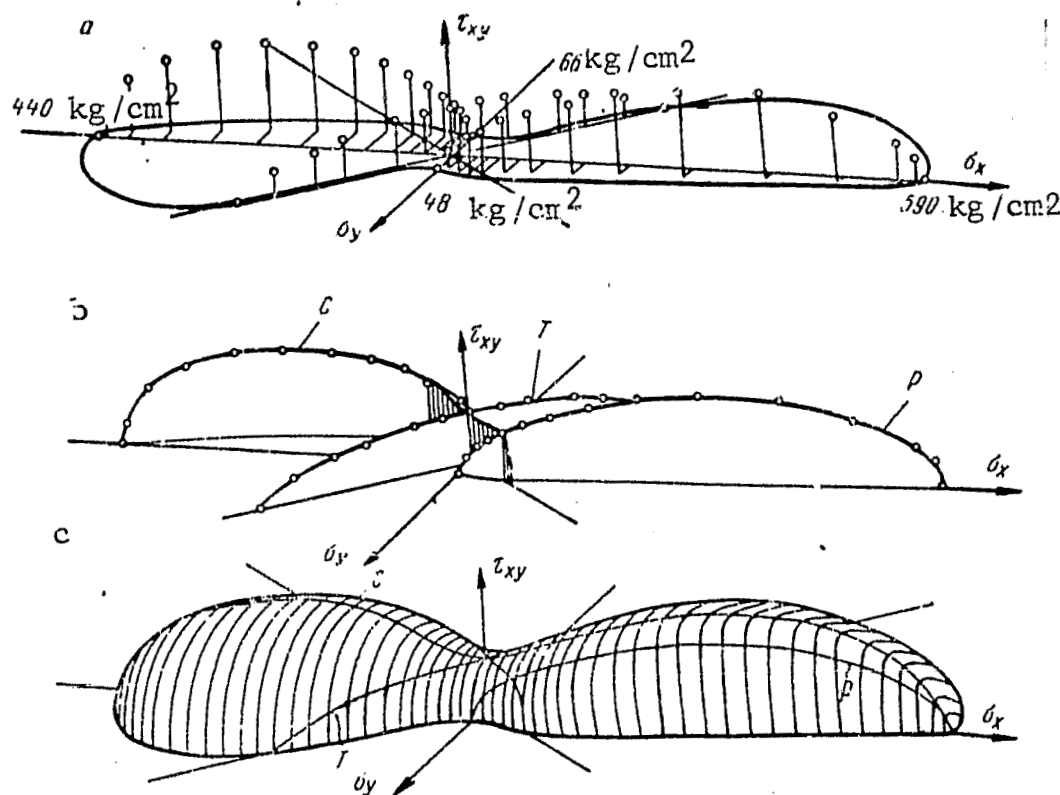


Figure 4.8. Surface of Equally Dangerous Planar Stresses for Pine

/152

The entire surface of equally dangerous states (limiting surface) is constructed in fig. 4.6c and 4.7 c for fiber glass-reinforced fabric plastic [117] and for aviation plywood [14] such that all the points that were obtained from testing results lie on this surface. The limiting surface for these comparatively weakly anisotropic materials by its appearance allows the hypothesis that it can be presented by an algebraic equation of the second order. After its intersection with the coordinate plane,  $\tau_{xy}=0$  can apparently be described by Mises' equation (4.7) or the equations suggested in the works of K. V. Zakharov [33,34] or J. Marin [105].

For pine, material with more pronounced anisotropy, these equations can no longer approximate experimental data. The limiting surface constructed for pine [14] in fig. 4.8c, is not convex everywhere. It consequently cannot be represented by a second order equation. An even

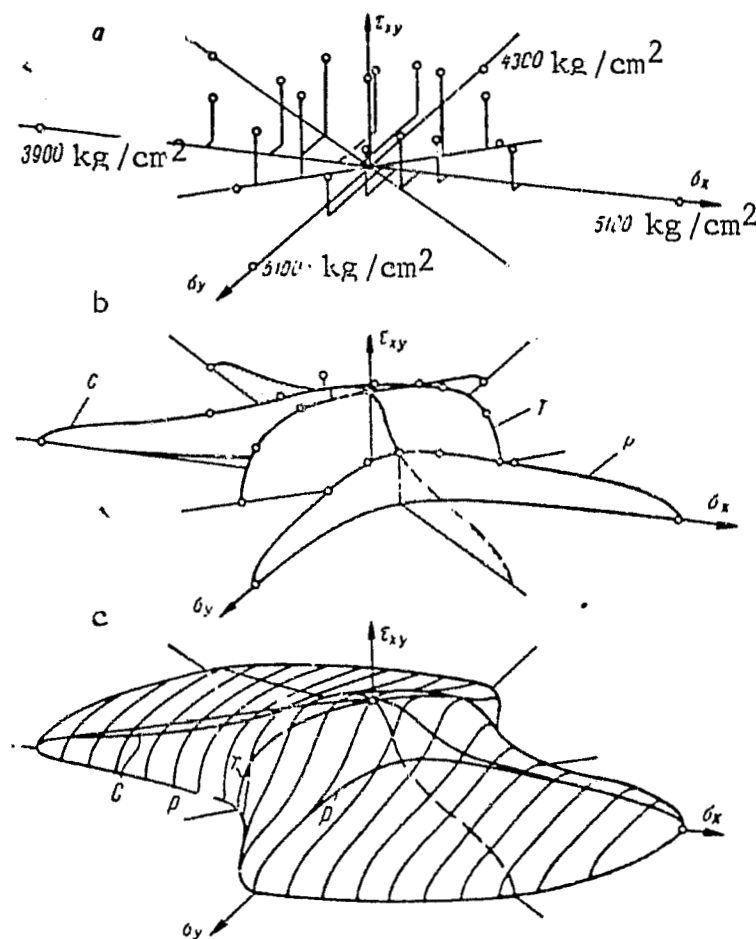


Figure 4.9. Surface of Equally Dangerous Planar Stresses for SVAM Fiber Glass-Reinforced Plastic on Epoxy-Phenol Binder with 1:1 Fiber Ratio

more complicated surface (fig. 4.9c) is obtained for SVAM fiber glass-reinforced plastic (see also article [14]).

However, one cannot draw any conclusions from the appearance of the limiting surfaces constructed above in regards to the plasticity functions of anisotropic materials, since the ultimate resistances  $\sigma_b$  and  $\tau_b$  were determined, as is customary in mechanical tests, in the majority of cases according to the failure of the samples, often of a quite brittle nature. Only for certain directions, mainly in compression, was the analysis made from that place on the testing diagram where the initial inclined section becomes a horizontal, or

almost horizontal line. Strength anisotropy for the examined materials has not only a quantitative, but also a qualitative nature. Undergoing brittle failure with one orientation of forces, the same material, with another orientation of the same forces, reveals clearly plastic properties. The limiting surfaces are surfaces of equally dangerous states. Constructed from the results of standard tests for stretching, compression and shear, they can be used for an approximate solution to the problem of the technical strength of the anisotropic material in the planar stressed state, as well as the problem that inevitably arises in designing machine parts made of reinforced plastics and other anisotropic materials.

The accuracy of the suggested solution to the problem depends on the number of points used to construct the surface, and on the degree of accuracy of defining the coordinates of these points. Here not only /155 the number of samples that guarantee the reliability of the experimental results is important, but also the most accurate possible correspondence between the calculated plan of uniform stress and the actual stress field that develops in the tested samples by the moment the amount of ultimate resistance is determined. This correspondence is fulfilled for anisotropic materials in the majority of cases in a worse form than for isotropic (see chapter II).

Of course it is necessary to observe the same temperature, humidity, rate of testing and order of sample dimensions for all orientations and all stresses.

By having a surface of equally dangerous planar stresses for a real anisotropic structural material, one can select the analytical expression for it.

#### 18. Possible Forms of Strength Condition for Strongly Anisotropic Bodies

We will examine the surfaces of equally dangerous planar stresses that were approximately constructed in the previous section from experimental data, from the viewpoint of their possible approximation to an equation in the form of a polynomial. For materials whose anisotropy is low (plywood, fiber glass-reinforced fabric plastic), the surfaces are primarily convex. They can be fully approximated by an

equation in the form of a second degree polynomial suggested by Mises and resulting in formulas (4.7) and (4.8). If the material resists stretching and compression in different ways, i.e., the segments on the coordinate axes  $\sigma_x$  and  $\sigma_y$  (fig. 4.6-4.9) vary in the positive and negative quadrants, then equation (4.7) and (4.8) should be written separately for that part of the limiting surface that lies on one side from the plane diagonal, and separately for the other side. By diagonal, we mean the vertical plane that forms a  $45^\circ$  angle with the coordinate planes. The curves T that are constructed from the shear testing results of variously oriented samples lie in the diagonal planes.

The works of K. V. Zakharov [34] suggest another equation of the limiting surface in the form of a nonuniform polynomial of the second degree with a free term.

The polynomial coefficients are determined based on experiments on uniaxial stretching and compression in the direction of two axes of symmetry ( $\sigma_0^p, \sigma_{90}^p, \sigma_0^c, \sigma_{90}^c$ ) and in pure shear in the direction of the same axes  $\tau_0$  at a  $45^\circ$  angle to it,  $\tau_{45}$ . The equation is confirmed by experiments conducted for weakly anisotropic brittle materials where the difference between the resistances in stretching in the direction of the two axes of symmetry is considerably smaller than the difference between the resistances to stretching and compression. For strongly anisotropic bodies, one can, in the first approximation, ignore the differences in the resistance to stretching and compression, since these differences are usually less significant than the differences between strength in stretching in the directions of the two axes of symmetry (for example, for oriented fiber glass-reinforced plastics when the fibers are primarily laid in one direction). Then one can consider

$$\frac{\sigma_0^p}{\sigma_0^c} \ll \frac{\sigma_{90}^p}{\sigma_{90}^c}$$

Equation (8) of Zakharov's work [34], after substitution of (4.9) and calculation of  $\sigma_b$  with  $\alpha=45^\circ$  results in formula (4.10) with all of its shortcomings.

Mises [106] made the note that the plasticity function can change little depending on the spherical stress tensor (Mises cited here the

experiments of Lode and the hypothesis advanced by Shleykher for isotropic bodies).

The problem of constructing the plasticity function for anisotropic bodies is solved in the works of V. O. Geogdzhayev [23], V. A. Lomakin [46] and certain other authors in the spirit of Mises' remark.

The invariant quantity that contains second degree components of the stress tensor and components of the anisotropy tensor, is written in these works depending on the invariant quantity that contains the first degrees of stress. The type of dependence is unknown and requires experimental analysis.

The condition that is written below based on systematization of the experimental results, can be viewed as an attempt to establish this relationship for strength (but not plasticity) of strongly anisotropic bodies.

Returning to the appearance of the surfaces of equally dangerous stresses, we note that the degree of the polynomial for wood must be higher than the second. The same conclusion can be drawn for the appearance of the limiting surface for SVAM fiber glass-reinforced plastic.

For the latter, the unique appearance of the limiting surface is a consequence of the relatively small quantity of ultimate strength ( $\tau_{45}$ ) in shear at a  $45^\circ$  angle to the fibers. A. L. Rabinovich [64] obtained roughly the same quantity with a completely different testing method.

It is possible that with more accurate tests for the pure shear plan, one could pinpoint this quantity, and correspondingly, the shape of the limiting surface. For wood this pinpointing can hardly attribute to the limiting surface a shape that is characteristic for the second order surfaces.

A higher order of limiting surface can be obtained if one starts from the tensor of ultimate resistances in the form adopted in chapter 1. We will take the higher, fourth, order of the polynomial that expresses the link between the invariants of the stress tensor and permits approximation of the surface of equally dangerous planar stresses for strongly anisotropic materials. /157

We will take the following polynomial as an example [117]

$$\begin{aligned} & \left[ \frac{\sigma_x^2}{\sigma_0} + \frac{\sigma_y^2}{\sigma_{90}} + \tau_x \tau_y \left( \frac{4}{\sigma_{45}} - \frac{1}{\sigma_0} - \frac{1}{\sigma_{90}} - \frac{1}{\tau_0} \right) + \frac{\tau_{xy}^2}{\tau_0} \right]^2 + \\ & - 2 \frac{\tau_x \tau_y - \tau_{xy}^2}{\tau_0} \left[ \tau_x \tau_y \left( \frac{1}{\sigma_0} + \frac{1}{\sigma_{90}} \right) + \frac{\sigma_x^2}{\sigma_0} + \frac{\sigma_y^2}{\sigma_{90}} \right] - \\ & - (\sigma_x \sigma_y - \tau_{xy}^2) [\tau_x \tau_y (\lambda + \mu) + \lambda \sigma_x^2 + \mu \sigma_y^2] - \rho (\tau_x - \tau_y) \times \\ & \times (\sigma_x \sigma_y - \tau_{xy}^2) - (\sigma_x^2 + \sigma_y^2 + \tau_{xy}^2 + \tau_x \tau_y) = 0. \quad (4.17) \end{aligned}$$

In equation (4.17), the coefficients  $\mu$ ,  $\lambda$  and  $\rho$  require experimental analysis with three biaxial stresses that comply with three different points in space  $\sigma_x, \sigma_y$  and  $\tau_{xy}$ . These can be, for example, stresses in which the main stresses  $\sigma_1 = 2\sigma_2$  form  $0.90^\circ$  and  $45^\circ$  angles to the x axis. The first two cases are illustrated by points on the coordinate plane  $\tau_{xy} = 0$ , and the third does not lie in this plane. One of these stresses can be replaced by a biaxial stress with  $\sigma_1 = \sigma_2$ . With any orientation in the plane, the latter conforms to the same point on the coordinate plane  $\tau_{xy} = 0$ . We therefore assume that the strength of the orthotropic material in biaxial equal compression or stretching, oriented as we please in the symmetry plane of the orthotropic material, remains fixed (does not depend on the orientation). The experiments described in section 15 confirm this conclusion to a certain measure. The polynomial (4.17) can be written in Gol'denblat's designations [122] that stress the tensorial dimensionality of the quantities included in it

$$\begin{aligned} & (\Pi_{i \lambda o p} \sigma_{ik} \sigma_{op})^2 + \frac{\tilde{\sigma}_{ik} \sigma_{ik} - \sigma_{ik} \sigma_{ik}}{2} [8 \Pi_{1212} \tilde{\sigma}_{ik} \sigma_{ik} (\tilde{\sigma}_{ik} \sigma_{ik} \Pi_{ikik}) - \\ & - \tilde{\sigma}_{ik} \sigma_{ik} (\tilde{\sigma}_{ik} \sigma_{ik} \Pi_{ik}) + \rho \tilde{\sigma}_{ik} \sigma_{ik}] - (\tilde{\sigma}_{ik} \sigma_{ik})^2 + \\ & + \frac{(\tilde{\sigma}_{ik} \sigma_{ik})^2 - \sigma_{ik} \sigma_{ik}}{2} = 0, \quad (4.18) \end{aligned}$$

where



$$\sigma_{ik} = \begin{vmatrix} \sigma_x & \tau_{xy} & 0 \\ \tau_{xy} & \sigma_y & 0 \\ 0 & 0 & 0 \end{vmatrix}; \quad \Pi_{ik} = \begin{vmatrix} \lambda & 0 & 0 \\ 0 & \mu & 0 \\ 0 & 0 & 0 \end{vmatrix}; \quad \delta_{ik} = \begin{cases} 1 & i = k \\ 0 & i \neq k \end{cases}$$

$$\Pi_{1111} = \frac{1}{\sigma_0}; \quad \Pi_{2222} = \frac{1}{\sigma_{90}}; \quad \Pi_{1212} = \frac{1}{4\tau_0};$$

$$\Pi_{1122} = \frac{1}{2} \left[ \frac{1}{\sigma_0} + \frac{1}{\sigma_{90}} - \frac{1}{\tau_{45}} \right].$$

/158

During simple stretching at angle  $\alpha$  to the x axis, the strength condition (4.18) after substitution of (4.9) results in formula (1.22). Thus, this condition is confirmed by the experiments in chapter III for different, including strongly anisotropic, materials with uniaxial stress states, randomly oriented in the material. During pure shear at angle  $\alpha$  to the x axis, condition (4.18) after substitution of (4.11) results in formula (1.23). In turn, this formula is confirmed by approximate experiments on shear of orthotropic materials presented in chapter III.

We do not have experimental data for an exhaustive, comprehensive verification of equation (4.18). It therefore should be viewed as one of the possible versions for solving the stated problem that is not in contradiction to the experimental data stated in chapter III, and is applicable in the case of materials that have varying resistance to stretching and compression with the help of the method of piecewise approximation.

### Conclusion

The study of strength problems of various wood and synthetic structural materials is complicated by their heterogeneous structure. This work made calculations based on a simplifying hypothesis that views all the materials as a homogeneous anisotropic continuum.

The structure of the majority of wood and many synthetic materials determines the existence of at least three mutually perpendicular symmetry planes. This allows us to attribute to them orthogonal or transverse symmetry of strength properties.

A study of the symmetry of mechanical properties permits generalization of the results from testing variously oriented samples by introducing an assumption regarding the tensoriality of the strength characteristics of anisotropic materials.

The assumption regarding the tensoriality of the strength characteristics is made here in the sense that their change depending on the stress orientation in the material occurs according to laws that can be approximated by formulas for the transformation of tensor components during rotation of the coordinate axes. /159

Since the phenomenon has a center of symmetry, the rank of the tensor must be even. The equality of the strength characteristics in the direction of three mutually perpendicular symmetry axes of the material still does not determine its isotropy. The second rank of the strength tensor is therefore insufficient. The nearest, smaller, fourth, rank of the tensor has been suggested to characterize the strength.

Examination of the figures for change in the elasticity moduli and the ultimate strengths of different orthotropic materials shows that the equations of the corresponding surfaces have the same (fourth) order, and consequently, the coefficients of these equations are components of the fourth order tensor that have the same physical dimensionality.

A concept has been introduced on the strength tensor whose components are suitable to approximate the laws for change in the strength characteristics of anisotropic bodies in stresses of stretching, compression and pure shear. The strength tensor is constructed analogously to the tensor of elastic constants.

Based on the concept regarding the fourth order strength tensor, formulas were obtained that were common for all materials for the change in the strength characteristics depending on orientation of the stress in the material. These formulas, called tensorial, can be used in static, impact and repeatedly variable loading on the condition that the same testing conditions are observed (same order of deformation rate, temperature, humidity, dimensions of the sample and nature of the stress) with all orientations of the material.

The tensorial formulas that determine the size of the strength characteristics of orthotropic and transtropic materials in stretching, compression and pure shear were obtained for a general case of random orientation of these stresses in relation to three axes of symmetry of the orthotropic material.

Separate examination was made of cases of shearing testing, in which

the resistances in mutually perpendicular directions can vary, and a case of pure shear in which the resistance is determined by the smaller of its two quantities experimentally obtained in shearing on two mutually perpendicular planes.

Based on the introduced concept regarding the strength tensor, it was established, how many and precisely which strength characteristics of the orthotropic material should be determined experimentally in order to be able to compute the amount of resistance of this material in any orientation of the stretching, compression and pure shear stresses. /160

It was established that the isotropy criterion, for example, of sheet material in the sheet plane can only be the equality of its three stretching resistances to each other in the following directions: longitudinal, transverse and diagonal. The equality of the first two is not an indicator of isotropy or equal strength of the material.

It has been shown that the sheet plates with nonorthogonal laying of the reinforcing fibers can be classified as orthotropic materials. In a particular case of placement of the fibers in three (or more) directions that form equal angles of  $60^\circ$  (or less), this material will be transverse-isotropic (transtropic) in its strength.

Experimental studies on the mechanical properties of different structural materials showed that the tensorial formulas of chapter I are good approximations of the law for change in the strength characteristics depending on the orientation in relation to the symmetry axes of the orthotropic materials.

The tensorial formulas were compared with the results of static (machine) tests for stretching, compression, shear, simple shearing, tests for impact compression and repeatedly changing pure bending. The tests were conducted partially by the author and partially by a group from the department of construction mechanics of the Forest Engineering Academy with the author's participation. Results were also used from works published in the literature.

The tensorial formulas were confirmed by experimental results for the following anisotropic materials:

pine, stripped birch veneer sheet, laminated wood plastics DSP-B and DSP-V, aviation and bakelite multilayer plywood, German wood plastics, parallel plywood glued out of birch veneer sheet layers of the

same orientation;

fiber glass-reinforced plastics on Butvar-phenol, epoxy-phenol and polyester binders with fabric and fibrous (SVAM) reinforcement. For the latter, cases were studied of orthogonal (with fiber ratio of 1:1, 1:5 and 1:13) and nonorthogonal arrangement in two and three directions;

metals: cold-rolled steel and aluminum alloys;

directed films of crystal polymers (caprone, polyethylene and lavsan).

It was thus demonstrated that instead of different empirical formulas used for this purpose, the strength of anisotropic materials depending on the orientation can be computed with sufficient accuracy by using the tensorial formulas of chapter I that are common for all materials

The tensorial formulas make it possible to determine the direction /161 of the greatest and least strength of the material depending on the ratio of its original characteristics. Selection of the material of the optimal anisotropy for each structural element affords new possibilities for implementing the principle of equal strength with regards for anisotropy.

According to the results of testing variously oriented samples, it is possible to approximately construct the surface of equally dangerous planar stresses that are randomly oriented in the symmetry planes of the orthotropic materials. These surfaces are constructed in the work for pine in a tangential plane, for aviation multilayer plywood, and for two fiber glass-reinforced plastics, fabric and fibrous.

The surface of equally dangerous stresses is a graphic presentation of the strength condition for an anisotropic body that is approximately constructed from experimental data. The nature of these surfaces permits us to draw the conclusion that the strength condition cannot be presented in the form of a second degree polynomial for all anisotropic materials. The constructed surfaces for wood and for SVAM fiber glass-reinforced plastic correspond to equations of a higher order.

Study of the plasticity condition suggested by Mises in the form of a uniform second degree polynomial shows that it is applicable as the strength condition for many anisotropic materials in form (4.8) in piecewise approximation.

For wood and certain other strongly anisotropic materials, the strength condition in the form of a second degree polynomial contradicts the results of tests for uniaxial stretching of variously oriented samples. For this case, the strength condition in the form of a fourth order polynomial can be suggested. Its use does not contradict the experimental data presented in this work.

The fourth rank of the strength tensor follows from the strength condition in the form of a second degree polynomial (Mises). Its components are quantities that are the inverse of the strength characteristics squared. The strength condition in the form of a fourth degree polynomial makes it possible to maintain the same physical dimensionality for the components of the strength tensor (fourth rank) as for the components of the tensor of elastic constants (the components are quantities that are the inverse of the strength characteristics taken in the first degree).

The conducted study does not pretend to exhaust the examination of the question. Its main task was to generalize the experimental data on the strength of anisotropic media into a single harmonious system, and at the same time, to promote the creation of a science on resistance of materials whose strength varies in different directions.

#### References

1. Ashkenazi, Ye. K. "Experimental Determination of Elastic Components of Wood as an Anisotropic Material," Trudy LTA, No. 70, 1950. /162
2. Ashkenazi, Ye. K. "Determination of Elastic Constants of Wood," Zavodskaya laboratoriya, No. 3, 1955.
3. Ashkenazi, Ye. K. "First Russian Tests on Wood for Strength," Vestnik mashinostroyeniya, No. 12, 1954.
4. Ashkenazi, Ye. K. "Strength Symmetry of Wood," Trudy LTA, No. 78, 1957.
5. Ashkenazi, Ye. K. et al. Anizotropiya mekhanicheskikh svoystv drevesiny i fanery ["Anisotropy of Mechanical Properties of Wood and Plywood"], Goslesbumizdat, 1958.
6. Ashkenazi, Ye. K. et al. "Determination of Wood Resistance to Impact Compression," Zavodskaya laboratoriya, No. 9, 1958.

7. Ashkenazi, Ye. K. "Strength Anisotropy of Structural Materials," ZhTF, AN SSSR, Vol. 29, No. 3, 1959.
8. Ashkenazi, Ye. K.; and Pozdnyakov, A. A. "Technique of Determining Elastic Constants of Anisotropic Materials," Trudy LTA, No. 94, 1962.
9. Ashkenazi, Ye. K. Methods of Determining Mechanical Properties of Structural Plastics," Zavodskaya laboratoriya, No. 6, 1960.
10. Ashkenazi, Ye. K.; and Pozdnyakov, A. A. "Tests of Fiber Glass-Reinforced Plastics for Fatigue," Zavodskaya laboratoriya, No. 10, 1961.
11. Ashkenazi, Ye. K. "Methods of Testing Anisotropic Materials for Shear," Zavodskaya laboratoriya, No. 4, 1961.
12. Ashkenazi, Ye. K. Anizotropiya mekhanicheskikh svoystv nekotorykh stekloplastikov ["Anisotropy of Mechanical Properties of Certain Fiber Glass-Reinforced Plastics"], verbatim report of lecture, publication of Leningrad House of Scientific and Technical Propaganda, 1961.
13. Ashkenazi, Ye. K. "Strength Anisotropy of Structural Materials," ZhTF AN SSSR, Vol. 31, No. 5, 1961.
14. Ashkenazi, Ye. K. "Construction of Limiting Surfaces for Anisotropic Materials from Experimental Data," Zavodskaya laboratoriya, No. 2, 1964.
15. Ashkenazi, Ye. K. "Anisotropy of Mechanical Properties of Uniaxially Oriented Films of Crystal Polymers," Plasticheskiye massy, No. 2, 1964.
16. Astakhov, Karavayev, Makarov and Suzdal'tsev, Spravochnaya kniga po raschetuy samoleta na prochnost' ["Reference Book to Design Airplanes for Strength"], Oborongiz, 1954.
17. Bazhenov, V. A. P'yezoelektricheskiye svoystva drevesiny ["Piezoelectric Properties of Wood"], Izd-vo AN SSSR, 1959.
18. Belyankin, F. P. Prochnost' drevesiny pri skalyvanii vdol' volokon ["Strength of Wood during Shearing along the Fibers"], Izd-vo AN UkrSSR, 1955.
19. Belyankin, F. P.; Yatsenko, V. F.; and Dybenko, G. I. Mekhanicheskiye kharakteristiki plastika DSP ["Mechanical Characteristics of DSP Plastic"], Izd-vo AN UkrSSR, Kiev, 1961.
20. Bol'shakov, V. V. "Dependence of Wood Strength on Angle of Incline of Fibers," Spravochnik proyektirovshchika. Tom Derevyannyye konstruktsii ["Reference of Designer. Volume Wood Designs"] ONTI, 1937.

/163

21. Burov, A. K.; and Andreyevskaya, G. D. Steklovoloknistyye anizotropnyye materialy i ikh tekhnicheskoye primeneniye ["Fiber Glass Anisotropic Materials and Their Technical Application"], Izd-vo AN SSSR, 1956.
22. Grigorovich, V. K.; Sobolev, N. D.; and Fridman, Ya. B. "Most Suitable Direction of Fibers in Items Made of Anisotropic Materials," DAN SSSR, Vol. 86, No. 4, 1952.
23. Geordzhayev, V. O. "Strength Criterion of Anisotropic Materials," Trudy Moskovskogo Fiziko-tekhnicheskogo instituta ["Proceedings of Moscow Physical Engineering Institute"], No. 5, Oborongiz, 1960.
24. Ganov, E. V. "Stretching and Compression in Random Direction of Cold Hardened Fiber Glass-Reinforced Plastic," Tekhnologiya sudostroyeniya, No. 6, 1964.
25. Gol'denblat, I. I. Nekotoryye voprosy mekhaniki deformiruyemykh sred ["Certain Questions of the Mechanics of Deformable Media"], Moscow, GTTI, 1955.
26. Gol'denblat, I. I. Lektsii po tenzornomu ischisleniyu i ego pri-lozheniyam k mekhanike ["Lectures on Tensor Calculation and its Applications to Mechanics"], Moscow, Oborongiz, 1958.
27. Gurevich, B. G.; and Strelyayev, V. S. "Study of Strength Characteristics of Certain Fiber Glass-Reinforced Plastics," Plasticheskiye massy, No. 5, 1963.
28. German, V. L. Nekotoryye voprosy teorii plastichnosti anizotropnykh sred ["Certain Questions of the Theory of Plasticity of Anisotropic Media"], Doctoral dissertation, Physical Engineering Institute of UkrSSR Acad. of Sci., Khar'kov, 1944.
29. Davidenkov, N. N. Nekotoryye problemy mekhaniki materialov ["Certain Problems of the Mechanics of Materials"], Lenizdat, 1943.
30. Dikareva, T. A.; and Slonimskiy, G. L. Vysokomolekulyarnyye soyedineniya, No. 1, 1964.
31. Drozd, M. Ye. "Constrained Torsion of Rod of Rectangular Cross Section," Nauchnyye trudy Volgogradskogo mekhanicheskogo instituta, ["Scientific Proceedings of Volgograd Mechanical Institute"], Vol. 1, 1952.
32. Yermakov, V. P. "General Theory of Equilibrium and Fluctuation in Elastic Solid States," Universitetskiye izvestiya Kiyevskogo uni-versiteta, No. 6-9, izd. Kievskiy universitet, 1871.
33. Zakharov, K. V. Trudy Leningradskogo politekhnicheskogo instituta, No. 196, 1958.
34. Zakharov, K. V. Plasticheskiye massy, No. 8, 1961 and No. 6, 1963.

35. Ivanov, Yu. M. "Physical States and Rheological Properties of Wood," Voprosy lesovedeniya i lesovodstva (Doklady na V Vsemirnom lesnom kongresse ["Questions of Forest Science and Silviculture. (Reports at Fifth World Forestry Congress)"], izd-vo AN SSSR, 1960.
36. Ivanov, Yu. M. "Resistance of Pine to Compression at Different Angles to Fibers," Trudy Instituta lesa AN SSSR ["Proceedings of Forestry Institute, USSR Acad. of Sci."], izd-vo AN SSSR, Vol. 9, 1953.
37. Kalmanok, A. K. "Theory of Compression Testing," Issledovaniya po teorii sooruzheniy ["Studies on the Theory of Structures"], No. 5, Stroyizdat, 1951.
38. Kosmodamianskiy, A. S. "Evaluation of the Accuracy of Saint-Venant's Principle during Stretching of Anisotropic Band," Izvestiya AN SSSR OTN, No. 9, 1958.
39. Kritsuk, A. A. "Solution to the Planar Problem for Wood as an Anisotropic Material under the Influence of a Load at an Angle to the Main Elasticity Axes," Inform. materialy No. 9, Institute of Construction Mechanics of the Ukr. SSR Acad. of Sci., izd-vo AN Ukr. SSR, 1957.
40. Kupch. L. Ya. "Plywood Made of Veneer Sheets Glued at an Angle," Izv. AN Latv. SSR, No. 5, 1959.
41. Karlsen, G. G. "Study of Ring Dowel of Tukhsheer," Trudy TsAGI ["Proceedings of Central Aerodynamic Institute, No. 13, Oborongiz, 1925.
42. Leont'yev, N. L. Statisticheskaya obrabotka resul'tatov nablyudeniy ["Statistical Processing of Observation Results"], Gosstatizdat, 1952.
43. Lekhnitskiy, S. G. Teoriya uprugosti anizotropnogo tela ["Theory of Elasticity of Anisotropic Body"], GTTI, 1950.
44. Lekhnitskiy, S. G. Anizotropnyye plastinki ["Anisotropic Plastics"] GITL, 1957.
45. Lyav, A. Matematicheskaya teoriya uprugosti ["Mathematical Theory of Elasticity"], ONTI, 1935.
46. Lom[il]in, V. A. "Theory of Nonlinear Elasticity and Plasticity of Anisotropic Media," Izv. AN SSSR OTN Mekhanika i mashinostroyeniye, No. 4, 1960. /164
47. Moskaleva, V. Ye. Stroyeniye drevesiny i ego izmeneniye pri fizicheskikh i mekhanicheskikh vozdeystviyakh ["Structure of Wood and Its Change in Physical and Mechanical Effects"], Izd-vo AN SSSR, 1957.



48. Myakinin, L. V. "Strength of Equal-Layer Plywood with Uniform Planar Stress," Trudy Leningradskogo politekhnicheskogo instituta, No. 197, 1959.
49. Mitinskiy, A. N. "Elastic Constants of Wood as Orthotropic Material," Trudy LTA, No. 63, 1948.
50. Mitinskiy, A. N. "Moduli of Torsion and Moduli of Shear of Wood as Anisotropic Material," Trudy LTA, No. 65, 1949.
51. Mitinskiy, A. N. "Elastic Constants of Wood as Transverse-Isotropic Material," Trudy LTA, No. 67, 1949.
52. Nay, Dzh. Fizicheskiye svoystva kristallov i ikh opisaniye pri pomoshchi tensorov i matrits ["Physical Properties of Crystals and Their Description with Help of Tensors and Matrices"], IL, 1960.
53. Ogibalov, P. M.; and Lomakin, V. A. "Mechanical Properties of Fiber Glass-Reinforced Plastics," Enzhenernyy sbornik, Vol. 30, 1960.
54. Okatov, M. F. Obshchaya teoriya ravnovesiya uprugikh tverdykh tel i razdeleniye ikh na klassy ["General Theory of Equilibrium of Elastic Solid States and Their Separation into Classes"], Dissertation, St. Petersburg University, 1865.
55. Pozdnyakov, A. A. Otsenka prochnosti konstruktsionnykh plastmass pri peremennykh nagruzkakh ["Evaluation of Strength of Structural Plastics in Variable Loads"], Textbook, Izd. LTA, 1960.
56. Pozdnyakov, A. A. "Study of Fatigue Strength of Wood Anisotropic Materials," Trudy LTA, No. 96, 1961.
57. Pozdnyakov, A. A. "Fatigue of Wood at Different Angles to Fiber Direction," Izv. Vuzov. Lesnoy zhurnal, No. 3, 1960.
58. Rabinovich, A. L. "Elastic Constants and Strength of Anisotropic Materials," Trudy TsAGI, Oborongiz, 1946.
59. Rabinovich, A. L. "Calculation of Orthotropic Laminated Panels for Stretching, Shear and Bending," Trudy MAP, Oborongiz, No. 675, 1948.
60. Rabinovich, A. L.; Shtarkov, M. G.; Dmitriyeva, Ye. I. "Methods of Determination and Quantity of Elastic Constants of Glass Textolite at Increased Temperature," Trudy MFTI, No. 1, Oborongiz, 1958.
61. Rabinovich, A. L. "Certain Mechanical Characteristics of Butvar-Phenol Polymer Films," Vysokomolekulyarnyye soyedineniya AN SSSR, Vol. 1, No. 7, 1959.
62. Rabinovich, A. L.; and Turazyan, A. V. "Effect of Rate of Deformation on Amount of Deformation and Strength of Oriented Fiber Glass-Reinforced Plastics," DAN SSSR, Vol. 148, No. 6, 1963.

63. Rabinovich, A. L.; and Bilik. Sh. M. "Determination of Ultimate Strength of Pipes Made of Fiber Glass-Reinforced Plastics in Compression," Vestnik mashinostroyeniya, No. 4, 1960.
64. Rabinovich, A. L.; and Avrasin, Ya. D. "Mechanical Characteristics of Certain Laminated Plastics in Relation to Strength of Bolt and Rivet Connections," Steklotekstolity i drugiye konstruktsionnyye plastiki ["Glass Textolites and Other Structural Plastics"], Oborongiz, 1960.
65. Sobolev, N. D.; and Fridman, Ya. B. "Strength of Bodies with Variable Mechanical Properties," ZhTF AN SSSR, Vol. 24, No. 3, 1954.
66. Stepanov, A. V. "Dislocation Theories of Strength and Plasticity," Izv. AN SSSR OTN, No. 9, 1954.
67. Smotrin, N. T.; and Chebanov, V. M. "Mechanical Properties of Anisotropic Laminated Plastics in Short-Term Tests," Collection No. 2 Issledovaniya po uprugosti i plastichnosti ["Studies of Elasticity and Plasticity"], Izd-vo LGU, 1963.
68. Serensen, S. V.; and Strelyayev, V. S. Zavodskaya laboratoriya, No. 4., 1962.
69. Timoshenko, S. P. Istoriya nauki o soprotivleniiy materialov ["History of the Science on Resistance of Materials"], GITI, 1957.
70. Ter-Mkrtich'yan, L. N. "Stresses and Deformations of Quasi-Isotropic Elastic Body," Trudy Lesotekhnicheskoy akademii, No. 94, 1962. /165
71. Flakserman, A. N. Effect of Incline of Fibers on Mechanical Properties of Pine, GNTI, 1931.
72. Fridman, Ya. B. Mekhanicheskiye svoystva metallov ["Mechanical Properties of Metals"], (preface of N. N. Davidenkov to 1946 edition), and second edition, Oborongiz, 1952.
73. Fridman, Ya. B.; and Morozov, Ye. M. "Effect of Anisotropy of Strength Materials on Their Mechanical Properties," Izvestiya Vuzov SSSR, Mashinostroyeniye, No. 10, 1960
74. Fridman, Ya. B. "Certain Results of Studying the Failure Characteristics of Materials," Sovremennyye metody ispytaniya materialov, ["Modern Methods of Testing Materials"], Mashgiz, 1956.
75. Hill, R. Matematicheskaya teoriya plastichnosti ["Mathematical Theory of Plasticity"], GITTL, 1956, Chapter 12, Plastic Anisotropy.
76. Chentsov, N. G. "Study of Plywood as Orthotropic Plastic," Tekhnicheskiye zametki TsAGI, No. 91, Oborongiz, 1936.

77. Chernetsov, M. M. "Study of Strength of Wood in Stretching Transverse to Fibers," Derevoobrabatyvayushchaya promyshlennost', No. 3, 1957.
78. Shmid, and Boas, Plastichnost' kristallov ["Plasticity of Crystals"] GONTI, 1938.
79. Shubnikov, A. V. "Symmetry of Vectors and Tensors," Izv. AN SSSR, vol. 13, 1949, pp. 347-391.
80. Shubnikov, A. V.; Flint, Ye. Ye.; and Boki, G. B. Osnovy kristallografii ["Fundamentals of Crystallography"], Izd-vo AN SSSR, 1940.
81. Shubnikov, A. V. P'yezoelektricheskiye tekstury ["Piezo-electric Textures"], Izd-vo AN SSSR, 1946.
82. Yagi, Yu. I. "New Methods of Calculating for Strength," Vestnik inzhenerov i tekhnikov, No. 6, 1931.
83. Ashkenazi, Ye. K.; Volkov, A. K.; Ganov, E. V.; and Sharapova, N. P. Effect of Cross Grain on Fatigue Strength of Fiber Glass-Reinforced Glass Fabrics," Tekhnologiya sudostroyeniya, No. 1, 1965.
84. Jlinen, A. A Comparative Study of Different Types of Shear Test of Wood, Helsinki, 1963.
85. Barkas, Hearmon, Rance (ed. Meredith), Mechanical Properties of Wood and Paper, Amsterdam, 1953.
86. Boller, K. "Fatigue Properties of Fibrous Glass-Reinforced Plastic Laminates," Modern Plastics, No. 6, 1957.
87. Donaldson, A. L.; and Velleu, R. B. "Design and Fabrication with Directionally Reinforced Plastic," Modern Plastics, No. 10, 1957, No. 2, 1958.
88. Findley, W. N.; and Mathur, P. N. "Anisotropy of Fatigue Strength of A Steel and Two Aluminum Alloys in Bending and Torsion," Proc. Amer. Soc. Testing Materials, Vol. 55, 1955.
89. Frey-Wyssling, A. "Die Ursache der anisotropen Schwindung des Holzes," Holz als Roh und Werkstoff, Vol. 3, 349, 1940.
90. Fischer, L. "How to Predict Structural Behavior of R P Laminates," Modern Plastics, No. 6, 1960.
91. Gaber, E. "Druckversuche quer zur Faser an Nadel und Laubhölzern," H.a.R.u.W., 7/8, 1940.
92. Gatto, and Mori, "Indagini sperimentali sull'anisotropia degli estrusi di leghe leggere ad alta resistenza," Alluminio, Vol. 24, No. 3, 1955.

93. Garofalo, F.; and Low, J. "The Effect of Prestraining in Simple Tension," Journal Mech. and Physics of Solids, Vol. 3, No. 4, 1957.
94. Hearmon, R. F. S. "The Elasticity of Wood and Plywood," Forest Product Laboratory Madison USA, Spec. Rep. No. 7, 1948.
95. Hoover, H. "The Measurement of Directional Strength in Straight and Cross Rolled Strip Steel," Amer. Soc. for Testing Materials, Proceed., Vol. 53, 1953.
96. Hörig, H. "Anwendung der Elactizitätstheorie anisotroper Körper auf Messungen an Holz," Ingenieur-Archiv B., Vol. 1.1935.
97. Hu, L.; and Marin, J. "Anisotropic Loading Function for Combined Stresses in Plastic Range," Journal of Appl. Mech., Vol. 22, No. 1 1955, /166
98. Jlinen, A. "Ein neues Messverfahren für die Bestimmung der Shub-meduln, H.a.R.u.W., Vol. 5, No. 11, 1942.
99. Keylwerth, R. "Die Anisotrope Elastizität des Holzes und der Lagenhölzer, V D J Forshungsheft, No. 430, 1951.
100. Keywerth, R. Erreichte und erreichbare Verminderung der Abisotropie und Holzwerkstoffplatten," H.a.R.u.W. Vol. 17, No. 6, 1959.
101. Kollmann, F. "Die Abhängigkeit der Festigkeit und der Dehnungszahl der Hölzer vom Faserverlauf," Bauingenieur, No. 19/20, 1934.
102. Kollmann, F. Technologie des Holzes und der Holzwerkstoffe, B. 1, Berlin, 1951.
103. Lin, T. H. "On the ASSociated Flow Rule of Plasticity Based on Crystalslip," Journal Franklin Inst. Vol. 270, No. 4, 1960.
104. Matschinski, M. "Sur les Symetries des proprietes physique," Comptes rendus L. acad. des Sciences, Paris, Vol. 240, No. 22, 1955.
105. Marin, J. "Theories of Strength for Combined Stresses and Nonisotropic Materials," Journal of Aeronautical Sciences, No. 24, No. 4, 1957.
106. Mises, R. "Mechanik der plastischen Formänderungen von Kristallen," Zeinschrift fur angew. Mathem. u. Mech., Vol. 8, No. 3, 1928.
107. Norris, C. B. Technique of Plywood, ed. Laucks, USA, 1942.
108. Norris, C. B. "The Elastic Theory of Wood Failure," Transactions of the ASME, Vol. 61, No. 3, 1939.
109. Raczkowski, J. "Anisotropia cisnienia pecznienia drewna," Folia Forestalia Polonica, No. 2, B, 1960.

110. Stüssi, F. "Zum Einfluss der Faserrichtung auf die Festigkeit und Elastizitätsmodul von Holz," Schweizerische Bauzeitung, Vol. 126, No. 22, 1945.
111. Späth, W. Der Schlagversuch, Berlin, 1957.
112. Schleicher, F. "Der Spannungszustand an der Fliessgrenze," ZAMM No. 6, 199, 1926.
113. Werren, F. "Mechanical Properties of Glass Plastic Laminates as Related to Direction of Stress," Transactions of ASME, Vol. 75, No. 4, 1953.
114. Voigt, W. Lehrbuch der Kristallphysik, 1910.
115. Skupin, L. Kačuk a plastike hmoty, No. 8, 1962, 290 (Czech).
116. Ashkenazi, Ye. K.; and Posdnyakov, A. A. "Shape of Sample for Testing Anisotropic Fiber Glass-Reinforced Plastics for Stretching," Zavodskaya laboratoriya, 1965, No. 10.
117. Ashkenazi, Ye. K. "Questions of Strength Anisotropy," Mekhanika polimerov, izd-vo AN Latv. SSR, No. 2, 1965.
118. Sidorin, Ya. S. "Experimental Study of Anisotropy of Fiber Glass-Reinforced Plastics," Izv. AN SSSR, No. 3, 1964.
119. Miklyayev, P. G.; and Fridman, Ya. B. "Technique of Evaluating Anisotropy of Mechanical Properties of Metals," Zavodskaya laboratoriya, No. 3, 1966.
120. Ashkenazi, Ye. K.; and Yelokhov, V. N. "One Principle of Dispersing Results of Testing Anisotropic Materials," Zavodskaya laboratoriya, No. 3, 1966.
121. Perekal'skiy, S. M. "Technique of Determining Elastic Constants of Fiber Glass-Reinforced Plastics," Standartizatsiya, No. 6, 1964.
122. Gol'denblat, I. I.; and Kopnov, V. A. "Strength of Fiber Glass Reinforced Plastics in Complex Stress," Mekhanika polimerov, Izd. AN Latv. SSR, No. 2, 1965.
123. Bridgman, P. W. J. Appl. Physics, Vol. 12, 1941.
124. Protasov, V. D.; Kochnov, V. A. Mekhanika polimerov, izd-vo AN Latv. SSR, No. 5, 1965.